



POLITECNICO DI TORINO

Department of Electronics and Telecommunications

PhD Dissertation

Study of Techniques For Reliable Data
Transmission In Wireless Sensor
Networks

by

Vahid Forutan

Tutor:

Carla-Fabiana Chiasserini

THESIS COMMITTEE

Carla Raffaelli
Universita di Bologna

Marco Gribaudo
Politecnico di Milano

Emilio Leonardi
Politecnico di Torino

Contents

Abstract	6
Organization of the thesis	7
List of Figures	12
List of Tables	16
1 Wireless Sensor Netowrks	19
1.1 Introduction	19
1.2 Design challenges in wireless sensor networks	23
1.2.1 Scalability	23
1.2.2 Lifetime	24
1.2.3 Fault tolerance	24
1.2.4 Localization	25
1.2.5 Synchronization	25
1.2.6 Data compression and aggregation	26
1.2.7 Security	26
1.2.8 Production costs	27
1.2.9 Hardware constraints	27
1.2.10 Transmission media	29
1.2.11 Power consumption	30
1.2.11.1 Communication	30

1.2.11.2	Data processing	31
1.3	Wireless sensor networks communication architecture	32
1.3.1	Transport layer	34
1.3.2	Network layer	34
1.3.3	Data link layer	35
1.3.3.1	Power saving modes of operation	36
1.3.3.2	Error control	37
1.3.4	Physical layer	38
1.3.4.1	Modulation schemes	39
1.3.4.2	Radio architecture	39
1.3.4.3	Bandwidth requirements	39
1.4	Cooperative communication and relaying in WSNs	40
2	Communication Strategies for Wireless Sensor Networks	42
2.1	Introduction	42
2.2	Network model and definitions	44
2.3	Communication Schemes	45
2.3.1	Proposed Schemes	45
2.3.1.1	Cooperative Sub-chains (CS)	45
2.3.1.2	Interlaced Chains (IC)	48
2.3.2	Conventional Schemes	49
2.3.2.1	Multi-hop (MH)	49
2.3.2.2	Multiple Access (MAC)	50
2.4	Results	51
2.5	Concluding Remarks	52
3	Network Information Theory of Linear Wireless Networks	57
3.1	Introduction	58
3.2	Multi-state Networks	60

3.3	System model	61
3.4	Cut-set bounds	63
3.4.1	Cut-set bound in multi-state networks	66
3.5	Cut-set bounds in linear wireless networks	67
3.5.1	Network with full-duplex nodes	67
3.5.1.1	One-hop, Full-duplex	70
3.5.1.2	One-hop, Full-duplex, Unidirectional traffic flow	72
3.5.2	Network with half-duplex nodes	74
3.5.3	Half-duplex nodes, One-hop communication	74
3.5.3.1	Three nodes, one destination ($n = 3$)	74
3.5.3.2	Four nodes, one destination ($n = 4$)	79
3.5.4	Half-duplex nodes, Two-hop communication	82
3.5.4.1	Two nodes, one destination ($n = 2$)	82
3.5.4.2	Three nodes, one destination ($n = 3$)	86
3.5.4.3	Four nodes, one destination ($n = 4$)	90
3.6	Concluding remarks	92
4	Fairness in Traffic Relaying in One-hop Linear Wireless Networks	93
4.1	Introduction	93
4.2	Related Work	95
4.3	System model	98
4.4	Fairness in achievable data rate	100
4.4.1	An upper bound to the achievable data rate	100
4.4.2	The Cooperative Sub-chains strategy	104
4.4.3	Results	108
4.5	Fairness in data rate and energy consumption	111
4.5.1	Link capacities providing fairness in average power consumption	112
4.5.2	An upper bound to the achievable rate	114

4.5.3	Multi-hop strategy with optimal link scheduling (Optimized Multi-hop)	116
4.5.4	Results	117
4.6	Concluding Remarks	118
5	Upper Bounds to the Performance of Cooperative Traffic Relaying in Linear Wireless Networks	120
5.1	Introduction	121
5.2	System model	124
5.3	Background on the cut-set bound	128
5.4	Cut-set bounds: Full-duplex radios	130
5.4.1	Upper bound to B_{FD}	131
5.4.2	Lower bound to B_{FD}	132
5.4.3	Results	134
5.5	Cut-set bounds: Half-duplex radios	137
5.5.1	Upper bound to B_{HD}	137
5.5.2	Lower bound to B_{HD}	141
5.5.3	Results	142
5.6	Conclusions	147
6	Two-hop Cooperative Communication Strategies for Wireless Sensor Networks	148
6.1	Introduction	148
6.2	Related Work	149
6.3	System Model	150
6.4	Communication strategies	152
6.4.1	The TTR strategy	152
6.4.1.1	Deriving the rate constraints in TTR strategy	155
6.4.1.2	Computing the average Achievable rate, R	157

6.4.2	The TTRR strategy	158
6.5	Results	167
6.6	Concluding Remarks	169

Abstract

This thesis addresses the problem of traffic transfer in wireless sensor networks (WSN). In such networks, the foremost challenge in the design of data communication techniques is that the sensor's transceiver circuitry consumes the major portion of the available power. Thus, due to stringent limitations on the nodes' hardware and power resources in WSN, data transmission must be power-efficient in order to reduce the nodes' power consumption, and hence to maximize the network lifetime while satisfying the required data rate. The transmit power is itself under the influence of data rate and source-destination distance. Thanks to the dense deployment of nodes in WSN, multi-hop communication can be applied to mitigate the transmit power for sending bits of information, i.e., gathered data by the sensor nodes to the destination node (gateway) compared to single-hop scenarios. In our approach, we achieve a reasonable trade-off between power-efficiency and transmission data rate by devising cooperative communication strategies through which the network traffic (i.e. nodes' gathered information) is relayed hop-by-hop to the gateway. In such strategies, the sensor nodes serve as data originator as well as data router, and assist the data transfer from the sensors to the gateway. We develop several data transmission schemes, and we prove their capability in transmitting the data from the sensor nodes at the highest possible rates allowed by the network limitations. In particular, we consider that

- (i) network has linear or quasilinear topology
- (ii) nodes are equipped with half-duplex radios, implying that they cannot transmit and receive simultaneously,
- (iii) nodes transmit their traffic at the same average rate.

We compute the average data rate corresponding to each proposed strategy. Next, we take an information-theoretic approach and derive an upper bound to the achievable rate of traffic transfer in the networks under consideration, and analyze its

tightness. We show that our proposed strategies outperform the conventional multi-hop scheme, and their average achievable rate approaches the upper bound at low levels of signal to noise ratios.

Organization of the thesis

The first part of the thesis is concentrated mainly on developing two simple but power-efficient cooperative data transmission strategies, namely *Cooperative sub-chains*, and *Interlaced chains*. The former is based on one-hop communication scheme, while the latter is basically a k -hop communication scheme. However, in both strategies the main assumption is that each node while being in transmit mode, communicates with only one node in the network that is located at one-hop distance (Cooperative sub-chains), or at k -hop distance (Interlaced chains). The idea is that each node in the network upon receiving its previous nodes' traffic, forwards them besides its own traffic to the next node located at one hop (in Cooperative sub-chains) or k hops (in Interlaced chains) distance farther. We analyze the performance of these strategies with respect to their average achievable rate of data transfer, and average power consumption, and compare them to the conventional multi-hop and multiple-access communication schemes. We show that the Cooperative sub-chains strategy outperforms the others with respect to the average achievable rate, while the Interlace chains does the same but with respect to the average power consumption. Thus, we conclude that "Cooperative sub-chains" is an efficient data transmission scheme in cases where the average data rate is the matter of concern in the network design, while the "Interlaced chains" is the appropriate solution when we concern mostly about the power consumption in the network.

In the next part of the thesis, we undertake an information-theoretic approach in finding the answer to the general question "what is the limit on the average rate of traffic transfer in a linear wireless network". In fact, the answer to this question provides us with some criteria in finding out how well our proposed strategies perform

with respect to average rate of data transmission. Toward this aim, we obtained the upper bounds on the rate of data transfer in linear wireless networks under the assumption of both full and half-duplex nodes in the network. Moreover, we show that extending the communication range beyond the two hop distance will lead to less benefits, implying that two-hop communication is an appropriate candidate as a traffic transfer scheme in such networks.

Finally, in the last part of the thesis, we consider extending the node's communication range to two hops, i.e., a node while being in transmit mode can communicate with two nodes located at most two hops distance from it. We design several traffic relaying strategies, namely *transmit-transmit-receive* (TTR) and *transmit-transmit-receive-receive* (TTRR) that are mainly based on having the node's transmission power or transmission rate to be assigned proportionally among the traffic that must be forwarded. We conclude through analysis that extending the communication range to two hops can be beneficial regarding the average achievable rate when compared to the case where the communication is restricted between two nodes only.

This thesis is organized in six chapters, we describe briefly the organization of the thesis and point out the main contributions of each chapter.

Chapter 1 This chapter is an introduction to wireless sensor networks, basically from the nodes communication point of view, and addresses some fundamental challenges that exist in such networks with respect to the data transmission among sensor nodes.

Chapter 2 In this chapter, we present cooperative traffic relaying strategies for half-duplex sensor networks with linear topologies, where sensors need to deliver the same amount of data to a sink node by sharing the same radio resources. Under such constraints, we devise two traffic transfer strategies, namely, Cooperative Sub-chains, and Interlaced Chains, and derive the expressions for the rate and the energy consumption they achieve. We then compare the two proposed strategies with the

multiple access and the multi-hop relaying strategies, highlighting which scheme is to be preferred as the system parameters vary.

Chapter 3 In this chapter, we use information theory to address the problem of finding the *cut-set* upper bounds to the average achievable rate of traffic transfer in linear wireless networks, where the nodes are supposed to send their own traffic as well as to relay other nodes' traffic toward the destination. Toward this end, first we construct a system model for such networks by considering the practical constraints, in particular, the half-duplex operation of network's nodes. Next we try to obtain such bounds as the solutions to the max-flow min-cut bound problem applied to linear wireless networks that consists of few nodes. The solutions obtained in these case, provide us with some useful insights into figuring out how do such networks with larger number of nodes such as (i) in the network with half-duplex nodes, and when the communication range is restricted to one-hop distance, the transfer of nodes' traffic to the destination requires the network to operate in just two distinct states, and that (ii) in linear wireless networks, the cut-set bounds corresponding to the last cuts – i.e., the cuts that separate the the near-destination nodes (and the destination) from the rest of the nodes – contribute to the max-flow min-cut bound to the rate of traffic transfer.

Chapter 4 This chapter is an extended analysis of the achievable data rate of cooperative relaying strategies in the multi-hop networks of half-duplex nodes, where every node needs to deliver its data to a gateway node at the same rate; also, nodes may have limited energy capabilities. Under such constraints, we first take an information-theoretic approach and derive cut-set upper bounds to the achievable rate. Then, we devise two communication strategies, each aiming at a different objective. The former ensures a high, fair rate allocation to the network nodes, but it neglects their energy constraints. By fairness in rate allocation, we mean that all nodes can have their data delivered to the gateway at the same average rate, as they exhibit equal traffic demand. The latter, instead does consider energy constraints

by meeting the requirements on the average power consumption at each node, and provides fairness in the data rate allocation. For each of the proposed strategies, we derive an expression for the achievable rate and average power consumption, and we compare their performance of the to the upper bounds and the classic multi-hop data transfer, showing their effectiveness and providing useful insights on the system behavior.

Chapter 5 In this chapter we study the rate performance limits of linear wireless network where n nodes have to deliver their traffic to a common destination node through multi-hop data transfers, for which (i) the nodes' transmissions can reach receivers farther than one-hop distance from the sender, (ii) the transmitters cooperate in the data delivery, and (iii) interference due to concurrent transmissions is taken into account. By adopting an information-theoretic approach, we derive analytical bounds to the achievable data rate accounting for the interference due to simultaneous transmissions, and in presence of full as well as half-duplex nodes. The expressions we provide are mathematically tractable and allow the analysis of multi-hop networks with a large number of nodes. Our analysis suggests two important facts. First, in order to design efficient communication strategies, it is sufficient to use pairs of transmitters that cooperate to forward the data to the destination. Second, in half-duplex networks, there exist some dominant network states whose contribution determines the achievable data rate. Effective communication strategies can therefore be obtained by considering pairs of cooperating nodes and by letting the network operate in such states. Future work will focus on the definition of cooperative traffic relaying schemes that provide an achievable rate as close as possible to the upper bound provided in this study.

Chapter 6 In this chapter, we focus on the design of two cooperative multi-hop communication strategies for linear wireless networks composed of a cascade of half-duplex nodes that may both generate their own traffic and relay other nodes' traffic toward the destination. However, unlike previous work, we account for the fact that the

transmission range of the source/relay nodes is allowed to span over more than one hop. Under these conditions, we derive the average rate that can be achieved by the node under each proposed strategy, and we compare it to the cut-set upper bound on the network data rate. We show that the proposed schemes exhibit good performances in terms of average achievable rate when compared to non-cooperative techniques as well as to the cut-set upper bound obtained in Chapter 5.

List of Figures

1.1	A typical sensor network (redrawn from [2]).	20
1.2	Components of a sensor node (redrawn from [2])	28
1.3	Protocol stack in a typical wireless sensor network (redrawn from [2]).	33
1.4	Detailed protocol stack in wireless sensor networks (redrawn from [4]).	34
2.1	Topology of the wireless sensor network.	45
2.2	Cooperative Sub-chains with $n = 7, k = 3$	46
2.3	Interlaced Chains with $n = 5, k = 2$	49
2.4	Multi-hop with $n = 5$	50
2.5	Multiple Access with $n = 5$	50
2.6	Achievable rate R versus k , in Cooperative Sub-chains (top), and Interlace chains (bottom), with $n = 20$ nodes, and $d = 20$ m.	53
2.7	Average achievable rate (top), and Average energy consumption per bit (bottom), obtained for $k = k^*$, with $n = 20$ nodes, and $d = 20$ m.	54
2.8	Average achievable rate, R , versus d , obtained for $k = k^*$, with $n = 20$ nodes, and $\gamma = 20$ dB (top), and $\gamma = 40$ dB (bottom).	55
2.9	Average energy consumption per bit, E , versus d , obtained for $k =$ k^* , with $n = 20, \gamma = 20$ dB (top), and $\gamma = 40$ dB (bottom)	56
3.1	Network topology.	62
3.2	An example of a linear network with $n = 3$ full-duplex nodes and a destination. The communication links are depicted by arrows.	67

3.3	A linear network with $n = 3$ full-duplex nodes and a destination. The communications are restricted to <i>one-hop</i> links only.	70
3.4	A linear network with $n = 3$ full-duplex nodes and a destination. The communications are restricted to one-hop unidirectional links only.	72
3.5	A network of $n = 3$ half-duplex nodes and a destination. The communication range is restricted to one-hop distance, and the information flow is unidirectional. The network operates in $M = 3$ states, namely, σ_1 , σ_2 , and σ_3	75
3.6	A network of $n = 3$ half-duplex nodes and a destination. It operates in $M = 2$ states.	78
3.7	A network of $n = 4$ half-duplex nodes and a destination. It operates in $M = 2$ states, namely, σ_1 , σ_2	79
3.8	A network of $n = 2$ half-duplex nodes and a destination. The communication range is limited to two-hop distance. The network operates in $M = 3$ states.	82
3.9	A network of $n = 3$ half-duplex nodes and a destination. We have appointed $M = 6$ states to it.	86
4.1	Network with linear topology, the gateway (sink) is shown in black.	98
4.2	Cooperative Sub-chains strategy for $n = 10$ and $k = 4$. Nodes in sleep state are not shown.	105
4.3	Average achievable rate as the number of nodes per sub-chain varies, for $n = 20$, $\alpha = 0.1$ (top), and $\alpha = 10$ (bottom), for different values of γ	109
4.4	Average achievable rate versus γ , for $n = 20$ and $\alpha = 0.1$ (top), and $\alpha = 10$ (bottom). The performance of the cut-set upper bound, the Cooperative Sub-chains strategy and the Multi-hop scheme are compared.	110

4.5	Per-node power consumption ($\pi_i, i = 1, \dots, n$) normalized to the average achievable rate, for $n = 20, \gamma = 30$ dB and $\alpha = 1$	111
4.6	Average achievable rate of the multi-hop scheme with optimal link scheduling (Optimized Multi-hop), for $n = 4, \alpha^{\max} = 100$ and $\gamma = 10, 50$ dB. The performance is compared to the cut-set bound, as the target average power consumption at the nodes (π) varies. . .	117
4.7	Achievable rate for the Optimized Multi-hop strategy, when $\alpha^{\max} = 100$ and both γ and n vary.	118
5.1	Network topology.	125
5.2	Full-duplex radios: bounds for $n = 10, a = 2$ (top), and $a = 4$ (bottom), $\rho_i = 1\forall i, k_C = 1, 2, 3$ hops and $k_I = 5$	136
5.3	Equivalent network for the computation of the bound in (5.21). . . .	140
5.4	Half-duplex radios: bounds for $n = 10, a = 2, 4, \rho_i = 1\forall i, k_C = 2$ hops and $k_I = 3$	143
5.5	Comparison between the cases of half-duplex and full-duplex radios. Bounds for $n = 5$ (top), and $n = 10$ (bottom), with $a = 2, 4, \rho_i = 1\forall i, k_C = 2$ hops and $k_I = 3$ hops.	144
5.6	Comparison between the cases of half-duplex and full-duplex radios. Bounds for $n = 5, a = 2, 4, k_C = 2$ hops, $k_I = 3$ hops, and different data generation rates at the nodes, namely, $\rho_i = i, i = 1, \dots, n$	145
5.7	Comparison between the cases of half-duplex and full-duplex radios. Bounds for $n = 5, 10, a = 2, k_C = 2$ hops, $k_I = 3$ hops, and different data generation rates at the nodes, namely, $\rho_i = i, i = 1, \dots, n$	146
6.1	Network with linear topology, the destination is shown in black. . .	151
6.2	TTR strategy in a network with $n = 6$ nodes.	154
6.3	TTRR strategy, Scenario 1; the network has $n = 7$ nodes.	159

6.4	Approaching the destination in Scenario 1; the number of active nodes in the last set is less than four, it is actually three (top), and two (bottom).	160
6.5	TTRR strategy, Scenario 2; delivery of W_1, W_2, W_5, W_6 to the destination in a network with $n = 7$ nodes.	162
6.6	Two consecutive quadruplets.	163
6.7	Special cases in TTRR strategy, where the number of active nodes in the last set is less than four, it is actually three (top), and two (bottom).	164
6.8	TTRR strategy, Scenario 3; a network with $n = 7$ nodes.	166
6.9	Average achievable rates in the absence of signal interference, $a = 1.5$ (top) and $a = 3$ (bottom).	168
6.10	Average achievable rates in the presence of signal interference, $a = 1.5$ (top) and $a = 3$ (bottom).	169

List of Tables

3.1	Cuts and their corresponding sum rates and cut-set bounds in a network of $n = 3$ full-duplex nodes and a destination.	68
3.2	Solution to the cut-set bounds and the resulted max-flow min-cut bound, referred to the network of $n = 3$ full-duplex nodes shown in Fig. 3.2.	69
3.3	Cuts and their corresponding sum rates and cut-set bounds in a network of $n = 3$ full-duplex nodes and a destination shown in Fig. 3.3.	70
3.4	Solution to the cut-set bounds and the resulted max-flow min-cut bound, referred to the network of $n = 3$ full-duplex nodes shown in Fig. 3.3.	72
3.5	Cuts and their corresponding cut-set bounds in a network of $n = 3$ full-duplex nodes and a destination, referred to the network shown in Fig. 3.4.	72
3.6	Solution to the cut-set bounds and the resulted max-flow min-cut bound, referred to the network of $n = 3$ full-duplex nodes shown in Fig. 3.4.	73
3.7	Node and network states in a network of $n = 3$ nodes.	75
3.8	Cuts in a network of $n = 3$ half-duplex nodes and a destination, referred to the netowrk shown in Fig. 3.5.	76
3.9	Cuts, sum rates, and cut-set bounds in a network of $n = 3$ half-duplex nodes and a destination shown in Fig. 3.5.	76

3.10	Cuts, sum rates, and cut-set bounds in a network of $n = 3$ half-duplex nodes and a destination shown in Fig. 3.5. $\mathcal{C} = (1/2) \log_2(1 + \gamma)$.	77
3.11	Cuts, sum rates, and cut-set bounds in a network of $n = 3$ half-duplex nodes and a destination shown in Fig. 3.6, where $\mathcal{C} = (1/2) \log_2(1 + \gamma)$.	78
3.12	Node and network states in a network of $n = 4$ half-duplex nodes.	79
3.13	Cuts in the network of $n = 4$ half-duplex nodes and a destination.	80
3.14	Cuts, sum rates, and cut-set bounds in the network of $n = 4$ half-duplex nodes and a destination.	81
3.15	Cuts, sum rates, and cut-set bounds in the network of $n = 4$ half-duplex nodes and a destination. $\mathcal{C} = (1/2) \log_2(1 + \gamma)$ denotes the one-hop link capacity.	81
3.16	Network and nodes' states appointed initially for a network of $n = 2$ nodes and a destination.	82
3.17	Cuts in a network of $n = 2$ half-duplex nodes and a destination.	83
3.18	Cuts, sum rates, and cut-set bounds in a network of $n = 2$ nodes and a destination, referred to the network shown in Fig. 3.8.	83
3.19	Cuts, sum rates, and cut-set bounds in a network of $n = 2$ nodes and a destination.	84
3.20	Time fractions of network states, referred to a network of $n = 2$ half-duplex nodes.	85
3.21	Cut-set bounds and the resulted max-flow min-cut bound in a network of $n = 2$ half-duplex nodes and a destination.	85
3.22	Network and nodes' states appointed initially for a network of $n = 3$ nodes and a destination.	86

3.23	Cuts, sum rates, and cut-set bounds, referred to a network of $n = 3$ half-duplex nodes, when the communication range is restricted to two-hop.	87
3.24	Time fractions of network states in a network of $n = 3$ half-duplex nodes when the communication range is two-hop.	89
3.25	Cut-set bounds and the resulted max-flow min-cut bound referred to a network of $n = 3$ half-duplex nodes.	90
3.26	Network and nodes' states appointed initially for a network of $n = 4$ half-duplex nodes and a destination.	90
3.27	Time fractions of network states, the network has $n = 4$ half-duplex nodes and one destination. Note that only t_1, t_2, t_5 and t_8 have nonzero values.	90
3.28	Actual (i.e. nontrivial) network states for a network of $n = 4$ half-duplex nodes.	91
3.29	Cut-set bounds obtained for a network of $n = 4$ half-duplex nodes (referred to cuts C_1, \dots, C_7).	91
3.30	Cut-set bounds and max-flow min-cut bound for a network of $n = 4$ half-duplex nodes (referred to cuts C_8, \dots, C_{15}).	91
4.1	Communication strategy achieving the bound	103
6.1	Power coefficients $\alpha_j^{(h)}$ and $\beta_j^{(h)}$ ($j = 1, 2, 3$) for $2 \leq h \leq n$, ($\alpha_3^{(h)} = 1 - \alpha_1^{(h)} - \alpha_2^{(h)}$ and $\beta_3^{(h)} = 1 - \beta_1^{(h)} - \beta_2^{(h)}$).	154

Chapter 1

Wireless Sensor Networks

1.1 Introduction

A wireless sensor network (WSN) is composed of a large set of multi-functional sensor nodes with limited power supply and constrained computational capability, which are deployed in an unattended manner over a geographical area for the purpose of gathering information or detecting special events in a collaborative way. It consists of hundreds to thousands of tiny, lightweight, and battery-operated devices (sensor nodes), each equipped with a sensing unit, a processing unit and memory, power supply, and a wireless communication unit (radio). The sensing unit is a micro-electromechanical system (MEMS) capable of measuring the changes in some physical parameter such as temperature or pressure within a monitoring environment (or *sensing field*). Indeed, the aggregation of sensing, processing, and communication into a very small device leads to many important applications such as environmental monitoring, target tracking and surveillance, seismic sensing and natural disaster relief, etc. [1]. The nodes, being stationary or moving, sense and collect an interested physical parameter within sensing field, and forward the gathered data through the wireless links to the base station node (or *sink*) in the network, possibly via *multiple hops*.

The deployment of the sensor nodes within the sensing field can be random or

follow a predefined order. This implies on the other hand that, sensor network protocols and algorithms must possess self-organizing capabilities [2]. As a distinctive feature, sensor networks are able to accomplish their tasks cooperatively. For example, instead of sending the raw data to the the base station, sensor nodes use their processing capabilities to locally carry out simple computations and transmit only the required and partially processed data toward the base station. Indeed, irrespective of the limited capabilities of an individual sensor node, the collaborative nature of the network operation makes WSNs an appropriate choice for the required tasks.

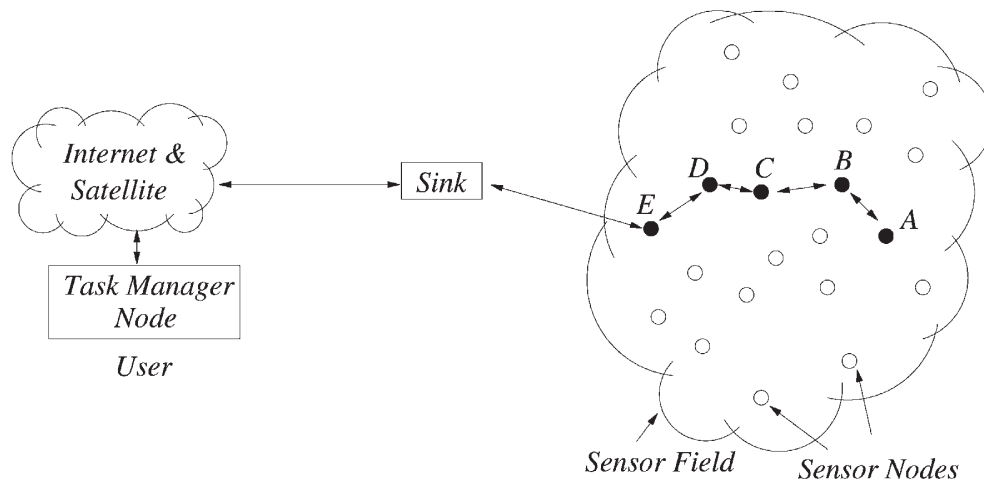


Figure 1.1: A typical sensor network (redrawn from [2]).

The nodes in WSN, in addition to playing the role of a *data source* in gathering information from the sensing field, should also act as a *data router* in communicating with their neighbor nodes in the network in order to transfer the information to the base station (or sink). This gives rise to a distributed computing, which itself poses many challenging issues such as real-time communication and coordination, since many constraints such as limited power, processing speed, storage capacity, and communication bandwidth must be satisfied simultaneously [3].

WSNs possess unique features and requirements that do not exist in the tra-

ditional wireless and *ad hoc* networking paradigms such as Wireless Local Area Networks (WLANs), and Mobile Ad hoc Networks (MANETs). In these traditional networks the primary concerns are, satisfying the quality of service (QoS), and high bandwidth efficiency, in which the tasks of organization, routing and mobility management are done considering such concerns. In other words, these networks are designed to provide good throughput/delay characteristics under high mobility conditions, while the energy consumption is of secondary importance, i.e., they do not have to cope with resource limitations in general [4]. This is in contrast to the WSNs, where the nodes are, in general, stationary after deployment, and the data rate is expected to be very low to the order of 1-100 kbps.

Accordingly, the main goals in the design of wireless sensor networks, are prolonging the lifetime of the network and maintaining the nodes connectivity through managing the network power consumption. In brief, among the most notable differences between WSNs and ad hoc networks are [2]

- huge number of nodes in WSNs, as compared to ad hoc networks,
- dense deployment of nodes,
- nodes are unreliable and prone to failures,
- frequent changes of the network topology,
- broadcast nature of communication in WSNs, point-to-point communication in ad hoc networks,
- *many-to-one* traffic pattern, i.e., data flow is unidirectional, from sensor nodes toward the sink(s),
- nodes are usually (very) small and battery-operated, hence there are severe constraints on power, processing capacity, and data storage,
- data redundancy, the sensed data are correlated to some extent,
- nodes in WSNs do not have necessarily a global identification (such as IP address).

A WSN typically has little or no infrastructure [5]. Regarding this, there are two types of WSNs: *structured* and *unstructured*. An unstructured WSN is one that contains a dense collection of sensor nodes that are deployed in an ad hoc manner into the sensing field. Once deployed, the network is left unattended to perform monitoring and reporting functions. In an unstructured WSN, network maintenance such as managing connectivity and detecting failures is difficult since there are so many nodes. In a structured WSN, however, all or some of the sensor nodes are deployed in a preplanned manner. The advantage of a structured network is that fewer nodes can be deployed with lower network maintenance and management cost. Fewer nodes can be deployed now since nodes are placed at specific locations to provide coverage while ad hoc deployment can have uncovered regions.

Unlike traditional networks, a WSN has its own design and resource constraints. Resource constraints include [5]

- limited amount of energy,
- short communication range,
- low bandwidth,
- limited processing and storage in each node.

The sensor nodes in WSNs are mainly battery-operated, thus, one of the most important constraints on sensor nodes is the low power consumption requirement. Indeed, it is widely recognized that energy is a strictly limited resource in wireless sensor networks, and that the consequences of this limitation must be considered [6].

Recharging or replacing batteries in a wireless sensor network is usually impossible due to the placement of the sensor nodes, and in most situations is practically and (or) economically infeasible. Therefore, the lifetime of a sensor network is defined by the time interval between which a certain amount of critical nodes run out of their battery power [7].

Because of the energy constrained operation of the sensor nodes, different activities in the network should be compromised in order to prolong the lifetime of WSN.

These compromises are needed on the node level as well as on the network level. Therefore, while traditional networks aim at achieving high quality of service (QoS) provisions, sensor network protocols in contrast must focus primarily on power conservation at the cost of lower throughput or higher transmission delay [2].

1.2 Design challenges in wireless sensor networks

Wireless sensor networks possess a distinguishing capability to carry out tasks in an unattended manner, i.e., without human intervention, and with limited energy resources [7]. Since replacing or recharging batteries in sensor networks are impractical in most cases, it is very likely that the lifetime of a sensor network expires as soon as the critical nodes run out of battery power. Moreover, since the nodes communicate with each other and with the sink(s) through a wireless medium, bandwidth scarcity could be a concern in WSNs as well. Therefore, and from nodes communication point of view, such energy and bandwidth constraints, along with the dense deployment of many nodes, poses challenges in the design, management, operation and maintenance of sensor networks.

However, there are also some other important factors that influence the design of protocols and algorithms for wireless sensor networks, some of which include fault tolerance, scalability, production costs, operating environment, sensor network topology, hardware constraints, transmission media, and power consumption [2].

1.2.1 Scalability

Due to the fact that the topology and node density of wireless sensor networks undergo dynamic changes, for example as a consequence of failures in individual nodes, WSNs should be scalable, implying that, they should be able to dynamically adapt to such changes. In particular, connectivity and coverage should be always ensured. *Connectivity* is achieved if the sink can be reached from any node, and

there is no isolated node in the network. *Coverage* is defined as how well a particular area can be observed by a network [8]. As stated in [9],

Multi-hop communication techniques can extend the coverage of the network well beyond the range of the radio technology alone.

The number of sensor nodes deployed in studying a phenomenon may be in the order of hundreds or thousands, depending on the application. Any algorithm and network protocol must be able to work with this number of nodes. They must also utilize the high density nature of the sensor networks [2].

1.2.2 Lifetime

Lifetime is perhaps the most critical concern in the design of any wireless sensor network, since the goal of most WSNs application is to have nodes deployed in the sensing field, unattended, for months or years [9]. The lifetime of a sensor network is defined as the time from the inception of the operation of the network, till a fraction of nodes drain out of their power, which results in either a *routing hole* within the network or a disconnected network, or a network with insufficient coverage [7, 10].

Basically, the lifetime of a sensor network is limited by the nodes' power consumption. In order to achieve the maximum network lifetime it is required that each node manages its local power supply. In many deployments, it is not the average node lifetime that is important, but rather the minimum node lifetime.

1.2.3 Fault tolerance

Fault tolerance is the ability to maintain the network functionality without any interruption due to sensor node or link failures. In other words, the fault tolerance in sensor networks attempts to ensure that failure of some nodes or link does not influence the overall task of the sensor network [2, 7]. In general, sensor nodes are prone to failure due to several reasons, e.g. lack of battery power, physical damages

due to unattended operation, and harsh environmental conditions.

In sensor networks, the sensed data are transmitted to the base station, possibly using multi-hop paths. In a flat architecture, sensor nodes themselves are responsible for routing the data. Therefore, fault-tolerant schemes in this architecture need to take into consideration all the sensor nodes within the network in the same way. But in hierarchical architectures, sensor nodes and cluster heads are treated differently. Each sensor nodes belongs to only one cluster and sends data only to its own cluster head in this architecture. Therefore, fault tolerance for sensor nodes attempts to ensure that in case a cluster heads fails, the underlying sensor nodes are still able to communicate with some other cluster head, so that the data generated by these nodes is not lost [7].

1.2.4 Localization

In WSNs, sensor nodes that are deployed into the environment in an ad hoc manner do not have prior knowledge of their location. The problem of determining the nodes location (position) is referred to as localization [5]. Existing localization methods include global positioning system (GPS), beacon (or anchor) nodes, and proximity-based localization. Equipping the sensor nodes with a GPS receiver is a simple solution to the problem. However, such a GPS-based system may impose further power requirements, and may not work when the sensors are deployed in an environment with obstructions.

1.2.5 Synchronization

From communications point of view, time synchronization in a WSN is critical for network routing, and therefore, for power conservation. The reason is that the timing inaccuracy can significantly reduce the network lifetime, since in many applications, the nodes should transmit data cooperatively and in a scheduled manner. In fact, energy is conserved when there are less collisions and retransmissions [5].

With respect to energy, many WSNs rely on sleep/wake protocols that allow a network to selectively switch off sensor nodes or let them enter low-power sleep modes. Here, temporal coordination among sensors is essential for nodes to know when they can enter a sleep mode and when to re-awake in order to ensure that neighboring nodes overlap in their wake periods to enable communication among them [17]. Furthermore, energy efficiency could be also achieved when the nodes operate in a duty-cycled manner. In duty-cycled operation paradigm, the sensor node would periodically turn its radio off to save energy and on to participate in network communication [5].

1.2.6 Data compression and aggregation

Data compression and aggregation reduce communication cost and increase reliability of data transfer. They are necessary for those WSN applications where there exists abundant data gathered by the network nodes that must be transferred to the sink across the network [5]. Upon Data-compression, the size of the data is compressed before transmission.

Since sensor nodes may generate significant redundant data, similar packets from multiple nodes can be aggregated so that the number of transmissions is reduced. Data aggregation technique has been used to achieve energy efficiency and data transfer optimization in a number of routing protocols [11].

For data aggregation, which in particular is the case in cluster-based WSNs, data is collected from multiple sensors and combined together to be transmitted to the sink. In this case, aggregated data is more important than individual readings.

1.2.7 Security

Because of its wireless transmission medium, a WSN may suffer from threats, in that an attacker can alter the integrity of data, eavesdrop messages, inject fake messages, and even waste network resource by compromising a sensor node. Hence,

wireless sensor networks must be capable of securing the gathered information, i.e., keeping them private from security attacking scenarios [5, 9]. However, the constraints on storage, communication, computation, and processing capabilities in WSNs, pose further challenges and limitations in incorporating security into a such networks.

1.2.8 Production costs

Since the sensor nodes are deployed in large numbers, from hundreds to thousands, and usually are not reusable, the cost of a single node is very important to justify the overall cost of the networks [2]. If the cost of the network is more expensive than deploying traditional sensors, then the sensor network is not cost-justified. As a result, the cost of each sensor node has to be kept low.

1.2.9 Hardware constraints

A sensor node consists of four basic components as shown in Fig. 1.2, a sensing unit, a processing unit, a wireless transceiver unit, and a power unit. They may also have application dependent additional components such as a location finding system [2]. Sensing units are usually composed of two subunits: sensors and analog to digital converters. The processing unit, which is generally associated with a small memory, manages the procedures that make the sensor node collaborate with the other nodes to carry out the assigned sensing tasks. A transceiver unit connects the node to the network. One of the most important components of a sensor node is the power unit. Power units may be supported by a power replenishing unit such as solar cells. Apart from the limitations on the node size, there are also some other stringent constraints for sensor nodes. These nodes must [2, 12]

- consume extremely low power,
- operate in high volumetric densities,

- have low production cost,
- be autonomous and operate unattended,
- be adaptive to the environment.

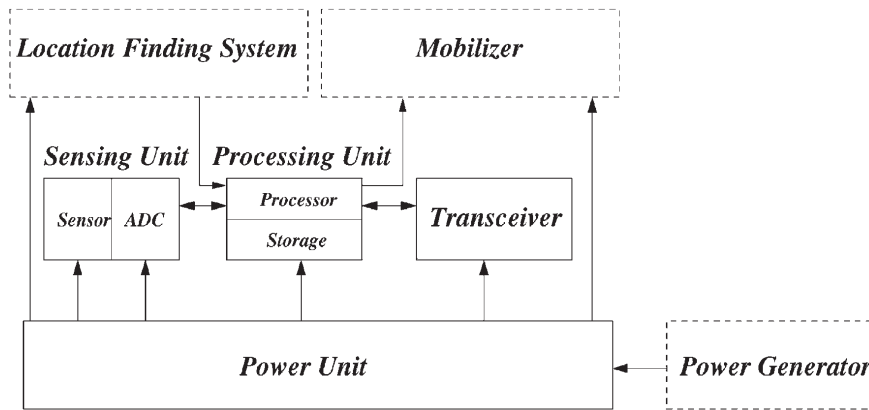


Figure 1.2: Components of a sensor node (redrawn from [2])

Since the sensor nodes are often inaccessible, the lifetime of a sensor network depends on the lifetime of the power resources of the nodes. Power is also a scarce resource due to the size limitations.

The transceiver unit of sensor nodes may be a passive or active optical or a radio frequency (RF) device. RF communications require modulation, bandpass filtering, demodulation and multiplexing circuitry, which make them more complex and expensive. Also, the path loss of the transmitted signal between two sensor nodes may be as high as the fourth order exponent of the distance between them, because the antennas of the sensor nodes are close to the ground [2, 13]. Nevertheless, RF communication is preferred in most cases, because the packets conveyed in sensor networks are small, data rates are low, and the frequency reuse is high due to short communication distances. These characteristics also make it possible to use low duty cycle radio electronics for sensor networks. However, designing energy efficient and low duty cycle radio circuits is still technically challenging, and current commercial radio technologies such as those used in Bluetooth is not efficient

enough for sensor networks because turning them on and off consumes much energy [2, 14].

Most of the sensing tasks require the knowledge of position. Since sensor nodes are generally deployed randomly and run unattended, they need to incorporate with a location finding system. Location finding systems are also required by many of the proposed sensor network routing protocols. It is often assumed that each sensor node will have a global positioning system (GPS) unit.

1.2.10 Transmission media

In a multi-hop sensor network, communicating nodes are linked by a wireless medium. These links can be formed by radio, infrared or optical media, however, radio communications is the dominant technique [2]. To enable global operation of these networks, the chosen transmission medium must be available worldwide. One option for radio links is the use of industrial, scientific and medical (ISM) bands, which offer license-free communication in most countries. The main advantages of using the ISM bands are the free radio, huge spectrum allocation and global availability. They are not bound to a particular standard, thereby giving more freedom for the implementation of power saving strategies in sensor networks. On the other hand, there are various rules and constraints, like power limitations and harmful interference from existing applications. These frequency bands are also referred to as unregulated frequencies. Much of the current hardware for sensor nodes is based upon RF circuit design.

Another possible mode of inter-node communication in sensor networks is by infrared. Infrared communication is license-free and robust to interference from electrical devices. Infrared based transceivers are cheaper and easier to build. This makes infrared a reluctant choice for transmission medium in the sensor network scenario.

1.2.11 Power consumption

The wireless sensor node, which is mainly a micro-electronic device, can only be equipped with a limited power source. In some application scenarios, replenishment of power resources might be impossible. Sensor node lifetime, therefore, shows a strong dependence on battery lifetime [2]. In a multi-hop ad hoc sensor network, each node serves as both the data originator and the data router. Therefore, the operation failure of just few nodes in the network, may prompt WSN to reroute the data packets, or reorganize the network. Hence, power conservation and power management take on additional importance.

Although power consumption is an important design consideration in other mobile and ad hoc networks, but it is not the primary concern, because power resources can be replaced by the user. In fact, in such networks, the emphasis is more on QoS provisioning than the power efficiency. However, this is not the case in wireless sensor networks, since power efficiency has a direct impact on the network lifetime, and hence on the performance. Thus, in design of network protocols, appropriate trade-off should be made between power efficiency and other performance metrics such as network delay and throughput.

The main task of a sensor node in a sensor field is to detect events, perform quick local data processing, and then transmit the data. Power consumption can hence be divided into three domains: sensing, communication, and data processing [2].

In the following subsections, we discuss the power consumption in data communication and processing units in more detail.

1.2.11.1 Communication

Data communication, i.e., both data transmission and reception, consumes the largest portion of the sensor node's energy. It can be shown that for short-range communication with low radiation power (~ 0 dBm), transmission and reception energy costs are nearly the same. Mixers, frequency synthesizers, voltage control oscilla-

tors, phase locked loops (PLL) and power amplifiers, all consume valuable power in the transceiver circuitry [2]. With this regard, in addition to the power consumption during the period where the transceiver is in active mode, i.e., when it is transmitting or receiving, one should also consider the startup power consumption in the transceiver circuitry. Indeed, the startup time, which may be in the order of hundreds of micro-seconds, makes the startup power non negligible [2]. For example, this startup time is imposed to the system by the PLL to lock. Moreover, as the transmission packet size is reduced, the startup power consumption even starts to dominate the active power consumption. Consequently, it is inefficient in turning the transceiver on and off, because a large amount of power is spent in turning the transceiver back ON each time. In [14], the radio power consumption (P_c) is formulated as

$$P_c = N_T(P_T(T_{\text{on}} + T_{\text{st}}) + P_{\text{out}}T_{\text{on}}) + N_R(P_R(R_{\text{on}} + R_{\text{st}}))$$

where $P_{T/R}$ is the power consumed by the transmitter/receiver; P_{out} , the output power of the transmitter; T/R_{on} , the transmitter/receiver ON time; T/R_{st} , the transmitter/receiver startup time and N/T_R , the number of times transmitter/receiver is switched ON per unit time, which depends on the task and medium access control (MAC) scheme used. T_{on} can further be rewritten as L/R , where L is the packet size and R , the data rate. [15] offers a small-sized, low-cost, ultra low power transceiver circuitry based on the direct-conversion architecture.

1.2.11.2 Data processing

Data processing requires much less power compared to data communication. The two most computationally intensive operations for a wireless sensor node are the in-network data processing and the management of the low-level wireless communication protocols [2]. There are strict real-time requirements associated with both communication and sensing [9]. The CPU is responsible for simultaneously con-

trolling the radio and record/decode the data as they arrive over the network. As the communication rates increase, faster computation and processing are required to be performed on sensor data. Common sensor processing operations include digital filtering, averaging, threshold detection, correlation and spectral analysis. It may even be necessary to perform a real-time FFT on incoming data in order to detect a high-level event [2]. Furthermore, some additional circuitry may be required by data encoding and decoding.

1.3 Wireless sensor networks communication architecture

The development of a reliable and energy-efficient protocol stack is important for supporting various WSN applications [5]. Each sensor node uses the protocol stack to communicate with one another and to the sink. Hence, the protocol stack must be energy efficient in terms of communication and be able to work efficiently across multiple sensor nodes.

The sensor nodes in WSN, collect data and route them back to the sink, via a multi-hop infrastructureless architecture [2]. The sink may also communicate with the task manager node via Internet or Satellite.

The protocol stack is shown in Fig. 1.3. It aims at integrating power and routing awareness to accommodate data with networking protocols, to communicate power efficiently via the wireless medium, and to employ the sensor nodes cooperatively. It consists of some *layers* such as application, transport, network, data link, physical layers, and also *planes* such as power management, mobility management, and task management planes [2]. In order to support various applications, it is of primary importance for a WSN to have a reliable and energy-efficient protocol stack.

The way through which a sensor node uses its power is managed by the power management plane. For example, in order to avoid receiving duplicate messages,

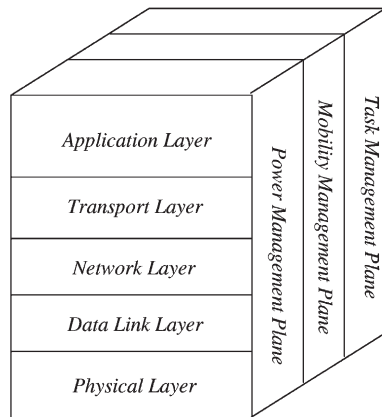


Figure 1.3: Protocol stack in a typical wireless sensor network (redrawn from [2]).

the sensor node may turn off its receiver after receiving a message from one of its neighbors. Also, when the power level of the sensor node is low, the sensor node broadcasts to its neighbors that it is low in power and cannot participate in routing messages. The remaining power is reserved for sensing.

The mobility management plane is responsible for detecting and keeping the record of the movement of sensor nodes, providing permanently a route back to the user, and assisting the sensor nodes in keeping track of who are their neighbor sensor nodes. This makes the sensor nodes capable of balancing their power and task usage.

The task management plane balances and schedules the sensing tasks given to a specific region, since depending to their power levels, not all sensor nodes in that region are required to perform the sensing task at the same time [2].

These management planes are necessary, since they enable nodes collaboration, leading to more power-efficient network operation, and hence prolonged network lifetime.

Fig. 1.4 illustrates the details of a WSN protocol stack, with emphasis on the interconnections among units.

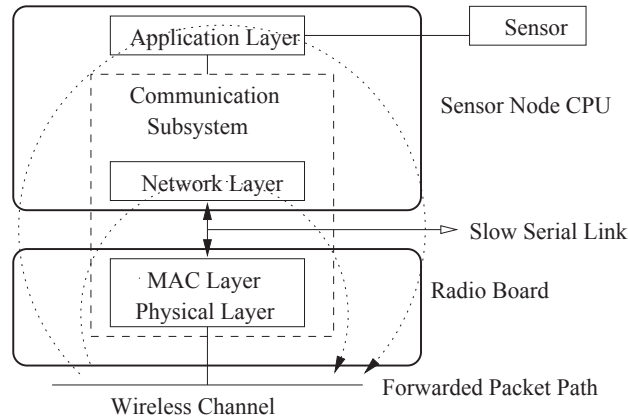


Figure 1.4: Detailed protocol stack in wireless sensor networks (redrawn from [4]).

1.3.1 Transport layer

The reliability and integrity of data at the sources and sink are guaranteed by the transport layer. Transport layer protocols in WSNs should support multiple applications, variable reliability, packet-loss recovery, congestion control mechanisms [5]. This layer is especially needed when the system is planned to be accessed through Internet or other external networks [2]. Any packet loss which may occur due to node failures, weak wireless links, congestion and packet collision, and memory overflow, can result in power wastage and degraded quality of service (QoS) in data delivery.

1.3.2 Network layer

The network layer manages source-to-destination data routing in the network. Routing protocols in WSNs are different from conventional routing protocols in some aspects. Sensor nodes do not have Internet protocol (IP) addresses, thus IP-based routing protocols are not applicable in WSNs. Furthermore, the design of network protocols in a WSN should be scalable. It should handle communication among many nodes, through which the sensor data is delivered to the base station. The protocol should cope with network resource constraints such as limited energy, communication bandwidth, memory, and computation capabilities, and should address

issues of efficiency, fault tolerance, fairness, and security [5] .

In summary, compared to other wireless networks such as mobile ad hoc or cellular networks, there are a number of characteristics of sensor networks that make the routing in them a challenging task including [7]

- The inability to apply classical IP-based protocols in sensor networks
- The flow of data from multiple sensor nodes to a single sink node
- Highly probable data redundancy due to sensing a common phenomena by large number of nodes
- Application-dependent design requirements
- Position awareness of sensor nodes is important since data collection is usually location based.
- The resource constraint of sensor nodes, such as limited power, limited processing and memory capability

1.3.3 Data link layer

The data-link layer is responsible for the data transfer between two nodes that share the same link, it ensures reliable point-to-point and point-to-multi-point connections within the network. In sensor networks, since the underlying network is wireless, and the wireless medium must be shared by multiple sensor nodes, therefore a mechanism is required to manage the access to the medium. In the design of medium access control (MAC) protocols for WSNs the following issues should be considered; energy efficiency, scalability to node density, frame synchronization, fairness in nodes power consumption, bandwidth utilization, flow control, and error control for data communication [5]. Error detection and correction services are offered at the data-link layer as well as the transport layer.

The MAC protocol in a wireless multi-hop self-organizing sensor network must achieve two goals [2]. The first is to establish the network infrastructure; since thousands of sensor nodes are densely scattered in a sensor field, the MAC scheme

must provide communication links for data transfer. The second objective is to fairly and efficiently share communication resources, i.e., power and bandwidth, between sensor nodes.

Providing high quality of service (QoS) and bandwidth efficiency is the primary goal of the MAC protocols in the conventional cellular and ad hoc networks, while power consumption management to be of secondary importance. This is in contrast, however, with the wireless sensor networks, where the primary concern is to minimize the energy consumption to extend the network lifetime. Indeed, for wireless sensor networks, MAC protocols are needed to effectively cope with the resource constraints and application requirements of sensor networks. Thus, the MAC protocols in WSNs should prevent energy wastage due to packet collisions, overhearing, excessive retransmissions, control overheads, and idle listening. It should also adapt to topology and network changes efficiently [5].

1.3.3.1 Power saving modes of operation

The medium access control (MAC) protocols must also provide the sensor nodes with the ability to operate in power saving modes, irrespective of the type of the protocol [2]. In general, MAC protocols must have full control over the wireless radio. Therefore, their design must comply thoroughly with the energy requirements of a sensor node. A common technique to preserve energy is dynamic power management (DPM), where a resource are switched between different operational modes such as *active*, *idle*, and *asleep* [17]. Without power management, most transceivers switch between *transmit*, *receive*, and *idle* modes, although the receive and idle modes are typically similar in their power consumption. However, dramatic energy savings can be obtained by putting the device into the low-power sleep mode.

Periodic traffic models are very common for sensor networks (e.g., environmental monitoring) and many networks can benefit from MAC schemes that do not require nodes to be active at all times. Instead they allow nodes to obtain periodic

access to the medium for transmission of data and to put their radios into low-power sleep modes between periodic transmissions. The fraction of time a sensor node spends in active mode is called the duty cycle, which is often very small due to the infrequent and brief data transmissions occurring in most sensor networks [17].

Significant power conservation is achievable by turning the transceiver off when it is not required. However, since the size of the communication packets in WSNs are short in general, the startup energy cannot be neglected. In fact, blind turning off the radio during each idling slot leads to more energy consumption compared to leaving the radio turned on over a period of time [2]. As a result, operation in a power saving mode is energy efficient only if the time spent in that mode is greater than a certain threshold.

1.3.3.2 Error control

The data link layer is also responsible for providing the transmission data with the error control mechanisms. Two important modes of error control in communication networks are the forward error correction (FEC) and automatic repeat request (ARQ). The application of either ARQ or FEC in wireless sensor networks have advantages and drawbacks. The main disadvantage of ARQ in WSNs applications is that it requires additional retransmissions cost and overhead [2]. FEC, on the other hand, imposes greater decoding complexity on the system. Thus, due to inherent constraints in WSNs, the error detection and correction mechanisms should be simple and meet the low complexity encoding and decoding requirements.

For reliable data communication, one should either increase the output transmit power P_{out} or apply suitable FEC. Increasing the transmit power is not an appropriate choice due to constraints on the power resources in WSNs. Thus, only FEC remains as a solution. Although, FEC yields significant reduction in the BER for any given value of P_{out} , however, extra processing power is imposed on the system for encoding and decoding, which might be in turn critical for sensor networks. As a result,

FEC is a feasible solution for the purpose of error detection and correction in WSNs whenever the sum of the encoding and decoding processing powers is less than the transmission power savings [2].

1.3.4 Physical layer

The physical layer performs frequency selection, carrier frequency generation, signal detection, modulation and data encryption. The challenge in the design of physical layer for wireless sensor networks is to minimize the power consumption, while combating the performance-degrading phenomena like signal scattering, shadowing, reflection, diffraction, multi-path and fading, that are common to all applications involving wireless medium. In general, the minimum output power required to transmit a signal over a distance d is proportional to d^a , with a to be the path loss exponent, and $2 \leq a < 4$. This exponent is closer to four for low-lying antennae and near-ground channels, as is typical in sensor network communication, and accounts for the partial signal cancellation by a ground-reflected ray [2].

Multi-hop communication can be applied in a wireless sensor network to effectively overcome shadowing and path-loss effects, if the node density is high enough. The choice of a good modulation scheme is critical for reliable communication in a sensor network [2]. In WSNs, minimizing energy consumption to maximize the network lifetime starts at the physical layer. For example, energy-efficient modulation schemes might be applied to minimize both transmission and circuit energy [5]. In [16], the physical layer requirements with a focus on digital communication and existing hardware technology is discussed. Small size of the sensor nodes besides their dense deployment in WSNs dictates the radio equipments to be cheap and small in size as well. With respect to energy, the radio must be low power. In fact, trade-offs must be made between the radio energy consumption, and other design factors such as data rate, error tolerance, transmission distance, and reliability.

Interference, synchronization, and multi-casting are other requirements that must

be considered at the physical layer as well [5]. Signal interference arises basically due to the dense deployment of sensor nodes in the environment. However, through proper synchronization between the link and physical layers and among sensor nodes, the sensor nodes can reduce their transmission power in order to alleviate the impact of interference.

1.3.4.1 Modulation schemes

Reducing the radio energy consumption in WSNs requires energy-efficient modulation schemes. Although M -ary schemes can reduce the transmit time by sending multiple bits per symbol, they need more complex circuitry, and hence increase the radio power consumption. Under startup power dominant conditions, the binary modulation scheme is more energy efficient [2, 14]. Hence, M -ary modulation are useful only for low startup power systems.

1.3.4.2 Radio architecture

Energy consumption at the physical layer accounts for both the circuit energy, and the transmission energy. A transmitter at its startup, consumes a excessive amount of time and energy. Even in some cases, the startup energy can be higher than the energy required for an actual transmission [5]. For a transmitter that switches between the sleep to active state, a fast startup transmitter architecture is needed to minimize both energy and time.

1.3.4.3 Bandwidth requirements

In WSNs, there are three classes of physical-layer technologies based on bandwidth; narrowband, spread spectrum, and ultra-wideband [5]. The resulted radio bandwidth in narrowband is on the order of symbol rate. Spread spectrum, however, spreads the narrow signal into a wideband signal. It has the ability to reduce power and still communicate effectively, and is more robust to interference and multi-path

channel impairment. Ultra-wideband employs even larger bandwidth, on the order of gigahertz. In ultra-wideband the interference to other radios is negligible. Like spread spectrum, ultra-wideband belongs to the low power communication schemes. Ultra-wideband employs baseband transmission, and thus, it requires no intermediate or radio carrier frequencies [2]. The main advantages of ultra-wideband are its robustness to multi-path, low transmission power and simple transceiver circuitry, which make makes it an attractive candidate for wireless sensor networks.

1.4 Cooperative communication and relaying in WSNs

The transmitter circuitry consumes the major portion of the power in a sensor node. In general, the required transmit power is itself under the influence of transmission data rate, and source-destination distance. The neighboring nodes in a WSN might be located in the nearly close vicinity of each other thanks to the dense deployment of the sensor nodes. This implies however that, multi-hop communication scenarios can be applied efficiently to mitigate the transmit power required to send bits of information from the source to the destination compared to other conventional single-hop communication. The transmitted signal in long-distance wireless communications suffers also from signal propagation effects that can be alleviated via multi-hop communication, as another advantage. Accordingly, among the schemes proposed for minimizing the power consumption in sensor networks, one is to introduce some special nodes, known as relays. In fact, some burden from the sensor nodes are taken by the relay nodes [7].

However, although multi-hop communication may have some benefits in reducing the overall energy consumption, some nodes, that are located near the base station, can be overloaded and deplete their energy prematurely and die, as compared to some other nodes in the network. In such situation, some regions may not be covered effectively or the connectivity of the network is damaged, although there are a large number of network nodes that still have much unused energy [7, 18, 19]. This

problem is known as *energy hole problem* in the literature, and causes functionality challenges for the networks, even making it inoperable. Various methods have been proposed to avoid the energy-hole problem, one of which is to reduce the burden on the overloaded nodes by deploying some as *relay-only* nodes, within the network so that they can share some of the load with the overloaded nodes [7].

Chapter 2

Communication Strategies for Wireless Sensor Networks

In this chapter, we present cooperative traffic relaying strategies for half-duplex sensor networks with linear topologies, where sensors need to deliver the same amount of data to a sink node by sharing the same radio resources. Under such constraints, we devise two schemes and derive the expressions for the rate and the energy consumption they achieve. We then compare the two proposed strategies with the multiple access and the multi-hop relaying strategies, highlighting which scheme is to be preferred as the system parameters vary.

2.1 Introduction

Wireless sensor networks are often used for monitoring applications in environments such as highways and urban roads, or for surveillance of corridors and borders. In these cases, the sensor network exhibits a linear topology and sensors need to deliver their measurements to a sink node, located at one end of the topology. In this chapter, we address such a network system and focus on the case of practical relevance where: (i) nodes are equipped with half-duplex radios (i.e., they cannot transmit and receive at the same time), (ii) they are energy constrained, (iii) they

share the same radio resources and generate data that need to be delivered to the sink at the same rate. Also, sensors can relay traffic towards the sink for other nodes and, when they do so, they adopt the decode-and-forward (DF) paradigm.

Under the above conditions, we devise two traffic relaying strategies that aim at achieving high data rate and low energy consumption. For each strategy, we derive an expression for the achievable rate and energy consumption, and compare the performance with that of a traditional multi-hop strategy and of the multiple access scheme.

Due to the inherent constraints on the available energy resources in wireless sensor networks (WSN), energy-efficient communication techniques are required to minimize the energy consumption while satisfying the data rate. In wireless sensor networks, contrary to the case of long-range communications, the circuit energy consumption is comparable to or even surpasses the transmission energy. In order to achieve a reasonable tradeoff between the energy consumption and the data rate, it is advisable to apply techniques that exploit nodes cooperation. In such cooperation techniques, it is typically considered that there are some information sources, and one or more information destinations where the source nodes also serve as potential relays intending to assist the information flow from sources to destinations. The problem of multi-source, multi-relay, and multi-destination and their potential application in WSN have been addressed in detail in [31]. Their approach has been so far based on the theoretical capacity aspects without considering energy consumption issues. There have been several articles proposing methods based on the concept of cooperative communications and relaying schemes (see e.g. [32–34]). In [32], they have proposed an energy-efficient cooperative communication scheme based on power control and relay selection in a distributed manner. The idea is that a set of potential relays determine their transmit power needed to participate in cooperation, and then the best relay is chosen to minimize the overall energy consumption. The energy efficiency of MIMO and cooperative MIMO communications in WSN has

been addressed in [33], where they have claimed that when both the transmission energy and the circuit energy consumption are considered, MIMO-based techniques are not necessarily superior than those SISO-based ones. They have shown that in short-range applications where the data rate and the modulation scheme are fixed, SISO may outperform MIMO as far as the energy efficiency is concerned. The idea of optimizing the transmission schemes to maximize the network lifetime by modeling the energy consumption in the transmitter circuit along with that for data transmission, and the bottom three layers of the network protocol stack has been proposed in [34]. They have suggested that the energy efficiency must be supported across the link layer, the medium access control layer, and the routing layer through a cross-layer design, and have introduced energy-efficient joint routing, scheduling, and link adaptation strategies maximizing the network lifetime.

2.2 Network model and definitions

The network consists of n sensors (or *nodes* hereafter) and one destination. The nodes (including destination) are equally spaced along a line, and the distance between every two nodes is denoted by d (Fig. 6.1). The noise is AWGN with zero mean and variance N_0 , and the signal to noise ratio corresponding to the *unit distance* is denoted by γ , defined as

$$\gamma = \frac{P_{\text{tx}} G_t G_r}{N_0 W} \left(\frac{\lambda}{4\pi} \right)^2 \quad (2.1)$$

with P_{tx} , G_t , and G_r to be, respectively, the sensor node's transmit power, and the transmit and receive gains of the sensor node's antenna. Also, λ and W denote the carrier wavelength, and the communication bandwidth shared among nodes. There is no fading present, and the policy for the communications through the relay channel is half-duplex Decode-and-Forward [35]. By half-duplex we mean that no node transmits and receives simultaneously.

Moreover, we denote by P_t and P_r , the amounts of *consumed* powers at each node during transmit and receive respectively. In calculating the total amount of power consumed in each scheme, we consider only the consumed power in the nodes and not in the destination. The data rate for node i is denoted by R_i , and we always constrain R_i to be equal to R . Time is divided into equal *slots*, and a *hop* is defined as a transmit-receive activity between every two nodes which may occur in one or more time slots.



Figure 2.1: Topology of the wireless sensor network.

2.3 Communication Schemes

2.3.1 Proposed Schemes

2.3.1.1 Cooperative Sub-chains (CS)

In this scheme nodes are grouped into sets, called *sub-chains*, each containing $k > 1$ adjacent nodes. We denote by q the number of sub-chains, which is equal to $q = \lceil n/k \rceil$. In general n is not a multiple of k , thus one of the sub-chains may contain less than k nodes. If so, in the following we assume that the sub-chain with fewer nodes is the closest to the destination. Data transmissions are scheduled in two phases as follows.

First phase;

The data generated within each sub-chain are transferred to the first node of the next sub-chain. As an example, consider the generic sub-chain including nodes $\{j, \dots, j+k-1\}$. In the first slot, node j sends its data to node $j+1$. In the next two slots, node $j+1$ sends j 's data as well as its own data to the third node, $j+2$. This procedure is repeated until, after k transmissions and

$k(k + 1)/2$ slots, the data originated by all nodes in the sub-chain reach the first node of the next sub-chain, i.e., node $j + k$.

Second phase;

At the beginning of this phase, the data to be forwarded are located only at nodes $k + 1, \dots, k(q - 1) + 1$, i.e., at the first node of sub-chains $2, \dots, q$. Each of these nodes transfer simultaneously the data to the sink in a hop-by-hop fashion. Thus, the data transfer to the sink is accomplished through $n - k$ transmissions, each requiring k slots.

Fig. 2.2 illustrates the Cooperative Sub-chains scheme for the case where $n = 7$ and $k = 3$ ($q = 3$); in the figure, the transmissions taking place simultaneously are represented by arrows along the same line and their duration is expressed in number of slots.

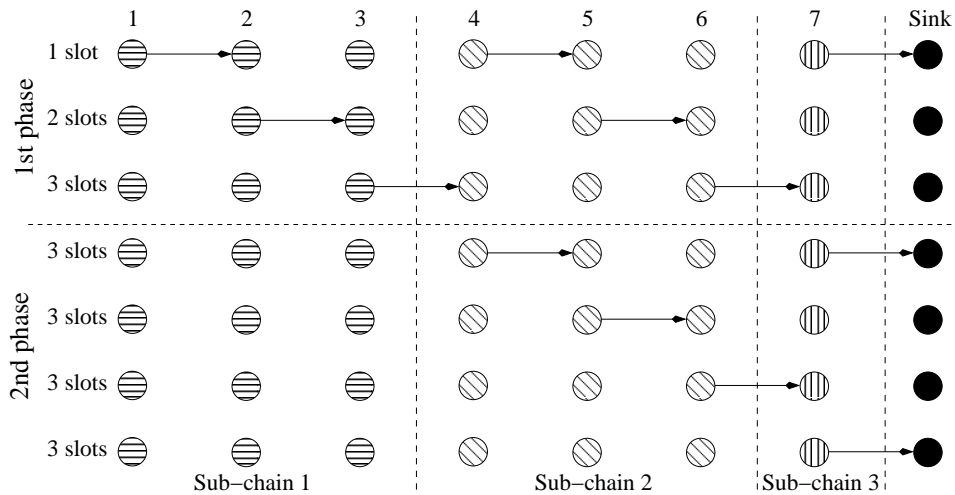


Figure 2.2: Cooperative Sub-chains with $n = 7$, $k = 3$.

According to the Cooperative Sub-chains strategy, only one node per sub-chain transmits in each slot, however there may be several simultaneous transmissions interfering with each other. Thus, for every receiving node located in sub-chain r

($1 \leq r \leq q$), the constraint on the achievable instantaneous rate is:

$$R_r \leq (1/2) \log_2 \left(1 + \frac{\gamma}{d^2 + \sum_{i=1}^{q-r} \frac{\gamma}{(ki-1)^2} + \sum_{i=1}^{r-1} \frac{\gamma}{(ki+1)^2}} \right) \quad (2.2)$$

The two sums at the denominator account for the interference due to the $q - r$ and $r - 1$ transmitters located, respectively, on the right and on the left side of the receiving node. The constraint on the achievable instantaneous rate is then given by

$$R_{CS} \leq \min_r R_r. \quad (2.3)$$

It is clear that the minimum over all R_r 's is represented by the rate associated to the sub-chain in the middle of the linear topology (i.e., $r = \lceil q/2 \rceil$), which indeed experiences the higher interference.

Furthermore, the total number of slots needed to transfer the data originated by all sensors to the sink is given by the sum of slots required by the two phases, i.e.,

$$S_{CS} = k(k+1)/2 + k(n-k). \quad (2.4)$$

The average rate is then given by R_{CS}/S_{CS} .

Finally, the energy consumption experienced by the generic i -th sensor, during the two-phase procedure (i.e., S_{CS} slots), can be easily derived by looking at Fig. 2.2. Indeed, according to the Cooperative Sub-chains strategy, sensor i receives the data generated by all sensors on its left side ($i - 1$ nodes) and retransmits them, along with its own data. Thus, we can write:

$$E_{CS}(i) = (i-1)P_r T + iP_t T, \quad i = 1, \dots, n. \quad (2.5)$$

2.3.1.2 Interlaced Chains (IC)

Again, we consider that the n sensors are grouped into q sub-chains of k adjacent nodes each, with q as defined before. In the Interlace Chains strategy, the data transmission to the sink is organized in k phases. Phase i only involves the i -th nodes of each sub-chain: during the first slot of the phase, the i -th node in the first sub-chain sends its data to the i -th node in the second sub-chain. Then, in the next two consecutive slots, the i -th node in the second sub-chain sends the received data, along its own data, to the i -th node in the next sub-chain, and so on. This transmission scheme is repeated till the data originated at the i -th nodes of the q sub-chains reach the sink. It is then repeated for $i = 1, \dots, k$, until all data generated in the network are delivered to the sink. An example of the Interlace Chains strategy is depicted in Fig. 2.3, for $n = 5$ and $k = 2$ ($q = 3$).

Differently from the Cooperative Sub-chains strategy, nodes do not transmit simultaneously, thus transmissions do not interfere with each other. We observe that the maximum distance covered by a transmission is kd , hence the minimum SNR at the receivers is given by $\gamma/(kd)^2$. It follows that the dominant constraint on the achievable instantaneous rate is

$$R_{\text{IC}} \leq (1/2) \log_2 \left(1 + \frac{\gamma}{(kd)^2} \right). \quad (2.6)$$

Also, note that in general n is not a multiple of k , and the last sub-chain may have only $k_1 \leq k$ nodes. Thus, k_1 phases of this strategy involve q nodes (requiring $q(q+1)/2$ slots each) and $k_2 = k - k_1$ phases involve $(q-1)$ nodes only (requiring $q(q-1)/2$ slots each). We conclude that the number of slots needed to complete the data transfer can be written as

$$S_{\text{IC}} = k_1 q(q+1)/2 + k_2 q(q-1)/2. \quad (2.7)$$

The average rate is given by $R_{\text{IC}}/S_{\text{IC}}$.

By looking at Fig. 2.3, we note that any sensor i ($i = 1, \dots, k$) belonging to sub-chain r receives the data generated by the i -th sensors in the $(r - 1)$ sub-chains on its left side and retransmits them, along with its own. It follows that the amount of energy consumed under the Interlace Chains strategy by sensor i belonging to sub-chain r is given by

$$E_{IC}(i) = (r - 1)P_r T + rP_t T, \quad i \in \text{sub-chain } r, r = 1, \dots, q. \quad (2.8)$$

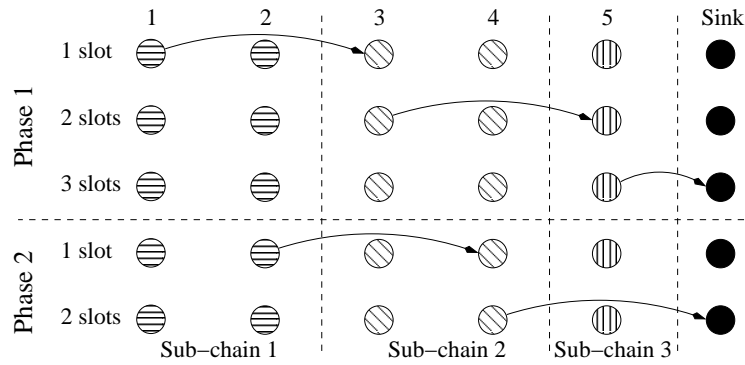


Figure 2.3: Interlaced Chains with $n = 5$, $k = 2$.

2.3.2 Conventional Schemes

2.3.2.1 Multi-hop (MH)

Multi-hop can be regarded as a special case of Cooperative Sub-chains when $k = n$, and of Interlace Chains when $k = 1$. Thus, we derive the number of slots needed to complete the data delivery under Multi-hop by replacing k with n in (2.4), i.e., $S_{MH} = \frac{1}{2}n(n + 1)$, while the constraint on the instantaneous rate becomes: $R_{MH} \leq (1/2) \log_2 (1 + \gamma/d^2)$. The average rate is R_{MH}/S_{MH} , while $E_{MH}(i) = E_{CS}(i)$ for any node i .

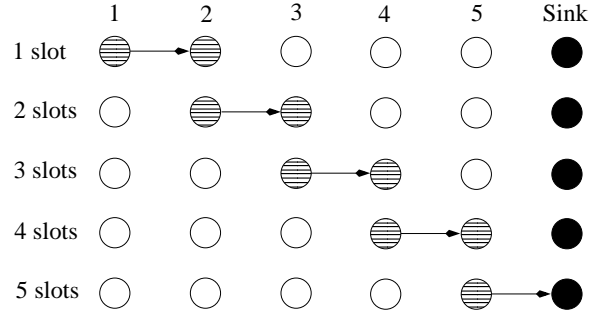


Figure 2.4: Multi-hop with $n = 5$.

2.3.2.2 Multiple Access (MAC)

In this case nodes do not act as relays, but they simultaneously transmit their data directly to the sink within one time slot ($S_{\text{MAC}} = 1$). Thus, using the result in [20] and considering our constraint on the common sensor rate, both the instantaneous and the average rates are given by:

$$R_{\text{MAC}} \leq \min_{i=1, \dots, n} \left(\frac{1}{i} \right) \log_2 \left(1 + \left(\frac{\gamma}{d^2} \right) \sum_{j=1}^i \frac{1}{(n-j+1)^2} \right) \quad (2.9)$$

The energy consumption is $E_{\text{MAC}}(i) = P_t T$ for any node i .

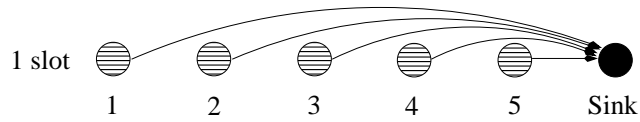


Figure 2.5: Multiple Access with $n = 5$.

2.4 Results

We compare the rate and power consumption performance of our proposed schemes, Cooperative Sub-chains and Interlaced Chains, with two conventional traffic transfer schemes, namely Multiple Access, and Multi-hop. For each scheme we obtain the average achievable rate by dividing the achievable rate R by the total number of slots S , and without loss of generality we assume that each slot duration is equal to one second.

For our two proposed schemes, with $n = 20$, $d = 20$ m, we present the plots of average achievable rate versus the number of nodes in each sub-chain, i.e., k , for $\gamma = 20, 30$ and 40 dB respectively. Fig. 2.6 depicts such plots for Cooperative Sub-chains and Interlace Chains. As implied by the plots, for each scheme there is one optimum amount of k , denoted by k^* , that maximizes the average achievable rate. As an example, for $\gamma = 40$ dB, the optimum k in Cooperative Sub-chains is $k^* = 2$, while in Interlace Chains it is $k^* = 5$.

The plot of average achievable rate versus γ for Multiple Access, Multi-hop, Cooperative Sub-chains, and Interlace Chains is shown in Fig. 2.7 with $n = 20$, and $d = 20$ m. For each scheme, the amounts are obtained for $k = k^*$. As we see in the first plot in Fig. 2.7, for the amounts of γ below 35 dB, Cooperative Sub-chains outperforms the other schemes. The superiority of Cooperative Sub-chains over Interlace Chains and Multi-hop is due to its smaller number of required time slots (refer to the equations (2.4) and (2.7)). However, as the signal power increases, due to the presence of interference in Cooperative Sub-chains, Multiple Access begins to prevail.

We also compare the average energy consumption versus γ in the bottom plot of Fig. 2.7 (again the results are obtained for $k = k^*$). The amounts of P_t and P_r are taken from a typical IEEE802.15.4 compliant wireless sensor with transmit power consumption of $P_t = 60$ mW for 1 mW transmit power, and receive power consumption of 69 mW reported in the device's data sheet. Based on the above

values, we can calculate P_t for any desired value of transmit power P_{tx} by using the following equation

$$P_t = (60 - 1) \text{ mW} + P_{tx} = 59 \text{ mW} + P_{tx} \quad (2.10)$$

As we observe, Multiple Access has the largest power consumption among the schemes. Indeed, the total power consumption for Cooperative Sub-chains, Interlace Chains, and Multi-hop is nearly the same for $\gamma \leq 35$ dB. But as γ increases, the power consumption of Interlace Chains becomes even smaller, and makes Interlace Chains as the candidate for the most power-efficient scheme.

The impact of inter-node distance d on the performance of the schemes is depicted in the following figures; In Figs. 2.8 and 2.9 the achievable rate and the average power consumption per bit are shown versus inter-node distance d for $n = 20$ and $\gamma = 20$, and 40 dB respectively.

2.5 Concluding Remarks

In this chapter, we proposed two new simple schemes, namely Cooperative Sub-chains, and Interlaced Chains, for sensor nodes traffic transfer in an almost linear wireless sensor networks. The results of the simulations prove that with respect to energy consumption and average achievable data rate, these schemes are superior than other common techniques such as Multiple Access and Multi-hop, particularly in lower amounts of signal to noise ratios.

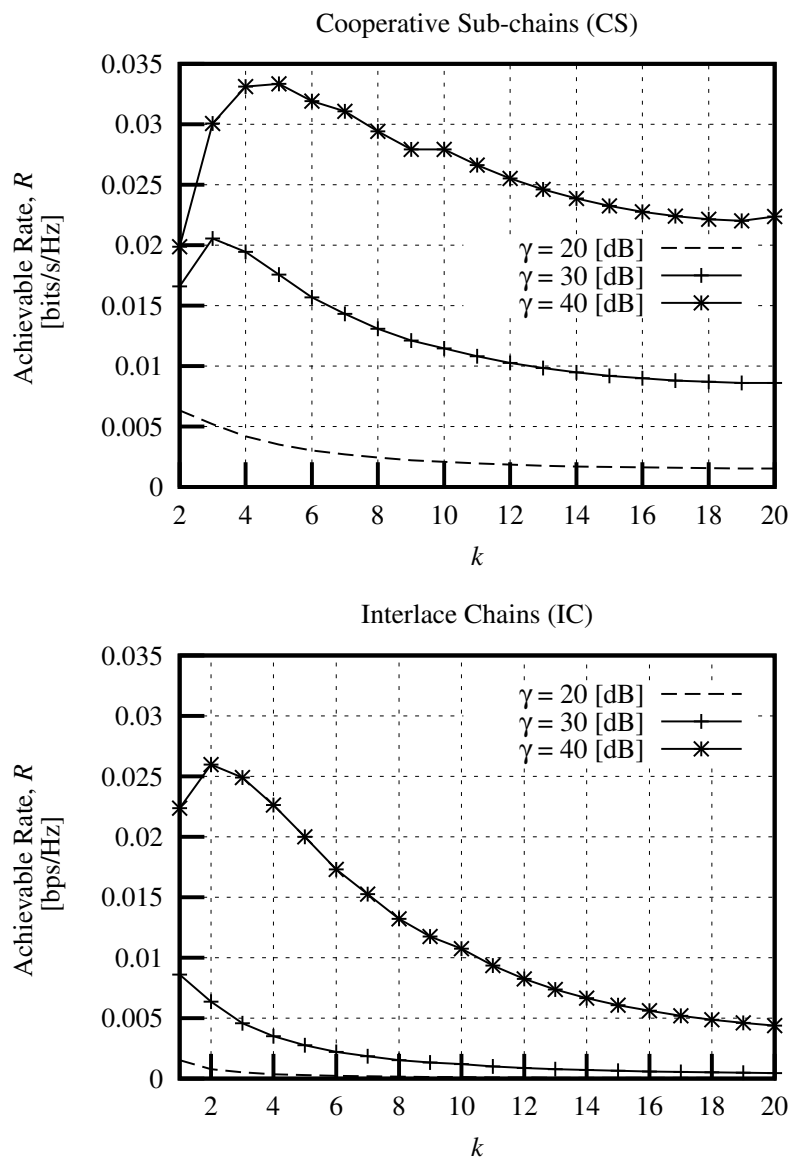


Figure 2.6: Achievable rate R versus k , in Cooperative Sub-chains (top), and Interlace chains (bottom), with $n = 20$ nodes, and $d = 20$ m.

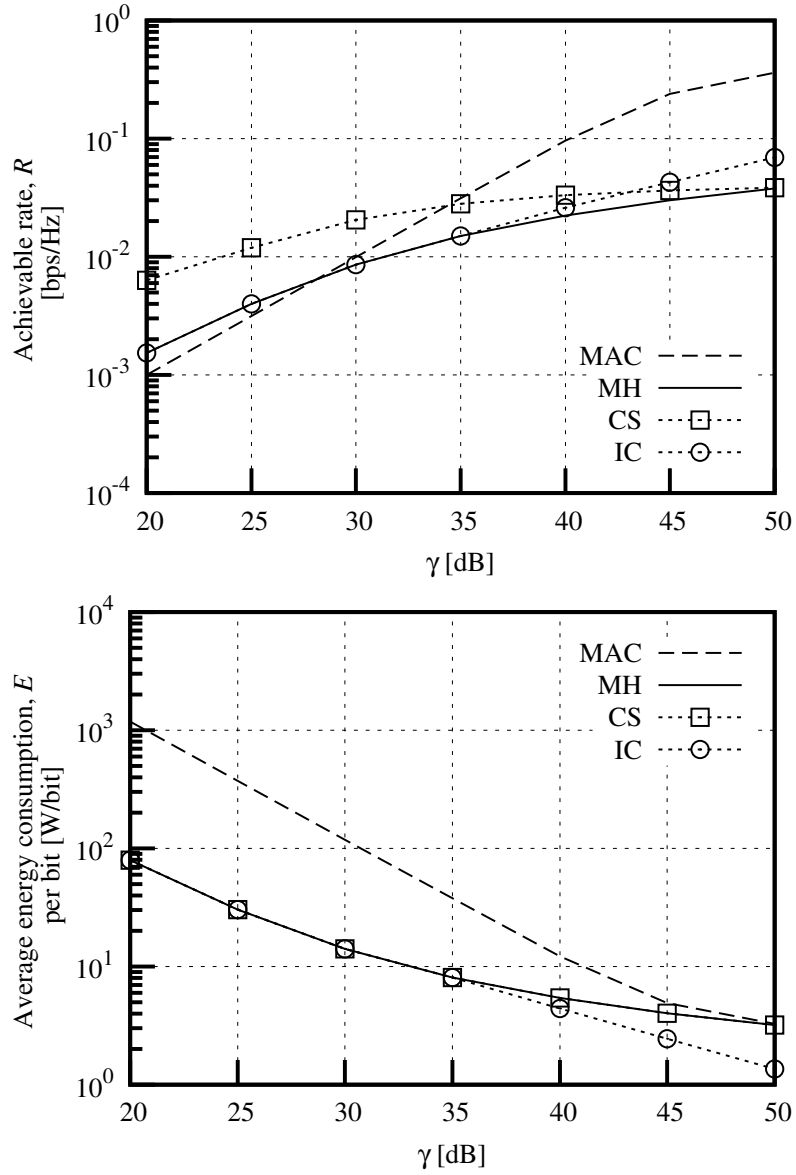


Figure 2.7: Average achievable rate (top), and Average energy consumption per bit (bottom), obtained for $k = k^*$, with $n = 20$ nodes, and $d = 20$ m.

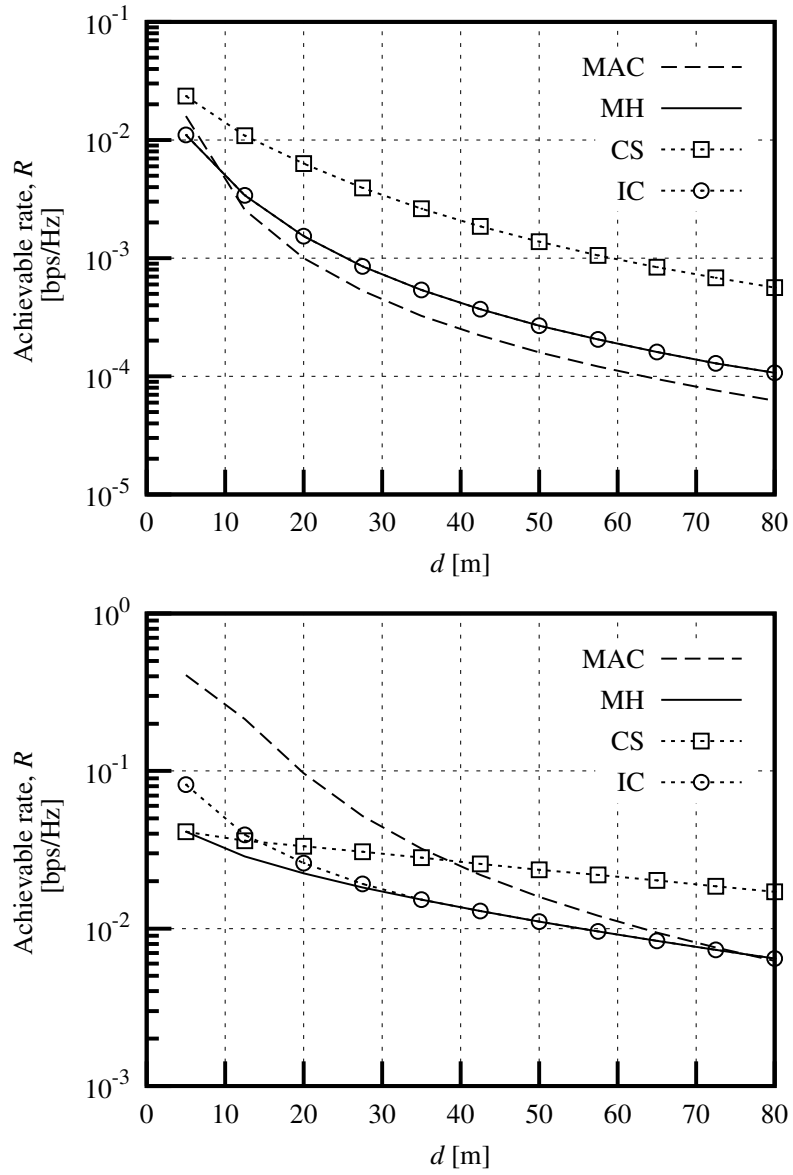


Figure 2.8: Average achievable rate, R , versus d , obtained for $k = k^*$, with $n = 20$ nodes, and $\gamma = 20$ dB (top), and $\gamma = 40$ dB (bottom).

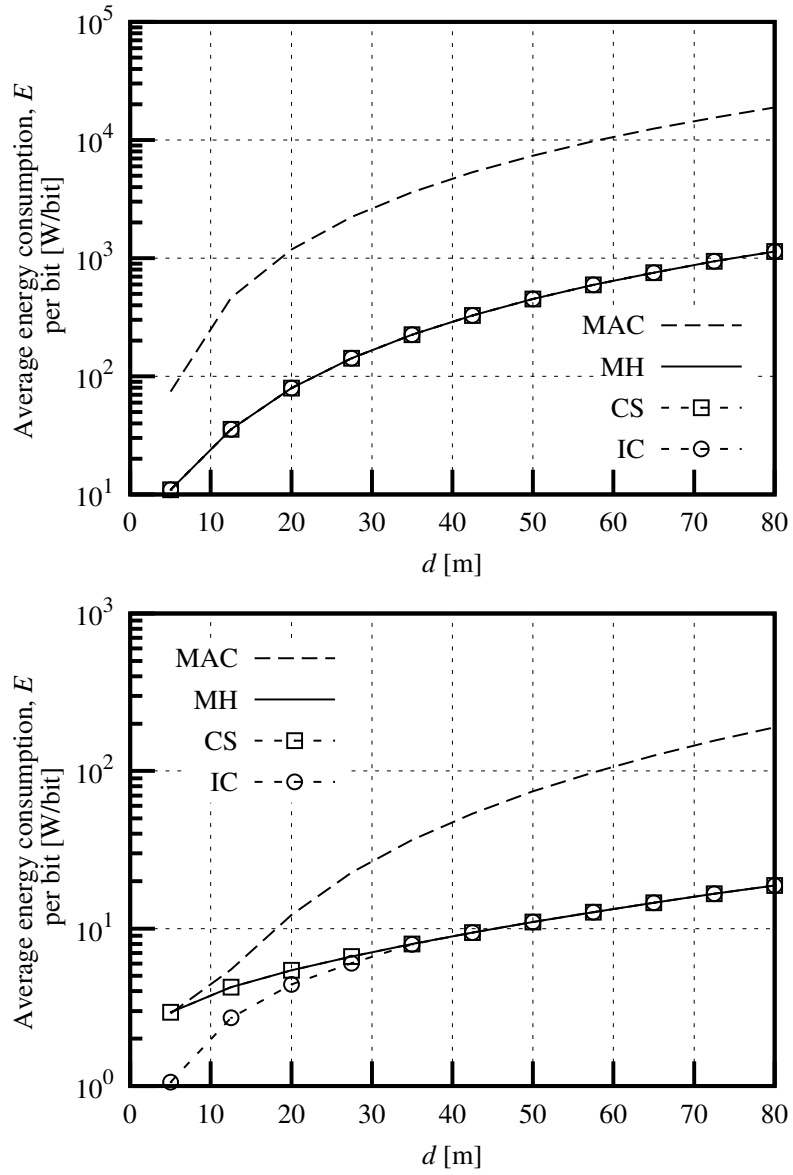


Figure 2.9: Average energy consumption per bit, E , versus d , obtained for $k = k^*$, with $n = 20$, $\gamma = 20$ dB (top), and $\gamma = 40$ dB (bottom)

Chapter 3

Network Information Theory of Linear Wireless Networks

Network information theory addresses basically the problem of reliable communication between multiplicity of source and destination nodes in a given wired or wireless network. Determining the ultimate (achievable) rate of reliable communication in a multi-terminal wireless network faces with many challenges, as the consequence of the coexistence of interference, cooperation, and feedback between the nodes [20, 21]. In fact, given an arbitrary wireless network, the exact *capacity*, i.e., the ultimate possible rate of information transfer is unknown in general, while it is known for only few simple situations. Therefore, one often relies on lower and upper *bounds* to understand the limits of communication efficiency. So far, one of the most useful and versatile bounds is known as *max-flow min-cut theorem* [20, 49], where in the cases in which the capacity of a network is known, it coincides with the achievable rates [21].

In this chapter, we take an information-theoretic approach to address the problem of finding the *cut-set* upper bounds to the average achievable rate of traffic transfer in linear wireless networks. Toward this end, first we construct a system model for such networks by considering the practical constraints, in particular, the half-duplex operation of network's nodes. Next we try to obtain such bounds as

the solutions to the max-flow min-cut bound problem applied to linear wireless networks consisting of few nodes.

As the number of communicating nodes in a network increases, say for example, beyond five, the complexity of finding the *exact* solution to such problem prompts us to rely on *approximate* solutions only, i.e., those bounds obtained to serve as *upper* and *lower bounds* to the cut-set bounds. This will be covered in detail in chapter 5. Thus, in this chapter, we focus only on computing the exact solution to the max-flow min-cut bounds in wireless networks with linear topology and of very few nodes, possessing full or half-duplex radios.

3.1 Introduction

One of the most fundamental questions that arises in the field of information theory of wireless networks is [23]

How much information can be transferred over a wireless network with a multiplicity of nodes, and how should the nodes cooperate to achieve the maximum information transfer?

Wireless networks possess two distinctive characteristics that do not exist in point-to-point wireless communications and wired networks [21, 22], which are

- *broadcast*: wireless nodes communicate over the air and signals from any one transmitter are heard by multiple nodes with possibly different signal strengths.
- *superposition*: a wireless node receives signals from multiple simultaneously transmitting nodes, with the received signals all superimposed on top of each other.

These two features imply that one cannot distinguish an isolated (i.e. point-to-point) link in wireless networks, and that the links interact in complex ways [22]. Although this could be beneficial in that the information is disseminated over the

network among the users, however, it could have possibly an adverse effect by causing *interference*. Moreover, frequency and power are two scarce resources in wireless communication. In fact, once a frequency is dedicated to a wireless link, it cannot be reused for other links in the networks. The scarcity of power is due to the potential mobility of the wireless nodes, which prompts the nodes to be power-limited. On the other hand, power attenuation due to path loss and channel variations poses even more challenges to communications in wireless environments. *Multi-hop* communication in which an intended sender-receiver pair communicate over multiple hops, is proved to be a promising solution to alleviate the impact of large distance on the communication reliability [21].

Most of the results obtained so far in information theory of wireless network in attempt to derive the corresponding capacity regions, are limited only to special cases, which are, *two-way channel*, *interference channel*, *multiple access channel*, *broadcast channel*, and *relay channel*. Finding the capacity of a communication channel is important not only to know the limit of the communication, but also to develop some kind of coding and transmission protocols to achieve this ultimate communication limit [21].

As the first work on multiple user information theory, Shannon introduced the *two-way channel* in his paper [24]. Although he did not present the capacity of this channel in general, however in his work he developed the preliminaries of two other important channel instances, namely, multiple access, and interference channels [21]. Later on, Ahlswede presented the multiple access channel, where several sources communicate with a single destination [25]. Concurrent with Shannon and Ahlswede, Cover introduced the broadcast channel, where a single source sends different pieces of information to several destinations [26]. In 1970, Van der Meulen proposed the concept of relay channel [27] for a network consisting of three nodes, namely, a source node, a node called relay, and a destination node. Furthermore, Cover worked also on the relay channel, and obtained some fundamental results on

the capacity of relay channel [28]. These pioneering works were the first efforts in finding the channel capacities corresponding to some simple but important cases, although deriving the general expressions for the capacity of even simple networks is still an open problem in information theory.

Due to the complications in determining the capacity of different communication channels, capacity results are only known for few channel instances under special constraints. In most of the cases where the capacity results are known, they comply with the cut-set bound on the achievable rates in a network. The bounds are obtained based on max-flow min-cut theorem, i.e., the rate of information flow across any boundary is less than or at most equal to the conditional mutual information between the inputs on one side of the boundary (senders' side) and the output on the other side (receivers' side) given the inputs on the receiver's side [21].

However, cut-set bounds do not always coincide with the derived upper bounds on the capacity, since in some situations, the former are found to be looser than the latter. This is the case for example in the general broadcast channel, where either the cut-set (outer) bounds are not sufficiently tight or the capacity region is not sufficiently large [21].

3.2 Multi-state Networks

In most applications of wireless sensor networks, due to the limitations on hardware and power resources, the nodes' radios are restricted to operate in *half-duplex* (HD) mode when the same frequency is used for transmission and reception. This implies that the sensor nodes cannot transmit and receive simultaneously. Thus, it is expected that the achievable rates in such network to be lower as compared to those in the network equipped with *full-duplex* (FD) nodes where simultaneous transmit and receive is allowed. This practical constraint prompts the sensor nodes to serve as either a sender or a receiver at any given time, which in turn causes the network to operate in more than just one state (mode). In other words, the network will have

a *multi-state* characteristics as stated in [29]:

In multi-state operation, each state in the network corresponds to the valid partitioning of the nodes into two disjoint subsets of sender and receiver nodes such that there is no node in the sender nodes set which is going to communicate with another node in that subset.

A network comprising of all full-duplex nodes has only one state of operation. In [29], the authors have addressed the problem of deriving the upper and lower bounds on the achievable rate of information transfer corresponding to the cases where the network has a finite number of states. Firstly, they obtain a *single cut* bound applicable to any arbitrary cut in the network that provides a bound on the sum of information flow from one side of the cut to the other side. As the second attempt, a more general bound is derived through repeated application of the already proposed single cut bound over multiple cuts. They have used this bound, in particular, to obtain an upper bound for a single *flow* between any arbitrary two nodes located multiple hops away from each other. Finally, they have presented a general approach in deriving an achievable rate for a single flow across the multi-state network. In their approach, they have shown that the derived bounds coincide with the known cut-set bound when the network has just one state. They have concluded that by considering the number of network states to be finite, the bounds hold for the network with the mentioned practical constraint if the number of nodes in the network is also finite.

3.3 System model

We consider a wireless network with linear topology composed of $n + 1$ nodes including the destination, each denoted by ν_i , $i = 1, \dots, n + 1$, as depicted in Fig. 5.1. Without loss of generality, we let node ν_1 be the node at the left end of the topology, while the destination is located at the right end and is denoted by ν_{n+1} . For simplicity, we assume that the nodes are equally spaced along the path

and denote by d the inter-node distance, which we refer to as the one-hop distance. It follows that the network has length $D = nd$ meters, or, equivalently, it includes n -hops.



Figure 3.1: Network topology.

Node ν_i , $i = 1, \dots, n$ generates messages at rate R_i , and it can decode and forward other nodes' messages. We consider an additive white Gaussian noise (AWGN) channel, and assume that all nodes transmit with power P while the noise power spectral density at each receiver is N_0 . We then write the SNR measured at distance d from a transmitting node as

$$\gamma = \frac{PG_tG_r}{N_0B} \left(\frac{\lambda}{4\pi} \right)^2 d^{-2} \quad (3.1)$$

where G_t, G_r are, respectively, the transmit and receive antenna gains, λ is the carrier wavelength, and B denotes the communication bandwidth common to all nodes.

Given the aforementioned scenario, we are interested in deriving a bound to the maximum achievable rate R , in both the FD and the HD case. FD nodes have the ability to transmit and receive simultaneously over the same frequency band; we denote the corresponding operational state by ft . HD nodes, instead, cannot do both tasks simultaneously, i.e., at a given time instant, they can either transmit (t) or receive (r). Under certain circumstances, an FD node may also operate in HD mode for a fraction of time, hence it may be in any of the states t , r and ft . However, for FD nodes, state t can be included in state ft since reception does not increase the interference level at other nodes and it does not decrease the system capacity either. Note also that a sleep state, denoted by s , could be considered, in which the nodes neither transmit nor receive but they just save energy. In conclusion, we can limit our attention to states r and ft for FD nodes, and to r and t for HD nodes.

Since any network node can operate in two states, while the destination node ν_{n+1} always receives, the number of possible states the network can take is $M = 2^n$. We denote the m -th network state ($m = 1, \dots, M$) by $\boldsymbol{\sigma}_m = [\sigma_{1m}, \dots, \sigma_{nm}]$ where σ_{im} is the state of node ν_i when the network is in state $\boldsymbol{\sigma}_m$, that is, $\sigma_{im} \in \{\mathfrak{r}, \mathfrak{tr}\}$ if ν_i is an FD node, and $\sigma_{im} \in \{\mathfrak{s}, \mathfrak{r}, \mathfrak{t}\}$ if ν_i is an HD node. Also, the time fractions the network spends in the possible states are represented by the vector $\mathbf{t} = [t_1, \dots, t_M]^T$, with $0 \leq t_m \leq 1$ and such that $\sum_{m=1}^M t_m = 1$.

3.4 Cut-set bounds

The cut-set bound is an upper-bound to the achievable data rate of a wireless network of generic topology where nodes exchange messages among each other. As mentioned, in our case the network is composed of n wireless nodes and a destination node (see Fig. 5.1). We define the set of network nodes as $\mathcal{T} = \{\nu_1, \dots, \nu_{n+1}\}$ and, as introduced in Section 3.3, we assume that node ν_i , $i = 1, \dots, n$, generates a message W_i , to be transferred to the destination. The messages W_i 's are assumed to be mutually independent.

We denote by x_i and y_i the random variables representing the signals, respectively, transmitted (channel inputs) and received (channel outputs), by node ν_i , $i = 1, \dots, n + 1$. Moreover, since we assume that the destination node (i.e., node ν_{n+1}) is always in receive state \mathfrak{r} , we set $x_{n+1} = 0$. The transmitted signals x_i 's are assumed to have zero mean, unit variance and joint distribution p_{x_1, \dots, x_n} . The destination node, on the base of the received signal y_{n+1} , derives estimates \widehat{W}_i of the messages W_i , $i = 1, \dots, n$.

In order to compute the cut-set bound, one should consider all possible partitions, hereinafter called *cuts*, of the network nodes \mathcal{T} into two non overlapping sets, \mathcal{S} and $\mathcal{S}_c = \mathcal{T} \setminus \mathcal{S}$. The former includes some of the nodes generating messages, while the latter contains the destinations of those messages (for which they compute an estimate). Note that, beside the sources and destinations of a set of tagged mes-

sages, \mathcal{S} and \mathcal{S}_c can include other nodes as well. In our network scenario, message estimates are derived only at the destination node, thus a valid cut is such that \mathcal{S}_c contains at least node ν_{n+1} .

Let us now consider a generic cut \mathcal{S} . We denote by

- $\mathcal{M}(\mathcal{S})$ the set of messages transmitted by nodes in the cut \mathcal{S} ,
- $R_{\mathcal{M}(\mathcal{S})}$ the sum of the rates of the messages in $\mathcal{M}(\mathcal{S})$,
- $\mathbf{x}_{\mathcal{S}} = \{x_k | \nu_k \in \mathcal{S}\}$ the set of channel inputs contained in \mathcal{S} ,
- $\mathbf{x}_{\mathcal{S}_c} = \{x_k | \nu_k \in \mathcal{S}_c\}$ the set of channel inputs contained in \mathcal{S}_c , and by
- $\mathbf{y}_{\mathcal{S}_c} = \{y_k | \nu_k \in \mathcal{S}_c\}$ the set of channel outputs contained in \mathcal{S}_c .
- $\mathbf{z}_{\mathcal{S}_c} = \{z_k | \nu_k \in \mathcal{S}_c\}$ the set of AWGN noise terms at the receiving nodes in \mathcal{S}_c .

By [30, Chapter 10.2], the rate $R_{\mathcal{M}(\mathcal{S})}$ can be written as $R_{\mathcal{M}(\mathcal{S})} = \sum_{\nu_i \in \mathcal{S}} R_i$, where R_i is the rate of message W_i . Then, the cut-set bound to the sum of the rates R_i is given by

$$\sum_{\nu_i \in \mathcal{S}} R_i \leq I(\mathbf{x}_{\mathcal{S}}; \mathbf{y}_{\mathcal{S}_c} | \mathbf{x}_{\mathcal{S}_c}) \quad (3.2)$$

and the network capacity region is

$$\mathcal{C} \subseteq \bigcup_{p_{x_1, \dots, x_n}} \bigcap_{\mathcal{S} \in \Omega} \left\{ R_1, \dots, R_n \mid \sum_{\nu_i \in \mathcal{S}} R_i \leq I(\mathbf{x}_{\mathcal{S}}; \mathbf{y}_{\mathcal{S}_c} | \mathbf{x}_{\mathcal{S}_c}) \right\} \quad (3.3)$$

where $\Omega = \{\mathcal{S} | \mathcal{S} \subseteq \mathcal{T}, \mathcal{S} \neq \emptyset\}$ is the set of network cuts, whose cardinality is $|\Omega| = 2^n - 1$. The term $I(\mathbf{x}_{\mathcal{S}}; \mathbf{y}_{\mathcal{S}_c} | \mathbf{x}_{\mathcal{S}_c})$ denotes the mutual information¹ between the random variables $\mathbf{x}_{\mathcal{S}}$ and $\mathbf{y}_{\mathcal{S}_c}$, given $\mathbf{x}_{\mathcal{S}_c}$ and a joint distribution p_{x_1, \dots, x_n} .

We recall the the mutual information $I(X; Y|Z)$ between two random variables X and Y , given the random variable Z , can be written as $I(X, Y|Z) = H(Y|Z) -$

¹The mutual information of two random variables measures the mutual dependence of the two variables [20].

$H(Y|X, Z)$, with $H(Y|Z) = H(Y, Z) - H(Z)$ being the differential entropy of the random variable Y given Z . Thus we have

$$\begin{aligned} I(\mathbf{x}_{\mathcal{S}}; \mathbf{y}_{\mathcal{S}_c} | \mathbf{x}_{\mathcal{S}_c}) &= H(\mathbf{y}_{\mathcal{S}_c} | \mathbf{x}_{\mathcal{S}_c}) - H(\mathbf{y}_{\mathcal{S}_c} | \mathbf{x}_{\mathcal{S}} \mathbf{x}_{\mathcal{S}_c}) \\ &= H(\mathbf{y}_{\mathcal{S}_c} \mathbf{x}_{\mathcal{S}_c}) - H(\mathbf{x}_{\mathcal{S}_c}) - H(\mathbf{z}_{\mathcal{S}_c}) \end{aligned} \quad (3.4)$$

In order to compute the entropies in (3.4), let $\mathbf{Y}_{\mathcal{S}_c}$ and $\mathbf{X}_{\mathcal{S}_c}$ denote two row vectors with elements drawn from all (ordered) members of $\mathbf{y}_{\mathcal{S}_c}$ and $\mathbf{x}_{\mathcal{S}_c}$ respectively. In other words, we have $\mathbf{Y}_{\mathcal{S}_c} = [y_i]_{\nu_i \in \mathcal{S}_c}$, and $\mathbf{X}_{\mathcal{S}_c} = [x_i]_{\nu_i \in \mathcal{S}_c \setminus \{n+1\}}$. Similarly, let $\mathbf{X} = [x_i]_{\nu_i \in \mathcal{T} \setminus \{n+1\}}$, and define the vector $\mathbf{Y} = [\mathbf{Y}_{\mathcal{S}_c} \ ; \ \mathbf{X}_{\mathcal{S}_c}]^T$, and $\mathbf{Z} = [\mathbf{Z}_{\mathcal{S}_c} \ ; \ \mathbf{0}_{1 \times (|\mathcal{S}_c| - 1)}]^T$ with $\mathbf{Z}_{\mathcal{S}_c} = [z_i]_{\nu_i \in \mathcal{S}_c}$, and $\mathbf{0}_{1 \times (|\mathcal{S}_c| - 1)}$, a row vector containing $|\mathcal{S}_c| - 1$ zeros.

The equation that relates the aforementioned vectors is

$$\mathbf{Y} = \mathbf{Q}\mathbf{X}^T + \mathbf{Z} \quad (3.5)$$

where the elements of matrix $\mathbf{Q}_{(2|\mathcal{S}_c|-1) \times (|\mathcal{T}|-1)}$ are the corresponding channel gains whenever the receiving node $\nu_j \in \mathcal{S}_c$ is within the transmission range of the sending node $\nu_i \in \mathcal{S}$, and zero otherwise.

According to (3.5), and by assuming the elements of \mathbf{Y} to be jointly Gaussian random variables, the entropies in (3.4) are computed as [20]

$$H(\mathbf{y}_{\mathcal{S}_c} \mathbf{x}_{\mathcal{S}_c}) = (1/2) \log_2 \left((2\pi e)^{2|\mathcal{S}_c|-1} \det(\boldsymbol{\Sigma}_{\mathbf{Y}}) \right) \quad (3.6a)$$

$$H(\mathbf{x}_{\mathcal{S}_c}) = (1/2) \log_2 \left((2\pi e)^{|\mathcal{S}_c|-1} \det(\boldsymbol{\Sigma}_{\mathbf{X}_{\mathcal{S}_c}}) \right) \quad (3.6b)$$

$$H(\mathbf{z}_{\mathcal{S}_c}) = (1/2) \log_2 \left((2\pi e)^{|\mathcal{S}_c|} \det(\boldsymbol{\Sigma}_{\mathbf{Z}_{\mathcal{S}_c}}) \right) \quad (3.6c)$$

where $\boldsymbol{\Sigma}_{\mathbf{Y}} = \mathbf{Q}\boldsymbol{\Sigma}_{\mathbf{X}}\mathbf{Q}^T + \boldsymbol{\Sigma}_{\mathbf{Z}}$ denotes the covariance matrix of \mathbf{Y} , and $\boldsymbol{\Sigma}_{\mathbf{X}}$, $\boldsymbol{\Sigma}_{\mathbf{Z}}$, $\boldsymbol{\Sigma}_{\mathbf{X}_{\mathcal{S}_c}}$ and $\boldsymbol{\Sigma}_{\mathbf{Z}_{\mathcal{S}_c}}$ are, respectively, the covariance matrices of \mathbf{X} , \mathbf{Z} , $\mathbf{X}_{\mathcal{S}_c}$, and $\mathbf{Z}_{\mathcal{S}_c}$.

3.4.1 Cut-set bound in multi-state networks

Applying the cut-set bound defined previously by (5.6) to the networks where the nodes operate under the assumption of half-duplexity will result to bounds that are not sufficiently tight. In [29] a multi-state max-flow min-cut theorem for multi-terminal networks with possible multiple states has been derived, and is shown to reduce to the well-known max-flow min-cut theorem [20] when applied to single-state networks. They have shown that if the network has multiple states, the new theorem provides a tighter upper bound than the bound in [20].

Theorem 3.4.1 (*Single cut cut-set bound in multi-state networks*) *In a general network with a finite number of states, M , the maximum sum rate of achievable information rates R_i across the cut-set $\mathcal{S} \subseteq \mathcal{T}$, and for any sequence of network states $\{\sigma_m\}_{m=1}^M$, is bounded by [29]*

$$\sum_{\nu_i \in \mathcal{S}} R_i \leq \sup_{t_m} \sum_m t_m I(\mathbf{x}_{\mathcal{S}}; \mathbf{y}_{\mathcal{S}_c} | \mathbf{x}_{\mathcal{S}_c}, \sigma_m) \quad (3.7)$$

where the supremum is over all $t_m \geq 0$ subject to $\sum_m t_m = 1$.

Proof The proof can be found in [29].

Theorem 3.4.2 (*Max-flow min-cut bound in multi-state networks*) *Consider a general network with a finite number of states, M . The sum rate of information transfer from an arbitrary set \mathcal{S}_1 (sender nodes) to an arbitrary disjoint set \mathcal{S}_2 (receiver nodes), where $\mathcal{S}_1, \mathcal{S}_2 \subset \mathcal{T}$ and for any sequence of network states $\{\sigma_m\}_{m=1}^M$, is bounded by [29]*

$$\sum_{\nu_i \in \mathcal{S}_1} R_i \leq \sup_{t_m} \min_{\mathcal{S}} \sum_m t_m I(\mathbf{x}_{\mathcal{S}}; \mathbf{y}_{\mathcal{S}_c} | \mathbf{x}_{\mathcal{S}_c}, \sigma_m) \quad (3.8)$$

when the minimization is taken over all set $\mathcal{S} \subseteq \mathcal{T}$ subject to $\mathcal{S} \cap \mathcal{S}_1 = \mathcal{S}_1, \mathcal{S} \cap \mathcal{S}_2 = \emptyset$ and the supremum is over all (non-negative) t_m subject to $\sum_{m=1}^M t_m = 1$.

Proof The proof is given in [29].

3.5 Cut-set bounds in linear wireless networks

In this section, we provide some examples in computing the cut-set bounds to the achievable rate of data transfer in linear wireless networks. We consider two different cases, one is the case where the network nodes are equipped with full-duplex transceivers, while the other is the case in which the network consists of nodes that can operate in half-duplex mode only. The former operates in only one state, while the latter might operate in several but finite states. We compute the exact bounds to the information flow across such networks based on the numerical solutions of max-flow min-cut problem applied to the network under study.

3.5.1 Network with full-duplex nodes

Refer to the generic linear network depicted in Fig. 5.1, and let us assume initially that the nodes are equipped with full-duplex radios, and that there is no limit on the transmission range. This latter assumption implies that the signal transmitted by the generic node ν_i , $i = 1, \dots, n$ is received (and decoded) by any other node in the network including the destination. Such network is illustrated in Fig. 3.2 with $n = 3$ nodes and a destination.

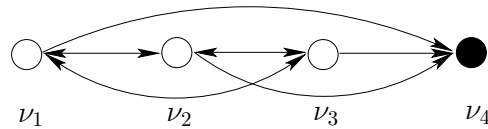


Figure 3.2: An example of a linear network with $n = 3$ full-duplex nodes and a destination. The communication links are depicted by arrows.

Let us denote by x_i and y_i , respectively, the signals transmitted from, and received by the node ν_i , $i = 1, \dots, n+1$. Hence, for the case of our network example, we have

$$y_i = \sqrt{\gamma} \sum_{\substack{k=1, \dots, n \\ k \neq i}} \frac{x_k}{|i - k|} + z_i \quad (3.9)$$

with z_i to be the additive white Gaussian noise, and $x_{n+1} = 0$.

In a network with $n = 3$ full-duplex nodes and a destination, and according to (3.9), the received signals are

$$\begin{aligned}
y_1 &= \sqrt{\gamma} \left(x_2 + \frac{x_2}{2} \right) + z_1 \\
y_2 &= \sqrt{\gamma} (x_1 + x_3) + z_2 \\
y_3 &= \sqrt{\gamma} \left(\frac{x_1}{2} + x_2 \right) + z_3 \\
y_4 &= \sqrt{\gamma} \left(\frac{x_1}{3} + \frac{x_2}{2} + x_3 \right) + z_4
\end{aligned} \tag{3.10}$$

The cuts and their corresponding cut-set bounds defined by the mutual informations, $I(\mathbf{x}_S; \mathbf{y}_{S_c} | \mathbf{x}_{S_c})$, are

cut, C_k	\mathcal{S}	\mathcal{S}_c	$\mathcal{R}_{\mathcal{M}(\mathcal{S})} = \sum_{\nu_i \in \mathcal{S}} R_i$	$I(\mathbf{x}_S; \mathbf{y}_{S_c} \mathbf{x}_{S_c})$
C_1	$\{\nu_1\}$	$\{\nu_2, \nu_3, \nu_4\}$	R_1	$I(x_1; y_2 y_3 y_4 x_2 x_3)$
C_2	$\{\nu_2\}$	$\{\nu_1, \nu_3, \nu_4\}$	R_2	$I(x_2; y_1 y_3 y_4 x_1 x_3)$
C_3	$\{\nu_3\}$	$\{\nu_1, \nu_2, \nu_4\}$	R_3	$I(x_3; y_1 y_2 y_4 x_1 x_2)$
C_4	$\{\nu_1, \nu_2\}$	$\{\nu_3, \nu_4\}$	$R_1 + R_2$	$I(x_1 x_2; y_3 y_4 x_3)$
C_5	$\{\nu_1, \nu_3\}$	$\{\nu_2, \nu_4\}$	$R_1 + R_3$	$I(x_1 x_3; y_2 y_4 x_2)$
C_6	$\{\nu_2, \nu_3\}$	$\{\nu_1, \nu_4\}$	$R_2 + R_3$	$I(x_2 x_3; y_1 y_4 x_1)$
C_7	$\{\nu_1, \nu_2, \nu_3\}$	$\{\nu_4\}$	$R_1 + R_2 + R_3$	$I(x_1 x_2 x_3; y_4)$

Table 3.1: Cuts and their corresponding sum rates and cut-set bounds in a network of $n = 3$ full-duplex nodes and a destination.

Regarding (3.4), $I(x_1; y_2 y_3 y_4 | x_2 x_3)$ is written, for example, as

$$I(x_1; y_2 y_3 y_4 | x_2 x_3) = H(y_2 y_3 y_4 | x_2 x_3) - H(x_2 x_3) - H(z_2 z_3 z_4) \tag{3.11}$$

We use (3.6a) – (3.6c) to compute the entropies in the above equation. First, we

note that according to (3.5) we have

$$\begin{bmatrix} y_2 \\ y_3 \\ y_4 \\ x_2 \\ x_3 \end{bmatrix} = \sqrt{\gamma} \begin{bmatrix} 1 & 0 & 1 \\ 1/2 & 1 & 0 \\ 1/3 & 1/2 & 1 \\ 0 & 1 & 0 \\ 0 & 0 & 1 \end{bmatrix} \begin{bmatrix} x_1 \\ x_2 \\ x_3 \end{bmatrix} + \begin{bmatrix} z_2 \\ z_3 \\ z_4 \\ 0 \\ 0 \end{bmatrix} \quad (3.12)$$

Hence, by assuming that x_i s are unit-variance and independent, the entropies are obtained for $\gamma = 20$ dB as

$$H(x_1 y_2 y_3 y_4) = 7.542$$

$$H(x_2 x_3) = 2.837$$

$$H(z_2 z_3 z_4) = 4.256$$

which result in $I(x_1; y_2 y_3 y_4 | x_2 x_3) = 7.065$ bits, and is the cut-set bound corresponding to the cut C_1 . The computation of other mutual informations are similar and straightforward, and the results are given in Table 3.2. As we observe in Ta-

γ [dB]	$\max_{p(x_1, \dots, x_n)} I(\mathbf{x}_{\mathcal{S}}; \mathbf{y}_{\mathcal{S}_c} \mathbf{x}_{\mathcal{S}_c});$							Max-flow min-cut bound;
	C_1	C_2	C_3	C_4	C_5	C_6	C_7	$\min_{C_k} \max_{p(x_1, \dots, x_n)} I(\mathbf{x}_{\mathcal{S}}; \mathbf{y}_{\mathcal{S}_c} \mathbf{x}_{\mathcal{S}_c})$
20	7.065	7.315	7.315	5.025	6.636	6.641	3.879	3.879

Table 3.2: Solution to the cut-set bounds and the resulted max-flow min-cut bound, referred to the network of $n = 3$ full-duplex nodes shown in Fig. 3.2.

ble 3.2, the cut-set bound corresponding to the last cut, C_7 , gives the max-flow min-cut bound in this case.

3.5.1.1 One-hop, Full-duplex

Consider again the network in Fig. 3.2, and assume that we pose a constraint on the nodes' communication range, i.e., we restrict it to be within the one-hop distance.

Such a network is shown in Fig. 3.3.

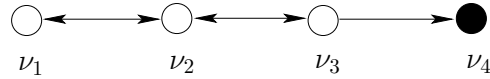


Figure 3.3: A linear network with $n = 3$ full-duplex nodes and a destination. The communications are restricted to *one-hop* links only.

The received signals in this case are

$$\begin{aligned}
 y_1 &= \sqrt{\gamma}x_2 + z_2 \\
 y_2 &= \sqrt{\gamma}(x_1 + x_3) + z_2 \\
 y_3 &= \sqrt{\gamma}x_2 + z_3 \\
 y_4 &= \sqrt{\gamma}x_3 + z_4
 \end{aligned} \tag{3.13}$$

The cut-set bounds are given through the mutual informations in Table 3.3.

cut, C_k	\mathcal{S}	\mathcal{S}_c	$\mathcal{R}_{\mathcal{M}(\mathcal{S})} = \sum_{\nu_i \in \mathcal{S}} R_i$	$I(\mathbf{x}_{\mathcal{S}}; \mathbf{y}_{\mathcal{S}_c} \mathbf{x}_{\mathcal{S}_c})$
C_1	$\{\nu_1\}$	$\{\nu_2, \nu_3, \nu_4\}$	R_1	$I(x_1; y_2 x_2 x_3)$
C_2	$\{\nu_2\}$	$\{\nu_1, \nu_3, \nu_4\}$	R_2	$I(x_2; y_1 y_3 x_1 x_3)$
C_3	$\{\nu_3\}$	$\{\nu_1, \nu_2, \nu_4\}$	R_3	$I(x_3; y_2 y_4 x_1 x_2)$
C_4	$\{\nu_1, \nu_2\}$	$\{\nu_3, \nu_4\}$	$R_1 + R_2$	$I(x_2; y_3 x_3)$
C_5	$\{\nu_1, \nu_3\}$	$\{\nu_2, \nu_4\}$	$R_1 + R_3$	$I(x_1 x_3; y_2 y_4 x_2)$
C_6	$\{\nu_2, \nu_3\}$	$\{\nu_1, \nu_4\}$	$R_2 + R_3$	$I(x_2 x_3; y_1 y_4 x_1)$
C_7	$\{\nu_1, \nu_2, \nu_3\}$	$\{\nu_4\}$	$R_1 + R_2 + R_3$	$I(x_3; y_4)$

Table 3.3: Cuts and their corresponding sum rates and cut-set bounds in a network of $n = 3$ full-duplex nodes and a destination shown in Fig. 3.3.

We assume the nodes' signals to be independent. Thus, we get

$$\begin{aligned}
I(x_1; y_2 | x_2 x_3) &= I(x_1; y_2) &&= (1/2) \log_2(1 + \gamma) \\
I(x_2; y_1 y_3 | x_1 x_3) &= I(x_2; y_1 y_3) &&= (1/2) \log_2(1 + 2\gamma) \\
I(x_3; y_2 y_4 | x_1 x_2) &= I(x_3; y_2 y_4) &&= (1/2) \log_2(1 + 2\gamma) \\
I(x_2; y_3 | x_3) &= I(x_2; y_3) &&= (1/2) \log_2(1 + \gamma) \\
I(x_1 x_3; y_2 y_4 | x_2) &= I(x_1; y_2) + I(x_3; y_4) &&= \log_2(1 + \gamma) \\
I(x_2 x_3; y_1 y_4 | x_1) &= I(x_2; y_1) + I(x_3; y_4) &&= \log_2(1 + \gamma) \\
I(x_3; y_4) &= (1/2) \log_2(1 + \gamma)
\end{aligned}$$

For instance, $I(x_2; y_1 y_3) = H(y_1 y_3) - H(z_2 z_3)$ is computed as follows. By writing the received signals $y_1 = \sqrt{\gamma}x_2 + z_1$ and $y_3 = \sqrt{\gamma}x_2 + z_3$ in matrix form, we obtain

$$\mathbf{Y} = \begin{bmatrix} y_1 \\ y_3 \end{bmatrix} = \begin{bmatrix} \sqrt{\gamma} \\ \sqrt{\gamma} \end{bmatrix} x_2 + \begin{bmatrix} z_1 \\ z_3 \end{bmatrix} = \mathbf{Q}x_2 + \mathbf{Z}.$$

According to (3.6a) and (3.6c)

$$I(x_2; y_1 y_3) = (1/2) \log_2 \left((2\pi e)^2 \det(\Sigma_{\mathbf{Y}}) \right) - (1/2) \log_2 \left((2\pi e)^2 \det(\Sigma_{\mathbf{Z}}) \right)$$

where

$$\Sigma_{\mathbf{Y}} = \mathbf{Q}\Sigma_{x_2}\mathbf{Q}^T + \Sigma_{\mathbf{Z}} = \begin{bmatrix} \sqrt{\gamma} \\ \sqrt{\gamma} \end{bmatrix} \begin{bmatrix} \sqrt{\gamma} & \sqrt{\gamma} \end{bmatrix} + \begin{bmatrix} 1 & 0 \\ 0 & 1 \end{bmatrix}.$$

and, we get finally $I(x_2; y_1 y_3) = (1/2) \log_2(1 + 2\gamma)$.

By computing the cut-set bounds corresponding to the the other cuts, the results are given in the Table 3.4.

γ [dB]	$\max_{p(x_1, \dots, x_n)} I(\mathbf{x}_S; \mathbf{y}_{S_c} \mathbf{x}_{S_c});$							Max-flow min-cut bound;
	C_1	C_2	C_3	C_4	C_5	C_6	C_7	$\min_{C_k} \max_{p(x_1, \dots, x_n)} I(\mathbf{x}_S; \mathbf{y}_{S_c} \mathbf{x}_{S_c})$
20	3.329	3.825	3.825	3.329	7.651	7.651	3.329	3.329

Table 3.4: Solution to the cut-set bounds and the resulted max-flow min-cut bound, referred to the network of $n = 3$ full-duplex nodes shown in Fig. 3.3.

3.5.1.2 One-hop, Full-duplex, Unidirectional traffic flow

Now let us assume the information flow to be *unidirectional*, i.e., from the lower-indexed nodes towards those with higher indexes as depicted in Fig. 3.4. Thus, the received signals become

$$\begin{aligned}
 y_2 &= \sqrt{\gamma}x_1 + z_2 \\
 y_3 &= \sqrt{\gamma}x_2 + z_3 \\
 y_4 &= \sqrt{\gamma}x_3 + z_4
 \end{aligned} \tag{3.14}$$



Figure 3.4: A linear network with $n = 3$ full-duplex nodes and a destination. The communications are restricted to one-hop unidirectional links only.

With respect to (3.14), the cut-set bounds are obtained to be as follows.

cut, C_k	$I(\mathbf{x}_S; \mathbf{y}_{S_c} \mathbf{x}_{S_c})$
C_1	$I(x_1; y_2 x_2 x_3)$
C_2	$I(x_2; y_3 x_1 x_3)$
C_3	$I(x_3; y_4 x_1 x_2)$
C_4	$I(x_2; y_3 x_3)$
C_5	$I(x_1 x_3; y_2 y_4 x_2)$
C_6	$I(x_3; y_4 x_1)$
C_7	$I(x_3; y_4)$

Table 3.5: Cuts and their corresponding cut-set bounds in a network of $n = 3$ full-duplex nodes and a destination, referred to the network shown in Fig. 3.4.

Upon assuming the independence of the transmitted signals, x_i , $i = 1, \dots, 3$, we expand the expressions of mutual information according to (3.4) to get

$$I(x_1; y_2 | x_2 x_3) = I(x_1; y_2) = H(y_2) - H(z_2) = (1/2) \log_2(1 + \gamma)$$

$$I(x_2; y_3 | x_1 x_3) = I(x_2; y_3) = (1/2) \log_2(1 + \gamma)$$

$$I(x_3; y_4 | x_1 x_2) = I(x_3; y_4) = (1/2) \log_2(1 + \gamma)$$

$$I(x_2; y_3 | x_3) = I(x_2; y_3) = (1/2) \log_2(1 + \gamma)$$

$$I(x_1 x_3; y_2 y_4 | x_2) = I(x_1; y_2) + I(x_3; y_4) = \log_2(1 + \gamma)$$

$$I(x_3; y_4 | x_1) = I(x_3; y_4) = (1/2) \log_2(1 + \gamma)$$

The cut-set bounds and the resulted max-flow min-cut bound are given in Table 3.6.

γ [dB]	$\max_{p(x_1, \dots, x_n)} I(\mathbf{x}_S; \mathbf{y}_{S_c} \mathbf{x}_{S_c});$							Max-flow min-cut bound;
	C_1	C_2	C_3	C_4	C_5	C_6	C_7	$\min_{C_k} \max_{p(x_1, \dots, x_n)} I(\mathbf{x}_S; \mathbf{y}_{S_c} \mathbf{x}_{S_c})$
20	3.329	3.329	3.329	3.329	6.658	3.329	3.329	3.329

Table 3.6: Solution to the cut-set bounds and the resulted max-flow min-cut bound, referred to the network of $n = 3$ full-duplex nodes shown in Fig. 3.4.

As we observe, the cut-set bound corresponding to the last cut, C_7 , contributes as the max-flow min-cut bound in all three instances of the linear network with $n = 3$ full-duplex nodes.

3.5.2 Network with half-duplex nodes

Now we turn to the the linear wireless networks comprising of half-duplex nodes, and we study the problem of finding the max-flow min-cut bound to the rate of traffic transfer assuming that the network has only a few number of nodes. Toward this end, first, we consider networks whose nodes' communication range is restricted to one-hop distance only. This means that each node can communicate with the node that is located either behind or after it. Next, we let the communication range to be extended to the two hops, implying that the signal transmitted from each node in the network can be received and decoded by the nodes that are located at most within two-hop distance, $2d$. To summarize, in the both cases of *one-hop* and *two-hop* scenarios, our basic assumptions are

- the nodes are equipped with half-duplex radios,
- the information flow is *unidirectional*,
- the nodes generate traffic at the same rate R , i.e., $R_i = R$. In other words, the nodes need to transfer their generated traffic at the same average rate, R .

3.5.3 Half-duplex nodes, One-hop communication

3.5.3.1 Three nodes, one destination ($n = 3$)

Consider a linear wireless network consisting of $n = 3$ half-duplex nodes and a destination. Since the nodes' transceivers are assumed to be half-duplex radios, the network might operate in some finite number of states. Let us appoint initially three states to such network, namely, $\sigma_1, \dots, \sigma_3$, along with their corresponding time fractions $\mathbf{t} = [t_1, \dots, t_3]$, where $\sum_i t_i = 1$, as defined earlier in section 3.3. The node and network states are listed in Table 3.7, and Fig. 3.5 depicts such network and its three operational states.

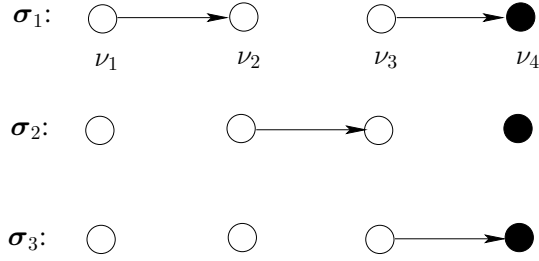


Figure 3.5: A network of $n = 3$ half-duplex nodes and a destination. The communication range is restricted to one-hop distance, and the information flow is unidirectional. The network operates in $M = 3$ states, namely, σ_1 , σ_2 , and σ_3 .

σ_m	σ_{1m}	σ_{2m}	σ_{3m}
σ_1	t	r	t
σ_2	s	t	r
σ_3	s	s	t

Table 3.7: Node and network states in a network of $n = 3$ nodes.

The received signals referred to each network state are

$$\sigma_1 : y_2 = \sqrt{\gamma}x_1 + z_2$$

$$y_4 = \sqrt{\gamma}x_3 + z_4$$

$$\sigma_2 : y_3 = \sqrt{\gamma}x_2 + z_3$$

$$\sigma_3 : y_4 = \sqrt{\gamma}x_3 + z_4.$$

Since there are three nodes and one destination in the network, there exist $2^3 - 1 = 7$ cuts, namely, C_1, \dots, C_7 as defined in Table 3.8. Furthermore, the cut-set bounds, $I(\mathbf{x}_S; \mathbf{y}_{S_c} | \mathbf{x}_{S_c}, \sigma_m)$, corresponding to each network state, σ_i , are given in Table 3.9.

cut, C_k	\mathcal{S}	\mathcal{S}_c
C_1	$\{\nu_1\}$	$\{\nu_2, \nu_3, \nu_4\}$
C_2	$\{\nu_2\}$	$\{\nu_1, \nu_3, \nu_4\}$
C_3	$\{\nu_3\}$	$\{\nu_1, \nu_2, \nu_4\}$
C_4	$\{\nu_1, \nu_2\}$	$\{\nu_3, \nu_4\}$
C_5	$\{\nu_1, \nu_3\}$	$\{\nu_2, \nu_4\}$
C_6	$\{\nu_2, \nu_3\}$	$\{\nu_1, \nu_4\}$
C_7	$\{\nu_1, \nu_2, \nu_3\}$	$\{\nu_4\}$

Table 3.8: Cuts in a network of $n = 3$ half-duplex nodes and a destination, referred to the network shown in Fig. 3.5.

cut, C_k	$\sum_{\nu_i \in \mathcal{S}} R_i$	$I(\mathbf{x}_{\mathcal{S}}; \mathbf{y}_{\mathcal{S}_c} \mathbf{x}_{\mathcal{S}_c}, \boldsymbol{\sigma}_1)$	$I(\mathbf{x}_{\mathcal{S}}; \mathbf{y}_{\mathcal{S}_c} \mathbf{x}_{\mathcal{S}_c}, \boldsymbol{\sigma}_2)$	$I(\mathbf{x}_{\mathcal{S}}; \mathbf{y}_{\mathcal{S}_c} \mathbf{x}_{\mathcal{S}_c}, \boldsymbol{\sigma}_3)$
C_1	R	$I(x_1; y_2 x_3)$	0	0
C_2	R	0	$I(x_2; y_3)$	0
C_3	R	$I(x_3; y_4 x_1)$	0	$I(x_3; y_4)$
C_4	$2R$	0	$I(x_2; y_3)$	0
C_5	$2R$	$I(x_1 x_3; y_2 y_4)$	0	$I(x_3; y_4)$
C_6	$2R$	$I(x_3; y_4 x_1)$	0	$I(x_3; y_4)$
C_7	$3R$	$I(x_3; y_4)$	0	$I(x_3; y_4)$

Table 3.9: Cuts, sum rates, and cut-set bounds in a network of $n = 3$ half-duplex nodes and a destination shown in Fig. 3.5.

Because of the statistical independence of x_1 and x_3 we have

$$\begin{aligned}
I(x_1; y_2 | x_3) &= I(x_1; y_2) = (1/2) \log_2(1 + \gamma) \\
I(x_3; y_4 | x_1) &= I(x_3; y_4) = (1/2) \log_2(1 + \gamma) \\
I(x_1 x_3; y_2 y_4) &= I(x_1; y_2) + I(x_3; y_4) = \log_2(1 + \gamma) \\
I(x_3; y_4 | x_1) &= I(x_3; y_4) = (1/2) \log_2(1 + \gamma)
\end{aligned} \tag{3.15}$$

Let us define the *link capacity* regarding one-hop distance, d as

$$\mathcal{C} = (1/2) \log_2(1 + \gamma) \tag{3.16}$$

cut, C_k	$\sum_{\nu_i \in \mathcal{S}} R_i$	$I(\mathbf{x}_{\mathcal{S}}; \mathbf{y}_{\mathcal{S}_c} \mathbf{x}_{\mathcal{S}_c}, \boldsymbol{\sigma}_1)$	$I(\mathbf{x}_{\mathcal{S}}; \mathbf{y}_{\mathcal{S}_c} \mathbf{x}_{\mathcal{S}_c}, \boldsymbol{\sigma}_2)$	$I(\mathbf{x}_{\mathcal{S}}; \mathbf{y}_{\mathcal{S}_c} \mathbf{x}_{\mathcal{S}_c}, \boldsymbol{\sigma}_3)$
C_1	R	\mathcal{C}	0	0
C_2	R	0	\mathcal{C}	0
C_3	R	\mathcal{C}	0	\mathcal{C}
C_4	$2R$	0	\mathcal{C}	0
C_5	$2R$	$2\mathcal{C}$	0	\mathcal{C}
C_6	$2R$	\mathcal{C}	0	\mathcal{C}
C_7	$3R$	\mathcal{C}	0	\mathcal{C}

Table 3.10: Cuts, sum rates, and cut-set bounds in a network of $n = 3$ half-duplex nodes and a destination shown in Fig. 3.5. $\mathcal{C} = (1/2) \log_2(1 + \gamma)$.

Thus, according to (3.8), the max-flow min-cut bound to the rate R is

$$\begin{aligned}
R &\leq \mathcal{C} \max_{\substack{t_m, \\ \text{s.t. } \sum t_m = 1}} \min \left\{ t_1, t_2, t_1 + t_3, \frac{t_2}{2}, t_1 + \frac{t_3}{2}, \frac{t_1 + t_3}{2}, \frac{t_1 + t_3}{3} \right\} \\
&= \mathcal{C} \max_{\substack{t_m, \\ \sum t_m = 1}} \min \left\{ t_1, \frac{t_2}{2}, \frac{t_1 + t_3}{3} \right\} \\
&= \mathcal{C}/5
\end{aligned}$$

with $t_1 = 1/5$, $t_2 = 2/5$, and $t_3 = 2/5$.

Now let us consider the same network of $n = 3$ half-duplex nodes as appeared in Fig. 3.5, but this time we integrate the first and the third states into one. The new network is depicted in Fig. 3.6.

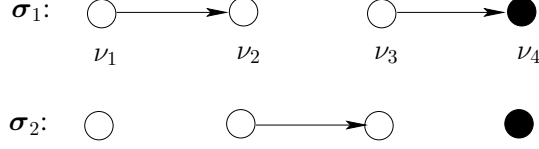


Figure 3.6: A network of $n = 3$ half-duplex nodes and a destination. It operates in $M = 2$ states.

Following the same procedure in computing the cut-set bounds corresponding the the cuts we have

cut, C_k	$\sum_{\nu_i \in \mathcal{S}} R_i$	$I(\mathbf{x}_S; \mathbf{y}_{S_c} \mathbf{x}_{S_c}, \sigma_1)$	$I(\mathbf{x}_S; \mathbf{y}_{S_c} \mathbf{x}_{S_c}, \sigma_2)$
C_1	R	\mathcal{C}	0
C_2	R	0	\mathcal{C}
C_3	R	\mathcal{C}	0
C_4	$2R$	0	\mathcal{C}
C_5	$2R$	$2\mathcal{C}$	0
C_6	$2R$	\mathcal{C}	0
C_7	$3R$	\mathcal{C}	0

Table 3.11: Cuts, sum rates, and cut-set bounds in a network of $n = 3$ half-duplex nodes and a destination shown in Fig. 3.6, where $\mathcal{C} = (1/2) \log_2(1 + \gamma)$.

According to (3.8), the max-flow min-cut bound to the rate R is

$$\begin{aligned}
 R &\leq \mathcal{C} \max_{\substack{t_m, \\ \text{s.t. } \sum t_m=1}} \min \left\{ t_1, t_2, t_1, \frac{t_2}{2}, t_1, \frac{t_1}{2}, \frac{t_1}{3} \right\} \\
 &= \mathcal{C} \max_{\substack{t_m, \\ \sum t_m=1}} \min \left\{ \frac{t_2}{2}, \frac{t_1}{3} \right\} \\
 &= \mathcal{C}/5
 \end{aligned}$$

with $t_1 = 3/5$, and $t_2 = 2/5$.

This example reveals that in a network of $n = 3$ half-duplex nodes and a destination, where the communication range is restricted to one-hop distance and the informa-

tion flow is unidirectional, the nodes' traffic is actually transferred to the destination in just two states.

3.5.3.2 Four nodes, one destination ($n = 4$)

Consider a linear wireless network of $n = 4$ half-duplex nodes and one destination. According to the results obtained previously in the case of $n = 3$ nodes, a four-node network requires just two states to transfer the nodes' traffic to the destination as shown in Fig. 3.7.

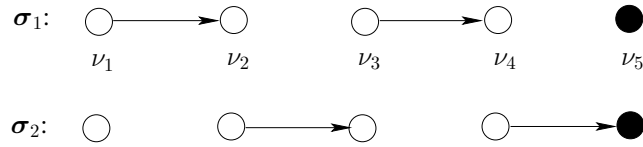


Figure 3.7: A network of $n = 4$ half-duplex nodes and a destination. It operates in $M = 2$ states, namely, σ_1, σ_2 .

The two network states, σ_1, σ_2 are given in Table 3.12.

σ_m	σ_{1m}	σ_{2m}	σ_{3m}	σ_{4m}
σ_1	t	r	t	r
σ_2	s	t	r	t

Table 3.12: Node and network states in a network of $n = 4$ half-duplex nodes.

In the following, we obtain the bound on the rate of traffic transfer, R , of such network. First we note that there exist $2^4 - 1 = 15$ cuts as defined in Table 3.13. Table 3.14 gives the cut-set bounds and the sum rates. Denoting by \mathcal{C} as the capacity of a one-hop link and defined as $\mathcal{C} = (1/2) \log_2(1 + \gamma)$, the resulted cut-set bounds corresponding to each network state are reported in Table 3.15.

cut, C_k	\mathcal{S}	\mathcal{S}_c
C_1	$\{\nu_1\}$	$\{\nu_2, \nu_3, \nu_4, \nu_5\}$
C_2	$\{\nu_2\}$	$\{\nu_1, \nu_3, \nu_4, \nu_5\}$
C_3	$\{\nu_3\}$	$\{\nu_1, \nu_2, \nu_4, \nu_5\}$
C_4	$\{\nu_4\}$	$\{\nu_1, \nu_2, \nu_3, \nu_5\}$
C_5	$\{\nu_1, \nu_2\}$	$\{\nu_3, \nu_4, \nu_5\}$
C_6	$\{\nu_1, \nu_3\}$	$\{\nu_2, \nu_4, \nu_5\}$
C_7	$\{\nu_1, \nu_4\}$	$\{\nu_2, \nu_3, \nu_5\}$
C_8	$\{\nu_2, \nu_3\}$	$\{\nu_1, \nu_4, \nu_5\}$
C_9	$\{\nu_2, \nu_4\}$	$\{\nu_1, \nu_3, \nu_5\}$
C_{10}	$\{\nu_3, \nu_4\}$	$\{\nu_1, \nu_2, \nu_5\}$
C_{11}	$\{\nu_1, \nu_2, \nu_3\}$	$\{\nu_4, \nu_5\}$
C_{12}	$\{\nu_1, \nu_2, \nu_4\}$	$\{\nu_3, \nu_5\}$
C_{13}	$\{\nu_1, \nu_3, \nu_4\}$	$\{\nu_2, \nu_5\}$
C_{14}	$\{\nu_2, \nu_3, \nu_4\}$	$\{\nu_1, \nu_5\}$
C_{15}	$\{\nu_1, \nu_2, \nu_3, \nu_4\}$	$\{\nu_5\}$

Table 3.13: Cuts in the network of $n = 4$ half-duplex nodes and a destination.

Upon solving the max-flow min-cut bound problem according to (3.8), we obtain

$$\begin{aligned}
R &\leq \mathcal{C} \max_{\substack{t_m, \\ \text{s.t. } \sum t_m=1}} \min \left\{ t_1, t_2, t_1, t_2, \frac{t_2}{2}, t_1, \frac{t_1+t_2}{2}, \frac{t_1}{2}, \right. \\
&\quad \left. t_2, \frac{t_2}{2}, \frac{t_1}{3}, \frac{2t_2}{3}, \frac{t_1+t_2}{3}, \frac{t_2}{3}, \frac{t_2}{4} \right\} \\
&= \mathcal{C} \max_{\substack{t_m, \\ \text{s.t. } \sum t_m=1}} \min \left\{ \frac{t_1}{3}, \frac{t_2}{4} \right\} \\
&= \mathcal{C}/7
\end{aligned} \tag{3.17}$$

with $\mathbf{t} = [t_1, t_2] = [3/7, 4/7]$.

The results show that the cut-set bounds referred to the last cuts C_{14} and C_{15} contribute in the derivation of max-flow min-cut bound.

cut, C_k	$\sum_{\nu_i \in \mathcal{S}} R_i$	$I(\mathbf{x}_{\mathcal{S}}; \mathbf{y}_{\mathcal{S}_c} \mathbf{x}_{\mathcal{S}_c}, \boldsymbol{\sigma}_1)$	$I(\mathbf{x}_{\mathcal{S}}; \mathbf{y}_{\mathcal{S}_c} \mathbf{x}_{\mathcal{S}_c}, \boldsymbol{\sigma}_2)$
C_1	R	$I(x_1; y_2 x_3)$	0
C_2	R	0	$I(x_2; y_3 x_4)$
C_3	R	$I(x_3; y_4 x_1)$	0
C_4	R	0	$I(x_4; y_5 x_2)$
C_5	$2R$	0	$I(x_2; y_3 x_4)$
C_6	$2R$	$I(x_1 x_3; y_2 y_4)$	0
C_7	$2R$	$I(x_3; y_4 x_1)$	0
C_8	$2R$	$I(x_1; y_2 x_3)$	$I(x_4; y_5 x_2)$
C_9	$2R$	0	$I(x_2 x_4; y_3 y_5)$
C_{10}	$2R$	0	$I(x_4; y_5 x_2)$
C_{11}	$3R$	$I(x_3; y_4)$	0
C_{12}	$3R$	0	$I(x_2 x_4; y_3 y_5)$
C_{13}	$3R$	$I(x_1; y_2)$	$I(x_4; y_5)$
C_{14}	$3R$	0	$I(x_4; y_5)$
C_{15}	$4R$	0	$I(x_4; y_5)$

Table 3.14: Cuts, sum rates, and cut-set bounds in the network of $n = 4$ half-duplex nodes and a destination.

cut, C_k	$\sum_{\nu_i \in \mathcal{S}} R_i$	$I(\mathbf{x}_{\mathcal{S}}; \mathbf{y}_{\mathcal{S}_c} \mathbf{x}_{\mathcal{S}_c}, \boldsymbol{\sigma}_1)$	$I(\mathbf{x}_{\mathcal{S}}; \mathbf{y}_{\mathcal{S}_c} \mathbf{x}_{\mathcal{S}_c}, \boldsymbol{\sigma}_2)$
C_1	R	\mathcal{C}	0
C_2	R	0	\mathcal{C}
C_3	R	\mathcal{C}	0
C_4	R	0	\mathcal{C}
C_5	$2R$	0	\mathcal{C}
C_6	$2R$	$2\mathcal{C}$	0
C_7	$2R$	\mathcal{C}	0
C_8	$2R$	\mathcal{C}	\mathcal{C}
C_9	$2R$	0	$2\mathcal{C}$
C_{10}	$2R$	0	\mathcal{C}
C_{11}	$3R$	\mathcal{C}	0
C_{12}	$3R$	0	$2\mathcal{C}$
C_{13}	$3R$	\mathcal{C}	\mathcal{C}
C_{14}	$3R$	0	\mathcal{C}
C_{15}	$4R$	0	\mathcal{C}

Table 3.15: Cuts, sum rates, and cut-set bounds in the network of $n = 4$ half-duplex nodes and a destination. $\mathcal{C} = (1/2) \log_2(1 + \gamma)$ denotes the one-hop link capacity.

3.5.4 Half-duplex nodes, Two-hop communication

We allow the communication range to be extended to two-hop interval, $2d$, implying that the signal transmitted by any node in the network can be received and decoded by the nodes located within, at most, the two-hop distance from the originating node. Again, we examine the upper bound to the rate of traffic transfer in linear wireless networks consisting of only few nodes, say for example $n = 2, 3, 4$, and under such condition.

3.5.4.1 Two nodes, one destination ($n = 2$)

Consider a linear network of $n = 2$ half-duplex nodes and a destination, and suppose initially that we appoint three operating states to this network. Fig. 3.8 depicts this network along with its states.

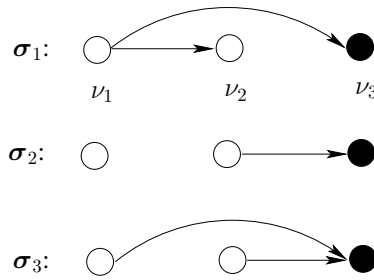


Figure 3.8: A network of $n = 2$ half-duplex nodes and a destination. The communication range is limited to two-hop distance. The network operates in $M = 3$ states.

The node and network states are listed in Table 3.16.

σ_m	σ_{1m}	σ_{2m}
σ_1	t	r
σ_2	s	t
σ_3	t	t

Table 3.16: Network and nodes' states appointed initially for a network of $n = 2$ nodes and a destination.

The cuts and their corresponding sum rates and cut-set bounds are mentioned respectively, in Tables 3.17 and 3.18.

cut, C_k	\mathcal{S}	\mathcal{S}_c
C_1	$\{\nu_1\}$	$\{\nu_2, \nu_3\}$
C_2	$\{\nu_2\}$	$\{\nu_1, \nu_3\}$
C_3	$\{\nu_1, \nu_2\}$	$\{\nu_3\}$

Table 3.17: Cuts in a network of $n = 2$ half-duplex nodes and a destination.

cut, C_k	$\sum_{\nu_i \in \mathcal{S}} R_i$	$I(\mathbf{x}_{\mathcal{S}}; \mathbf{y}_{\mathcal{S}_c} \mathbf{x}_{\mathcal{S}_c}, \boldsymbol{\sigma}_1)$	$I(\mathbf{x}_{\mathcal{S}}; \mathbf{y}_{\mathcal{S}_c} \mathbf{x}_{\mathcal{S}_c}, \boldsymbol{\sigma}_2)$	$I(\mathbf{x}_{\mathcal{S}}; \mathbf{y}_{\mathcal{S}_c} \mathbf{x}_{\mathcal{S}_c}, \boldsymbol{\sigma}_3)$
C_1	R	$I(x_1; y_2 y_3)$	0	$I(x_1; y_3 x_2)$
C_2	R	0	$I(x_2; y_3)$	$I(x_2; y_3 x_1)$
C_3	$2R$	$I(x_1; y_3)$	$I(x_2; y_3)$	$I(x_1 x_2; y_3)$

Table 3.18: Cuts, sum rates, and cut-set bounds in a network of $n = 2$ nodes and a destination, referred to the network shown in Fig. 3.8.

Under such situation, the received signals are

$$\begin{aligned}
\boldsymbol{\sigma}_1 : y_2 &= \sqrt{\gamma} x_1 + z_2 \\
y_3 &= \frac{1}{2} \sqrt{\gamma} x_1 + z_3 \\
\boldsymbol{\sigma}_2 : y_3 &= \sqrt{\gamma} x_2 + z_3 \\
\boldsymbol{\sigma}_3 : y_3 &= \sqrt{\gamma} \left(\frac{1}{2} x_1 + x_2 \right) + z_3
\end{aligned}$$

Let us compute, for example, the cut-set bound given through the mutual information $I(x_1 x_2; y_3)$ in Table 3.18, which is referred to the cut C_3 in the third state $\boldsymbol{\sigma}_3$, as follows

$$\begin{aligned}
I(x_1 x_2; y_3) &= H(y_3) - H(y_3 | x_1 x_2) \\
&= H(y_3) - H(z_3)
\end{aligned}$$

According to the received signal y_3 in state $\boldsymbol{\sigma}_3$,

$$y_3 = \begin{bmatrix} \frac{1}{2} \sqrt{\gamma} & \sqrt{\gamma} \end{bmatrix} \begin{bmatrix} x_1 \\ x_2 \end{bmatrix} + z_3$$

Regarding (3.6a), $H(y_3) = \frac{1}{2} \log_2 (2\pi e \det(\Sigma_{y_3}))$ where

$$\Sigma_{y_m} = \begin{bmatrix} \frac{1}{2}\sqrt{\gamma} & \sqrt{\gamma} \end{bmatrix} \begin{bmatrix} 1 & 0 \\ 0 & 1 \end{bmatrix} \begin{bmatrix} \frac{1}{2}\sqrt{\gamma} \\ \sqrt{\gamma} \end{bmatrix} + 1 = 1 + \frac{5}{4}\gamma$$

by assuming that x_1 and x_2 are independent, and $\Sigma_{z_3} = 1$. Thus

$$\begin{aligned} H(y_3) &= \frac{1}{2} \log_2 (2\pi e (1 + \frac{5}{4}\gamma)) \\ H(z_3) &= \frac{1}{2} \log_2 (2\pi e) \end{aligned}$$

and we get

$$I(x_1 x_2; y_3) = \frac{1}{2} \log_2 (1 + \frac{5}{4}\gamma) := \mathcal{C}_1$$

Similarly, other mutual informations are computed to be

$$\begin{aligned} I(x_1; y_2 y_3) &= \frac{1}{2} \log_2 (1 + \frac{5}{4}\gamma) \\ I(x_2; y_3 | x_1) &= I(x_2; y_3) = \frac{1}{2} \log_2 (1 + \gamma) := \mathcal{C}_2 \\ I(x_1; y_3 | x_2) &= I(x_1; y_3) = \frac{1}{2} \log_2 (1 + \frac{1}{4}\gamma) := \mathcal{C}_3 \end{aligned}$$

We substitute the these values into Table 3.18, an get

cut, \mathcal{C}_k	$\sum_{\nu_i \in \mathcal{S}} R_i$	$I(\mathbf{x}_{\mathcal{S}}; \mathbf{y}_{\mathcal{S}_c} \mathbf{x}_{\mathcal{S}_c}, \boldsymbol{\sigma}_1)$	$I(\mathbf{x}_{\mathcal{S}}; \mathbf{y}_{\mathcal{S}_c} \mathbf{x}_{\mathcal{S}_c}, \boldsymbol{\sigma}_2)$	$I(\mathbf{x}_{\mathcal{S}}; \mathbf{y}_{\mathcal{S}_c} \mathbf{x}_{\mathcal{S}_c}, \boldsymbol{\sigma}_3)$
\mathcal{C}_1	R	\mathcal{C}_1	0	\mathcal{C}_3
\mathcal{C}_2	R	0	\mathcal{C}_2	\mathcal{C}_2
\mathcal{C}_3	$2R$	\mathcal{C}_3	\mathcal{C}_2	\mathcal{C}_1

Table 3.19: Cuts, sum rates, and cut-set bounds in a network of $n = 2$ nodes and a destination.

The max-flow min-cut bound is obtained according to (3.8) as

$$R \leq \max_{\substack{t_m \\ \text{s.t. } \sum t_m = 1}} \min \left\{ \mathcal{C}_1 t_1 + \mathcal{C}_3 t_3, \mathcal{C}_2 (t_2 + t_3), \frac{1}{2} (\mathcal{C}_3 t_1 + \mathcal{C}_2 t_2 + \mathcal{C}_1 t_3) \right\}$$

and the solution is

The results suggest that the network operates actually in just two states, one is

γ [dB]	t_1	t_2	t_3
-10	0.884	0	0.115
10	0	0	1
30	0.162	0	0.837

Table 3.20: Time fractions of network states, referred to a network of $n = 2$ half-duplex nodes.

γ [dB]	$\max_{\mathbf{t}} \sum_m t_m I(\mathbf{x}_S; \mathbf{y}_{S_c} \mathbf{x}_{S_c}, \boldsymbol{\sigma}_m);$			Max-flow min-cut bound;
	C_1	C_2	C_3	$\min_{C_k} \sum_m t_m I(\mathbf{x}_S; \mathbf{y}_{S_c} \mathbf{x}_{S_c}, \boldsymbol{\sigma}_m)$
-10	0.077	0.008	0.008	0.008
10	0.903	1.729	0.848	0.848
30	4.174	4.174	8.91	4.174

Table 3.21: Cut-set bounds and the resulted max-flow min-cut bound in a network of $n = 2$ half-duplex nodes and a destination.

$\boldsymbol{\sigma}_1$ and the other is $\boldsymbol{\sigma}_3$, since the time fraction t_2 corresponding to the second state $\boldsymbol{\sigma}_2$ is always obtained to be equal to zero. Moreover, the max-flow min-cut bound is determined by the cut-set bound referred to the last cut C_3 .

3.5.4.2 Three nodes, one destination ($n = 3$)

We have a network of $n = 3$ half-duplex nodes and the communication range is restricted to two hops. Initially, we appoint six distinct states to such network as shown in Fig. 3.9.

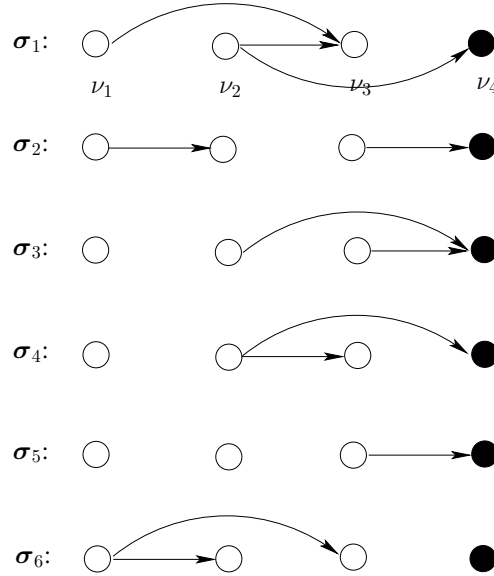


Figure 3.9: A network of $n = 3$ half-duplex nodes and a destination. We have appointed $M = 6$ states to it.

The six distinct states are

σ_m	σ_{1m}	σ_{2m}	σ_{3m}
σ_1	t	t	r
σ_2	t	r	t
σ_3	s	t	t
σ_4	s	t	r
σ_5	s	s	t
σ_6	t	r	r

Table 3.22: Network and nodes' states appointed initially for a network of $n = 3$ nodes and a destination.

The cuts and their corresponding sum rates with respect to the six states are listed in Table 3.23.

cut, C_k	$\sum_{v_i \in S} R_i$	$I(\mathbf{x}_S; \mathbf{y}_{S_c} \mathbf{x}_{S_c}, \boldsymbol{\sigma}_1)$	$I(\mathbf{x}_S; \mathbf{y}_{S_c} \mathbf{x}_{S_c}, \boldsymbol{\sigma}_2)$	$I(\mathbf{x}_S; \mathbf{y}_{S_c} \mathbf{x}_{S_c}, \boldsymbol{\sigma}_3)$	$I(\mathbf{x}_S; \mathbf{y}_{S_c} \mathbf{x}_{S_c}, \boldsymbol{\sigma}_4)$	$I(\mathbf{x}_S; \mathbf{y}_{S_c} \mathbf{x}_{S_c}, \boldsymbol{\sigma}_5)$	$I(\mathbf{x}_S; \mathbf{y}_{S_c} \mathbf{x}_{S_c}, \boldsymbol{\sigma}_6)$
C_1	R	$I(x_1; y_3 x_2)$	$I(x_1; y_2 x_3)$	0	0	0	$I(x_1; y_2 y_3)$
C_2	R	$I(x_2; y_3 y_4 x_1)$	0	$I(x_2; y_4)$	$I(x_2; y_3 y_4)$	0	0
C_3	R	0	$I(x_3; y_4 x_1)$	$I(x_3; y_4 x_2)$	0	$I(x_3; y_4)$	0
C_4	R	$I(x_2; y_3 y_4)$	$I(x_2; y_4 x_3)$	$I(x_2; y_3 y_4)$	0	$I(x_1; y_3)$	
C_5	$2R$	0	$I(x_1 x_3; y_2 y_4)$	$I(x_3; y_4 x_2)$	0	$I(x_3; y_4)$	$I(x_1; y_2)$
C_6	$2R$	$I(x_2; y_4 x_1)$	$I(x_3; y_4 x_1)$	$I(x_2 x_3; y_4)$	$I(x_2; y_4)$	$I(x_3; y_4)$	0
C_7	$2R$	$I(x_2; y_4)$	$I(x_3; y_4)$	$I(x_2 x_3; y_4)$	$I(x_2; y_4)$	$I(x_3; y_4)$	0

Table 3.23: Cuts, sum rates, and cut-set bounds, referred to a network of $n = 3$ half-duplex nodes, when the communication range is restricted to two-hop.

The received signals are written as

$$\begin{aligned}
\boldsymbol{\sigma}_1 : y_3 &= \sqrt{\gamma}(\frac{1}{2}x_1 + x_2) + z_3 \\
y_4 &= \frac{1}{2}\sqrt{\gamma}x_2 + z_4 \\
\boldsymbol{\sigma}_2 : y_2 &= \sqrt{\gamma}x_1 + z_2 \\
y_4 &= \sqrt{\gamma}x_3 + z_4 \\
\boldsymbol{\sigma}_3 : y_4 &= \sqrt{\gamma}(\frac{1}{2}x_2 + x_3) + z_4 \\
\boldsymbol{\sigma}_4 : y_3 &= \sqrt{\gamma}x_2 + z_3 \\
y_4 &= \frac{1}{2}\sqrt{\gamma}x_2 + z_4 \\
\boldsymbol{\sigma}_5 : y_4 &= \sqrt{\gamma}x_3 + z_4 \\
\boldsymbol{\sigma}_6 : y_2 &= \sqrt{\gamma}x_1 + z_2 \\
y_3 &= \frac{1}{2}\sqrt{\gamma}x_1 + z_3
\end{aligned} \tag{3.18}$$

For example, we compute $I(x_1x_2; y_3y_4)$ by noting that with respect to the received signals in the first state, $\boldsymbol{\sigma}_1$, we have

$$\mathbf{Y} = \begin{bmatrix} y_3 \\ y_4 \end{bmatrix} = \begin{bmatrix} \frac{1}{2}\sqrt{\gamma} & \sqrt{\gamma} \\ 0 & \frac{1}{2}\sqrt{\gamma} \end{bmatrix} \begin{bmatrix} x_1 \\ x_2 \end{bmatrix} + \begin{bmatrix} z_3 \\ z_4 \end{bmatrix} = \mathbf{Q}\mathbf{X} + \mathbf{Z}.$$

Since

$$\begin{aligned}
I(x_1x_2; y_3y_4) &= H(y_3y_4) - H(y_3y_4|x_1x_2) \\
&= H(y_3y_4) - H(z_3z_4)
\end{aligned}$$

thus, according to (3.6a), $H(y_3y_4) = \frac{1}{2} \log_2 ((2\pi e)^2 \det(\boldsymbol{\Sigma}_{\mathbf{Y}}))$, and upon the assumption of independence of x_1 and x_2 ,

$$\boldsymbol{\Sigma}_{\mathbf{Y}} = \begin{bmatrix} \frac{1}{2}\sqrt{\gamma} & \sqrt{\gamma} \\ 0 & \frac{1}{2}\sqrt{\gamma} \end{bmatrix} \begin{bmatrix} 1 & 0 \\ 0 & 1 \end{bmatrix} \begin{bmatrix} \frac{1}{2}\sqrt{\gamma} & 0 \\ \sqrt{\gamma} & \frac{1}{2}\sqrt{\gamma} \end{bmatrix} + \begin{bmatrix} 1 & 0 \\ 0 & 1 \end{bmatrix} = \begin{bmatrix} \frac{5}{4}\gamma + 1 & \frac{1}{2}\gamma \\ \frac{1}{2}\gamma & \frac{1}{4}\gamma + 1 \end{bmatrix}.$$

Finally, we get

$$I(x_1x_2; y_3y_4) = \frac{1}{2} \log_2 \left(1 + \frac{3}{2}\gamma + \frac{1}{16}\gamma^2 \right) := \mathcal{C}_1$$

Similarly, by considering the independence of the transmitted signals, the other mutual informations are obtained as

$$\begin{aligned}
I(x_1; y_2 y_3) &= I(x_2; y_3 y_4 | x_1) = I(x_2; y_3 y_4) = I(x_2 x_3; y_4) = \frac{1}{2} \log_2 \left(1 + \frac{5}{4} \gamma\right) := \mathcal{C}_2 \\
I(x_1; y_2 | x_3) &= I(x_3; y_4 | x_1) = I(x_3; y_4 | x_2) = I(x_3; y_4) = I(x_1; y_2) = \frac{1}{2} \log_2 (1 + \gamma) := \mathcal{C}_3 \\
I(x_1; y_3 | x_2) &= I(x_2; y_4 | x_1) = I(x_2; y_4) = I(x_2; y_4 | x_3) = I(x_1; y_3) = \frac{1}{2} \log_2 \left(1 + \frac{1}{4} \gamma\right) := \mathcal{C}_4
\end{aligned}$$

We obtain the max-flow min-cut bound to the rate of traffic transfer, R , according to (3.8)

$$\begin{aligned}
R \leq \max_{\substack{t_m, \\ \text{s.t. } \sum t_m = 1}} \min \left\{ \mathcal{C}_4 t_1 + \mathcal{C}_3 t_2 + \mathcal{C}_2 t_6, \mathcal{C}_2 t_1 + \mathcal{C}_4 t_3 + \mathcal{C}_2 t_4, \mathcal{C}_3 (t_2 + t_3 + t_5), \right. \\
\left. \frac{1}{2} (\mathcal{C}_1 t_1 + \mathcal{C}_4 (t_3 + t_6) + \mathcal{C}_2 t_4), \mathcal{C}_3 t_2 + \frac{1}{2} \mathcal{C}_3 (t_3 + t_5 + t_6), \right. \\
\left. \frac{1}{2} (\mathcal{C}_4 t_1 + \mathcal{C}_3 t_2 + \mathcal{C}_2 t_3 + \mathcal{C}_4 t_4 + \mathcal{C}_3 t_5), \right. \\
\left. \frac{1}{3} (\mathcal{C}_4 t_1 + \mathcal{C}_3 t_2 + \mathcal{C}_2 t_3 + \mathcal{C}_4 t_4 + \mathcal{C}_3 t_5) \right\}
\end{aligned}$$

By solving the above optimization problem, we get

γ [dB]	t_1	t_2	t_3	t_4	t_5	t_6
-10	0.314	0.211	0.474	0	0	0
10	0.248	0.180	0.571	0	0	0
30	0.093	0.258	0.647	0	0	0

Table 3.24: Time fractions of network states in a network of $n = 3$ half-duplex nodes when the communication range is two-hop.

The values of t_i 's reveals that among all six possible states considered initially, only the first three are non-trivial. The solution of the optimization problem is given in Table 3.25.

As we observe, for all values of γ , the cut-set bound corresponding the last cut, C_7 , determines the upper bound.

γ [dB]	$\max_{\mathbf{t}} \sum_m t_m I(\mathbf{x}_S; \mathbf{y}_{S_c} \mathbf{x}_{S_c}, \boldsymbol{\sigma}_m);$							Max-flow min-cut bound;
	C_1	C_2	C_3	C_4	C_5	C_6	C_7	$\min_{C_k} \sum_m t_m I(\mathbf{x}_S; \mathbf{y}_{S_c} \mathbf{x}_{S_c}, \boldsymbol{\sigma}_m)$
-10	0.020	0.035	0.047	0.020	0.030	0.030	0.020	0.020
10	0.536	0.982	1.299	0.536	0.805	0.804	0.536	0.536
30	1.664	3.062	4.515	1.664	2.902	2.497	1.664	1.664

Table 3.25: Cut-set bounds and the resulted max-flow min-cut bound referred to a network of $n = 3$ half-duplex nodes.

3.5.4.3 Four nodes, one destination ($n = 4$)

For the case of a linear network with $n = 4$ half-duplex nodes assuming the two-hop communication scenario, we nominate initially twelve distinct states as mentioned in Table 3.26.

	σ_{1m}	σ_{1m}	σ_{1m}	σ_{1m}
σ_1	t	r	t	t
σ_2	t	t	r	t
σ_3	r	t	r	t
σ_4	t	r	r	t
σ_5	s	t	t	r
σ_6	t	r	t	r
σ_7	s	s	s	t
σ_8	s	s	t	t
σ_9	t	r	r	s
σ_{10}	s	s	t	r
σ_{11}	t	t	r	r
σ_{12}	s	t	r	r

Table 3.26: Network and nodes' states appointed initially for a network of $n = 4$ half-duplex nodes and a destination.

We neglect the details on the computation of the cut-set bounds in this case, and present here the final solution only. The time fractions of network states obtained by solving the optimization problem are given in Table 3.27.

γ [dB]	t_1	t_2	t_3	t_4	t_5	t_6	t_7	t_8	t_9	t_{10}	t_{11}	t_{12}
-10	0.185	0.190	0.084	0	0.354	0	0	0.184	0	0	0	0
10	0.210	0.241	0	0	0.336	0	0	0.212	0	0	0	0
30	0.232	0.304	0	0	0.215	0	0	0.248	0	0	0	0

Table 3.27: Time fractions of network states, the network has $n = 4$ half-duplex nodes and one destination. Note that only t_1, t_2, t_5 and t_8 have nonzero values.

Consequently, there are only four non-trivial states in this case as

	σ_{1m}	σ_{1m}	σ_{1m}	σ_{1m}
σ_1	t	r	t	t
σ_2	t	t	r	t
σ_5	s	t	t	r
σ_8	s	s	t	t

Table 3.28: Actual (i.e. nontrivial) network states for a network of $n = 4$ half-duplex nodes.

Tables 3.29 and 3.30 present the solutions to the cut-set bounds and the max-flow min-cut bound for different amounts of signal-to-noise ratio γ .

γ [dB]	$\max_t \sum_m t_m I(\mathbf{x}_S; \mathbf{y}_{S_c} \mathbf{x}_{S_c}, \boldsymbol{\sigma}_m);$						
	C_1	C_2	C_3	C_4	C_5	C_6	C_7
-10	0.016	0.025	0.036	0.044	0.014	0.024	0.030
10	0.581	0.721	1.013	1.147	0.378	0.688	0.864
30	2.369	2.374	3.023	3.910	1.211	2.090	3.140

Table 3.29: Cut-set bounds obtained for a network of $n = 4$ half-duplex nodes (referred to cuts C_1, \dots, C_7).

C_8	C_9	C_{10}	C_{11}	C_{12}	C_{13}	C_{14}	C_{15}	Max-flow min-cut bound;
								$\min_{C_k} \sum_m t_m I(\mathbf{x}_S; \mathbf{y}_{S_c} \mathbf{x}_{S_c}, \boldsymbol{\sigma}_m)$
0.021	0.031	0.028	0.014	0.022	0.023	0.014	0.014	0.014
0.567	0.781	0.756	0.378	0.533	0.625	0.378	0.378	0.378
1.817	2.713	2.423	1.211	1.824	2.001	1.211	1.211	1.211

Table 3.30: Cut-set bounds and max-flow min-cut bound for a network of $n = 4$ half-duplex nodes (referred to cuts C_8, \dots, C_{15}).

The results show that similar to the case of the network with $n = 3$ nodes, in a network of $n = 4$ nodes, the cut-set bound referred to the last cut C_{15} , i.e. the cut that separates the nodes from the data destination node, provides the *max-flow min-cut* bound.

3.6 Concluding remarks

In this chapter, we considered computing the cut-set bounds to the average achievable rates of traffic transfer in the linear wireless network, where the nodes are supposed to send their own traffic as well as to relay other nodes' traffic toward the destination. Indeed, we studied such network scenario for the two cases of full-duplex and half-duplex nodes. Half-duplexity refers to the situation where due to practical limitations on hardware and power resources in the network nodes, they are not able to transmit and receive simultaneously. This in turn prompts the network to operate in several states other than just one. The *exact* solution to the max-flow min-cut problem in such networks is only computable in the networks with very few nodes, otherwise, solving such problem demands for extravagant numerical computations, and hence is not tractable. However, the solutions obtained in the networks consisting of only a few number of nodes, provide us with some useful insights into figuring out how do such networks with larger number of nodes such as

- In the network with half-duplex nodes, and when the communication range is restricted to one-hop distance, the transfer of nodes' traffic to the destination requires the network to operate in just two distinct states.
- In linear wireless networks, the cut-set bounds corresponding to the last cuts – i.e., the cuts that separate the the near-destination nodes (and the destination) from the rest of the nodes – contribute to the max-flow min-cut bound to the rate of traffic transfer.

Chapter 4

Fairness in Traffic Relaying in One-hop Linear Wireless Networks

In this chapter we analyze the achievable data rate of cooperative relaying strategies in networks where nodes operate in half-duplex mode. Every node needs to deliver its data to a gateway node at the same rate; also, nodes may have limited energy capabilities, as in the case of energy-harvesting communication networks. Under such constraints, we first take an information-theoretic approach and derive cut-set upper bounds to the achievable rate. Then, we devise two communication strategies, each aiming at a different objective. The former ensures a high, fair rate allocation to the network nodes, but it neglects their energy constraints. The latter does consider energy constraints by meeting the requirements on the average power consumption at each node, and provides fairness in the data rate allocation. We compare the performance of the aforementioned communication strategies to the upper bounds, showing their effectiveness and providing useful insights on the system behavior.

4.1 Introduction

Multi-hop communications are often used in wireless networks for traffic delivery when source and destination are not within each other's radio range. In this case, the

sequence of links over which data should be routed, i.e., the source-destination path, and the link scheduling, i.e., when and for how long the links should be activated, need to be determined.

In this chapter, we address the latter issue by taking an information-theoretic approach. More specifically, we consider a wireless network with linear topology whose nodes need to deliver their traffic to a gateway node through multi-hop data transfers. Nodes share the same radio resources and generate their own data (that need to be delivered to the gateway) at the same rate. Such a system well represents, e.g., sensor networks for path and street monitoring, and multi-hop networks for road or traffic videosurveillance [36].

We assume that, when nodes relay data for others, they adopt the decode-and-forward (DF) paradigm [20]. Also, the node transmission rates and powers correspond to optimal coding over a discrete-time additive white Gaussian noise (AWGN) channel, although more general channels and coding schemes could be considered as well. While modeling the network system, we account for practical aspects by considering that nodes are equipped with half-duplex radios (i.e., they cannot transmit and receive at the same time) and they may be energy constrained.

Under the above conditions, the scheduling of traffic links is of primary importance, as it determines both the maximum data rate achievable by the network nodes and the energy consumption they experience. Specifically, with regard to the latter issue, link scheduling may help address (i) the energy hole problem [37,38], i.e., the unfairness arising in the energy consumption experienced by the nodes depending on their distance from the gateway, and (ii) the time-dependent power availability in energy-harvesting communication systems, where energy becomes available only at certain known instants thus imposing a maximum power consumption rate at the nodes.

In this context, we devise two traffic relaying strategies. The former aims at achieving high data rate performance while providing fairness in the rate allocation

at the network nodes. By fairness in rate allocation, we mean that all nodes can have their data delivered to the gateway at the same average rate, as they exhibit equal traffic demand. The latter, instead, aims at maximizing the achievable data rate while ensuring fairness in both the data rate and the energy consumption at every node. For each of the proposed strategies, we derive an expression for the achievable rate and average power consumption, and compare the performance to that of classic multi-hop data transfer. Furthermore, we derive the cut-set upper bound [29, 30] to the achievable rate for our network scenario, both with and without the constraint on the energy consumption, and compare the maximum data rate attained by each proposed strategy to the corresponding bound.

4.2 Related Work

We highlight that several papers appeared in the literature have dealt with traffic relaying in wireless networks by adopting an information-theory perspective, however our study significantly differs from previous work. Indeed, some of the earlier papers have considered sources that transfer their data with the help of other nodes, but the latter only act as relays (i.e., they do not generate any data) [20,35,39]. Other works have studied the case of sources that can also relay other nodes' traffic, however they assume that the nodes are full-duplex [31,40], or that the network includes just a small number of half-duplex nodes [41]. In addition, previous studies have maximized the sum rates of the source nodes, while in our work we aim at maximizing the node rate under the constraint that all nodes achieve the same performance. A work that analyzes a cascade of source and relay nodes with half-duplex constraints is in [42]. There, the information transfer is carried out by applying a coding scheme that allocates the transmission and reception time slots at the relays depending on the amount of information to be transferred. Through numerical results, the authors show that their strategy achieves the cut-set bound when the rates of nodes acting as both sources and relays fall below certain thresholds. Unlike our

study, however, the work in [42] assumes that adjacent node pairs are connected via error-free links and that the nodes are synchronized at the symbol level.

As for energy consumption, a number of energy-efficient cooperative communication schemes have been proposed in the literature, e.g., [32, 33]. The scope and methodology of these works differ from ours, as they focus either on the design of algorithms and protocols for sensor networks, or target totally different scenarios (e.g., MIMO communications). Approaches, as the one adopted in [43, 44], assume that traffic can be buffered at the nodes and minimize the energy consumption of the *whole* network when the data must be delivered within a given time deadline. Furthermore, these studies consider that the energy consumption is proportional to the output transmit power, an assumption that does not hold for most wireless communication devices where the power consumption due to the transceiver cannot be neglected. The problem of minimizing energy consumption considering both the output transmit power and the transceiver contribution has been addressed by designing suitable routing and MAC protocols. Very few works have dealt with such an issue from a theoretical viewpoint, and, again, they aim either at minimizing the energy consumption of the whole network [45, 46], i.e., they do not address the energy hole problem, or at maximizing the network lifetime [34, 47]. Note that, besides having a different scope, the study in [34] considers a variable-length TDMA scheme but, unlike our work, it takes the data rates of the source nodes as an input to the problem of the transmissions scheduling.

In summary, the key contributions of our work are:

- i) We pose the problem of defining relaying strategies for attaining fairness in the nodes data rate in networks of arbitrary size, under the practical assumptions that all nodes are half duplex and can act as both sources and relays (Section 4.3);
- ii) We derive the cut-set upper bound [29, 30] to the achievable rate for our network scenario. Based on that, we propose a strategy that ensures a high data

rate to all nodes and fairness in the rate allocation, while taking interference (i.e., due to hidden terminals) into account. We then compare the performance of our strategy to the bound as well as to the performance of classic multi-hop data transfer (Section 4.4);

- iii) We address the energy-hole problem and derive the cut-set upper bound to the achievable data rate when the average power consumption at the nodes is constrained to a target value. Furthermore, we envision a classic multi-hop strategy but with optimized link scheduling. In particular, the link scheduling we implement maximizes the nodes data rate while ensuring fairness in both the energy consumption and the data rate allocation at each network node. The performance of such a scheme is then compared to the bound (Section 4.5).

Before introducing our analysis and main results, in the next section we describe the system model under study.

4.3 System model

Network topology. We consider a network composed of n wireless nodes; each node generates independent information messages that need to be delivered to a gateway node, G . We assume the network topology to be linear and we label the $n + 1$ nodes forming the path as $1, \dots, n, G$, with the last node being the gateway. For simplicity, in our analysis we also assume that the nodes are equally spaced along the path, and the inter-node distance is denoted by d , as depicted in Figure 5.1; we will refer to it as the one-hop distance.



Figure 4.1: Network with linear topology, the gateway (sink) is shown in black.

Node and network states. The nodes work in half-duplex mode. While the gateway node is assumed to be always in receiving mode, the nodes $1, \dots, n$ can operate in three different states, namely transmission, reception, and sleep, in the following denoted by \mathfrak{t} , \mathfrak{r} , \mathfrak{s} , respectively. The state of the generic node is indicated as $\sigma \in \{\mathfrak{t}, \mathfrak{r}, \mathfrak{s}\}$. Moreover, for $i = 1, \dots, n$, we denote by t_i^σ the fraction of time spent by node i in state σ , with

$$t_i^{\mathfrak{t}} + t_i^{\mathfrak{r}} + t_i^{\mathfrak{s}} = 1. \quad (4.1)$$

The state of the network is therefore represented by the vector $\boldsymbol{\sigma} = [\sigma_1, \dots, \sigma_n]$, with $\sigma_i \in \{\mathfrak{t}, \mathfrak{r}, \mathfrak{s}\}$ being the state of node i ($i = 1, \dots, n$). Since each node may be in three possible states, the network can take up to 3^n states. The variable t^σ denotes the fraction of time that the network spends in state $\boldsymbol{\sigma}$, with $\sum_{\boldsymbol{\sigma}} t^\sigma = 1$.

Power consumption. We denote by P_e the power consumption of the transceiver electronics at each node. In the following, we use such a quantity as a reference

value, by normalizing the powers involved in our analysis with respect to P_e . In particular, we assume that the normalized power consumption at the generic node i ($i = 1, \dots, n$) is as follows:

$$\frac{P_i^\sigma}{P_e} = \begin{cases} 1 + \alpha_i & \text{if } \sigma = \text{t} \\ 1 & \text{if } \sigma = \text{r} \\ 0 & \text{if } \sigma = \text{s} \end{cases} \quad (4.2)$$

where $\alpha_i = P_i^{\text{tx}}/P_e$ and P_i^{tx} is the power irradiated by the antenna of node i . Also, when neither transmitting nor receiving, a node can enter a sleep mode, characterized by negligible power consumption. Then, the average power consumption of node i (normalized to P_e) is given by

$$\pi_i = \mathbb{E}_\sigma \left[\frac{P_i^\sigma}{P_e} \right] = (1 + \alpha_i)t_i^{\text{t}} + t_i^{\text{r}} \quad i = 1, \dots, n. \quad (4.3)$$

When energy constraints are considered, we denote by π the (normalized) average power consumption that every node should experience. Such a constraint well represents the case of networks composed of energy harvester nodes, in which the power consumption at each node, averaged over time, cannot exceed a given maximum value [48].

Communication channel. Nodes share the same frequency channel of bandwidth W and are willing to relay traffic for others toward the gateway G , by adopting a DF relaying technique [20]. Since our network topology represents a multi-hop path toward G , in the following we consider that each node carries out single-hop transmissions. Also, every node i ($i = 1, \dots, n$) has the same amount of data to deliver to the gateway in the unit time. Hence, in order to ensure fairness among the n nodes, we impose that each of them needs to achieve the same average data rate.

As for the propagation model, we assume that the signal power decays exponentially with the distance, and the path loss exponent is a . Furthermore, we consider an AWGN channel with same noise power spectral density, N_0 , at all the receivers.

We then define γ as the signal-to-noise ratio (SNR) observed at a receiver located at one-hop distance (d meters) from the transmitter, when the sender transmits at a power level equal to P_e and in absence of interferers. In other words,

$$\gamma = \frac{P_e G_t G_r}{N_0 W} \left(\frac{\lambda}{4\pi d} \right)^a \quad (4.4)$$

where G_t and G_r are the transmit and receive antenna gains, respectively, and λ is the signal carrier wavelength. Then, given a generic transmitter-receiver node pair at one-hop distance from each other, the transmitter-receiver point-to-point link is assigned an instantaneous transmission rate, which is assumed to correspond to optimal coding over the above discrete-time channel. Clearly, such a rate will depend on γ , the transmit output power that is used, and the number of interfering links (i.e., the hidden terminals) that are simultaneously active.

4.4 Fairness in achievable data rate

We first focus on a cooperative relaying strategy whose goal is to maximize the achievable data rate of the network nodes in a fair manner. In order to get some insight on the design of such a strategy, we start by deriving an upper bound, based on the cut-set bound, to the maximum data rate that the network nodes can achieve.

4.4.1 An upper bound to the achievable data rate

We adopt the notation introduced in [30], and derive the cut-set bound by extending to our network scenario the results obtained in [29]. Note that [29] addresses half-duplex networks, but including one source node only.

Specifically, since in our case all nodes are data sources, we assume that any node i ($i = 1, \dots, n$) generates independent messages W_i with the same rate $R_b = \mathcal{R}(W_i)$, and that estimates of these messages have to be obtained at the gateway G . In order to ease the derivation of the bound, we consider the network as a cascade of

n discrete memoryless channels (see Figure 5.1), where the generic node i receives the output of the channel $i - 1$, y_i , and transmits the signal x_i to node $i + 1$ via the i -th channel. Also, since here we are not concerned with energy consumption, we assume that a node in state t irradiates an arbitrary power $P_i^{\text{tx}} = P^{\text{tx}}$, which is the same for any node of the network. It follows that, for any i , the capacity of the i -th link, i.e., the link connecting node i to node $i + 1$, is given by $\mathcal{C} = \log_2(1 + \alpha\gamma)$ where $\alpha = P^{\text{tx}}/P_e$.

In general, the computation of the cut-set bound for the network under study requires us to consider $2^n - 1$ network cuts, each of them separating some of the messages from their corresponding estimates. However, thanks to the above assumptions, we can apply the max-flow min-cut theorem [49] and restrict the number of cuts to n . We denote the generic cut of the network by the pair $(\mathcal{S}_i, \bar{\mathcal{S}}_i)$, where \mathcal{S}_i is the set of nodes $\{1, \dots, i\}$ and $\bar{\mathcal{S}}_i = \{i + 1, \dots, n, G\}$. We recall that all nodes are sources of messages with rate R_b , thus the sum of the rates of the messages generated in \mathcal{S}_i is iR_b . For such a cut, the rate R_b for reliable communications is given by

$$R_b \leq \frac{W}{i} I(x_{\mathcal{S}_i}; y_{\bar{\mathcal{S}}_i} | x_{\bar{\mathcal{S}}_i}) \stackrel{a}{=} \frac{W}{i} I(x_i; y_{i+1}) \quad (4.5)$$

where $x_{\mathcal{S}_i} = \{x_1, \dots, x_i\}$, $y_{\bar{\mathcal{S}}_i} = \{y_{i+1}, \dots, y_n, y_G\}$, $x_{\bar{\mathcal{S}}_i} = \{x_{i+1}, \dots, x_n\}$, and I denotes the mutual information. In (4.5), the equality (a) is due to the assumption that the channel output y_{i+1} depends only on the channel input x_i .

Since the network nodes operate in half-duplex mode, the mutual information in (4.5) can be rewritten by conditioning over the network state σ :

$$I(x_i; y_{i+1}) = \sum_{\sigma} t^{\sigma} I(x_i; y_{i+1} | \sigma) = t_i^t \mathcal{C} \quad (4.6)$$

where we recall that t^{σ} represents the fraction of time the network spends in state σ . Since the i -th link is active only when node i is transmitting, then the mutual information in (4.6) is proportional to the fraction of time, t_i^t , spent by node i in

state \mathfrak{t} .

Considering all cuts $(\mathcal{S}_i, \bar{\mathcal{S}}_i)$, for $i = 1, \dots, n$ and maximizing over the time spent by the network in each state, the expression of the bound is given by

$$R_b \leq WC \max_{\sum_{\sigma} t_i^{\sigma} = 1} \min_i \frac{t_i^{\mathfrak{t}}}{i}. \quad (4.7)$$

In order to solve (4.7), we first note that the amount of data that node i has to transmit through the i -th link must be i times the information transmitted through link 1 by node 1. Since links 1 and i have the same capacity, we can write $t_i^{\mathfrak{t}}/i = t_1^{\mathfrak{t}}$, i.e., the argument of (4.7) does not depend on i . We can therefore arbitrarily set $i = n$ and remove the min operator in (4.7). We also note that the data that node i has to receive, through link $i - 1$, is $i - 1$ times the information transmitted by node 1. It follows that $t_i^{\mathfrak{r}} = (i - 1)t_1^{\mathfrak{t}}$. By using these expressions for $t_i^{\mathfrak{t}}$ and $t_i^{\mathfrak{r}}$ in (4.1) and setting $i = n$, we obtain $t_n^{\mathfrak{s}} = 1 - (2n - 1)t_1^{\mathfrak{t}}$, i.e., $t_1^{\mathfrak{t}} = (1 - t_n^{\mathfrak{s}})/(2n - 1)$. By substituting this result in (4.7), we can rewrite the bound as

$$R_b \leq WC \max_{\sum_{\sigma} t_n^{\sigma} = 1} \frac{1 - t_n^{\mathfrak{s}}}{2n - 1}$$

which is maximized for $t_n^{\mathfrak{s}} = 0$. Thus, the average rate achieved by the nodes is limited by

$$R_b \leq \frac{WC}{2n - 1}. \quad (4.8)$$

Since the rate achieved by the first node is $t_1^{\mathfrak{t}}WC$, from (4.8) it follows immediately that $t_1^{\mathfrak{t}} = 1/(2n - 1)$. It follows that, for $i = 1, \dots, n$, we have

$$\begin{aligned} t_i^{\mathfrak{t}} &= i/(2n - 1); & t_i^{\mathfrak{r}} &= (i - 1)/(2n - 1) \\ t_i^{\mathfrak{s}} &= 2(n - i)/(2n - 1). \end{aligned} \quad (4.9)$$

We remark that the derivation of the bound outlined above does not account for interference among simultaneous transmissions. A communication strategy that,

		Node state							
	σ	t^σ	σ_1	σ_2	σ_3	σ_4	\dots	σ_{n-1}	σ_n
Network state	σ_1	$\frac{1}{2n-1}$	t	r	t	r	\dots	r	t
	σ_2	$\frac{2}{2n-1}$	s	t	r	t	\dots	t	r
	σ_3	$\frac{2}{2n-1}$	s	s	t	r	\dots	r	t
	σ_4	$\frac{2}{2n-1}$	s	s	s	t	\dots	t	r
	σ_5	$\frac{2}{2n-1}$	s	s	s	s	\dots	r	t
	\vdots	\vdots	\vdots	\vdots	\vdots	\vdots	\dots	\vdots	\vdots
	σ_{n-1}	$\frac{2}{2n-1}$	s	s	s	s	\dots	t	r
	σ_n	$\frac{2}{2n-1}$	s	s	s	s	\dots	s	t
		t_i^t	$\frac{1}{2n-1}$	$\frac{2}{2n-1}$	$\frac{3}{2n-1}$	$\frac{4}{2n-1}$	\dots	$\frac{n-1}{2n-1}$	$\frac{n}{2n-1}$
		t_i^r	0	$\frac{1}{2n-1}$	$\frac{2}{2n-1}$	$\frac{3}{2n-1}$	\dots	$\frac{n-2}{2n-1}$	$\frac{n-1}{2n-1}$
	t_i^s	$\frac{2n-2}{2n-1}$	$\frac{2n-4}{2n-1}$	$\frac{2n-6}{2n-1}$	$\frac{2n-8}{2n-1}$	\dots	$\frac{2}{2n-1}$	0	

Table 4.1: Communication strategy achieving the bound

under the same conditions, achieves the bound in (4.8) is outlined in Table 4.1.

In this strategy, the network has n states, denoted by $\sigma_1, \dots, \sigma_n$, with associated time fractions $t^{\sigma_1}, \dots, t^{\sigma_n}$ such that $\sum_{m=1}^n t^{\sigma_m} = 1$. For each network state $\sigma_m = [\sigma_{j1}, \dots, \sigma_{jn}]$, the table shows the state of the nodes $\sigma_{j1}, \dots, \sigma_{jn}$. Specifically, in network state σ_m :

- nodes $1, \dots, m-1$ are in sleep mode (s);
- nodes $m+2h$, with $h = 0, \dots, \lfloor (n-m)/2 \rfloor$, are transmitting (t);
- nodes $m+2h+1$, with $h = 0, \dots, \lfloor (n-m-1)/2 \rfloor$, are receiving (r).

The last three rows of Table 4.1 show the time fractions t_i^σ for any node i , defined as $t_i^\sigma = \sum_{m=1}^n 1\{\sigma_{ji} = \sigma\} t^{\sigma_m}$, for $i = 1, \dots, n$ and $\sigma \in \{t, r, s\}$. Such time fractions coincide with those obtained in (4.9). Note that this strategy allows more than one transmission to occur at the same time, but, as mentioned, interference among them is not considered.

Finally, using (4.3), the average (normalized) power consumption of the generic node i can be written as:

$$\pi_{b,i} = (1 + \alpha)t_i^t + t_i^r = \frac{i(\alpha + 2) - 1}{2n - 1}. \quad (4.10)$$

4.4.2 The Cooperative Sub-chains strategy

The communication strategy summarized in Table 4.1, which achieves the cut-set upper bound to the average rate, suggests that:

- (i) the i -th node needs to transmit (resp. receive) for a time fraction that is i (resp. $i - 1$) times the transmission period of node 1;
- (ii) nodes should transmit as often as possible, provided that the half-duplex constraints are met, hence $t_n^s = 0$.

However, the strategy in Table 4.1 does not account for the interference that may affect simultaneous transmissions, hence degrade the achievable rate. Based on the above observations, we propose a communication strategy that adheres to the two aforementioned requirements, but it groups nodes into different sets, called *sub-chains*. Within each sub-chain, at most one node at a time can transmit, so as to limit the interference between simultaneous transmissions. We recall this strategy as *Cooperative Sub-chains* introduced already in Chapter 2.

More specifically, according to the Cooperative Sub-chains scheme, each sub-chain contains $k > 1$ adjacent nodes, thus q sub-chains can be formed, with $q = \lceil n/k \rceil$. In general, n is not a multiple of k . If so, one of the sub-chains will contain less than k nodes, namely, $k_1 = n - k(q - 1)$ nodes; without loss of generality, we assume that this is the closest sub-chain to the gateway node. Again, we assume that all nodes use the same output transmission power (i.e., $\alpha_i = \alpha$ for any node i); also, time is discretized into slots of equal duration t . An example of the Cooperative Sub-chains strategy for $n = 10$ and $k = 4$ is depicted in Figure 4.2. In the example, we have $q = \lceil 10/4 \rceil = 3$ sub-chains, with the last sub-chain including $k_1 = 2$ nodes.

$$R_r \leq W \log_2 \left(1 + \frac{\gamma}{(1 + \alpha)^{-1} + \gamma \sum_{i=1}^{q-r} (ki - 1)^{-a} + \sum_{i=1}^{r-1} (ki + 1)^{-a}} \right) \quad (4.11)$$

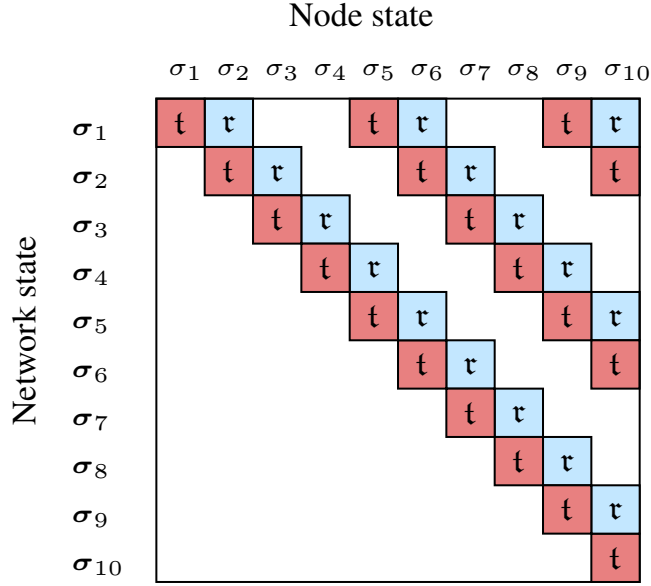


Figure 4.2: Cooperative Sub-chains strategy for $n = 10$ and $k = 4$. Nodes in sleep state are not shown.

Initially, classic multi-hop data transfer, i.e., a hop-by-hop data transfer with only one node transmitting at a time, is applied within each sub-chain. Hereinafter, we refer to classic multi-hop data transfer as Multi-hop. For instance, in sub-chain r , $r = 1, \dots, q$, the first node generates some data and transmit them to the second node, in one slot. Node 2 will relay the received data and transmit its own, in the next two slots. This procedure is repeated till all data originated within sub-chain r are transferred to the first node of the next sub-chain (i.e., node 1 of sub-chain $r + 1$). This procedure is applied simultaneously to all sub-chains $r = 1, \dots, q$. Overall, this phase lasts $k(k + 1)/2$ slots, however in the first $k_1(k_1 + 1)/2$ slots q nodes transmit simultaneously while in the remaining time only $q - 1$ transmit at the same time (see the example in Figure 4.2).

Next, every sub-chain needs to relay the data (if any) received from the upstream sub-chain to the downstream one. As before, at any time instant, there is at most one transmitting node per sub-chain, however each transmission now requires k slots as it has to transfer the bulk of data generated within one of the upstream sub-chains.

As the data flow downstream, the sub-chains that are farther away from the gateway G become inactive (i.e., all their nodes enter the sleep state), and only the

nodes closer to G need to transmit/receive.

Let us define as T_{cs} the total number of slots needed to transfer to G the data originated by all nodes, under the Cooperative Sub-chains strategy. We note that the number of states taken by the network under the Cooperative Sub-chains scheme is equal to n , namely, $\sigma_1, \dots, \sigma_n$. In particular, state σ_m , with $m = 1, \dots, k$, has an associated time fraction $t^{\sigma_m} = m/T_{cs}$ while state σ_m , with $m = k + 1, \dots, n$, has an associated time fraction $t^{\sigma_m} = k/T_{cs}$. Thus, we can write

$$T_{cs} = k(k + 1)/2 + k(n - k).$$

As for the time spent by a node in each state, from the above description, one can infer that node i has to transmit for i slots and receive for $i - 1$ slots, and then it is in sleep mode for the rest of the time, i.e.,

$$\begin{aligned} t^t &= i/T_{cs}, \\ t^r &= (i - 1)/T_{cs} \text{ and} \\ t^s &= 1 - (2i - 1)/T_{cs}. \end{aligned}$$

As for the achievable rate, we observe that, for every node located in sub-chain r ($1 \leq r \leq q$), the constraint on the achievable instantaneous rate is as in (10). In the equation, the second term in the logarithmic function is the SINR at the receiver node in the r -th sub-chain. In particular, the two sums at the denominator account for the interference due to the $q - r$ and $r - 1$ transmitters (i.e., hidden terminals) located, respectively, in the $q - r$ sub-chains on the right side and in the $r - 1$ sub-chains on the left side of sub-chain r . The constraint on the achievable instantaneous rate is then given by $\min_r R_r$. It is clear that the minimum over all R_r 's is represented by the rate associated to the sub-chain in the middle of the linear topology (i.e., $r = \lceil q/2 \rceil$), which indeed experiences the highest interference. The

average achievable rate can be therefore written as:

$$R_{cs} = \min_r R_r / T_{cs} .$$

For completeness, we also derive the average power consumption of the generic node i , during the Cooperative Sub-chains procedure (i.e., T_{cs} slots). In general, node i receives the data generated by all nodes on its left side ($i - 1$ nodes) and retransmits them, along with its own data; it is then in sleep state for the rest of the time. Thus, by using (4.2), the average power consumption at node i ($i = 1, \dots, n$) is given by:

$$\pi_{cs,i} = \frac{(2i - 1) + i\alpha}{T_{cs}} .$$

As the last remark, we highlight that, under the same assumptions made for the Cooperative Sub-chains scheme, classic multi-hop data transfer can be regarded as a special case of Cooperative Sub-chains for $k = n$. Indeed, as already mentioned, in Multi-hop there is only one node transmitting at any time instant in the whole network. The generic node i employs node $i + 1$ as a relay and acts, in its turn, as a relay for node $i - 1$; thus, node n ends up transmitting all other nodes' traffic toward G . It follows that, by setting $k = n$ in the expressions derived for the Cooperative Sub-chains strategy, we can readily obtain the data transfer duration, the average node rate, and the average node power consumption under the Multi-hop scheme, i.e.,

$$\begin{aligned} T_{mh} &= \frac{n(n + 1)}{2} \\ R_{mh} &\leq W \frac{\log_2(1 + \alpha\gamma)}{T_{mh}} \\ \pi_{mh,i} &= \frac{(2i - 1) + i\alpha}{T_{mh}} \end{aligned} \quad (4.12)$$

4.4.3 Results

We first evaluate the performance of the Cooperative Sub-chains strategy for different values of the parameter k , i.e., the number of nodes per sub-chain. By doing so, we identify the value of k that allows the highest achievable rate. While deriving our results, we set $n = 20$, $a = 3$, and let d vary so as to consider different values of γ .

Fig. 4.3 shows the average maximum rate that can be achieved through the Cooperative Sub-chains as k varies between 2 and 20, for $\alpha = 0.1$ and $\alpha = 10$, respectively. Note that 2 is the minimum value that k can take, while for $k = n = 20$ the Cooperative Sub-chains degenerates into the Multi-hop strategy. Interestingly, for low values of α (i.e., output transmit power), short sub-chains are always to be preferred, while, for a large value of α ($\alpha = 10$), small k 's (between 3 and 4) are optimal only for low values of γ . Indeed, large values of γ and α correspond to high interference between simultaneous transmissions, which reduces the achievable rate. As a consequence, the Multi-hop, which does not involve simultaneous transmissions, becomes the best strategy and, consistently, the optimal size of the sub-chains becomes 20.

Next, we compare the results obtained for the Cooperative Sub-chains strategy, with the above optimal value of k , to the cut-set upper bound as well as to the performance of the Multi-hop scheme.

Fig. 4.4 depicts the average maximum rates that can be achieved through the Multi-hop and the Cooperative Sub-chains schemes for, respectively, $\alpha = 0.1$ and $\alpha = 10$, and compares them to the cut-set upper bound in (4.8). Looking at Fig. 4.4 (top), we observe that the Cooperative Sub-chains strategy achieves very close performance to the upper bound for low-medium values of γ , while it behaves as the Multi-hop scheme for high values of SNR. Indeed, the upper bound does not account for interference between simultaneous transmissions, thus it becomes less tight when such a contribution dominates. This suggests that, by varying k , the

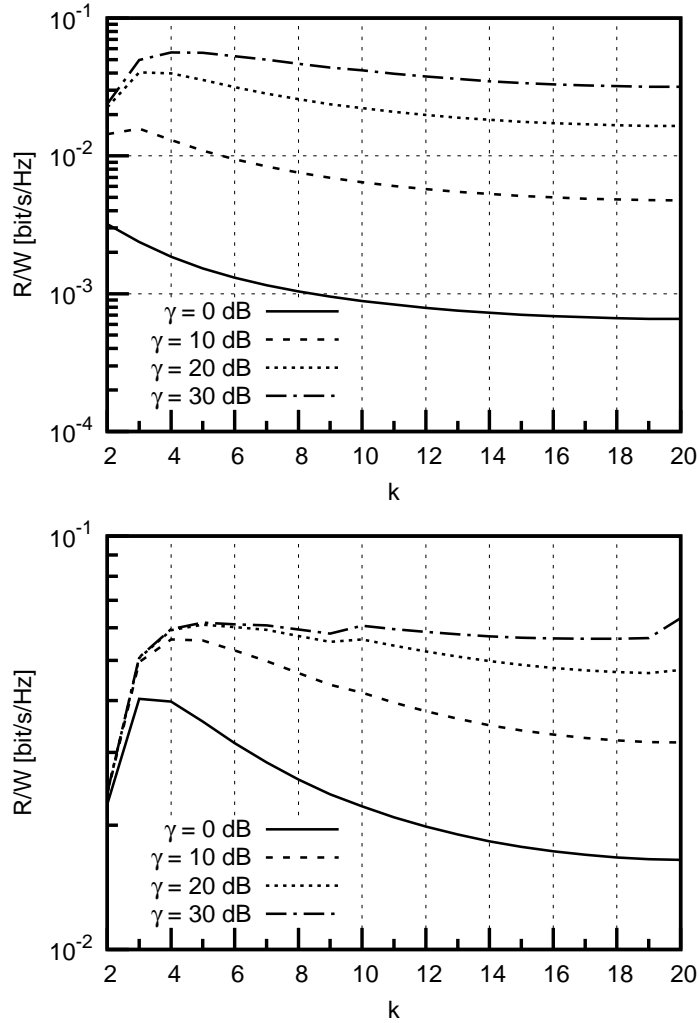


Figure 4.3: Average achievable rate as the number of nodes per sub-chain varies, for $n = 20$, $\alpha = 0.1$ (top), and $\alpha = 10$ (bottom), for different values of γ .

Cooperative Sub-chains strategy can adapt to the communication conditions and provide always excellent performance. As the contribution of the interference becomes more significant (i.e., α grows), Fig. 4.4 (bottom) shows that the bound is less and less tight, especially for high γ 's.

Finally, Fig. 4.5 presents the ratio of the per-node average power consumption ($\pi_i, i = 1, \dots, n$) to the average rate that can be obtained under (i) the Cooperative Sub-chains, (ii) the Multi-hop, and (iii) the communication strategy achieving the value of the bound on the average rate, in absence of interference (labeled by Bound in the plot). We first note that the Multi-hop shows the same performance as the Bound. This is explained by the fact that the Bound neglects the interference due

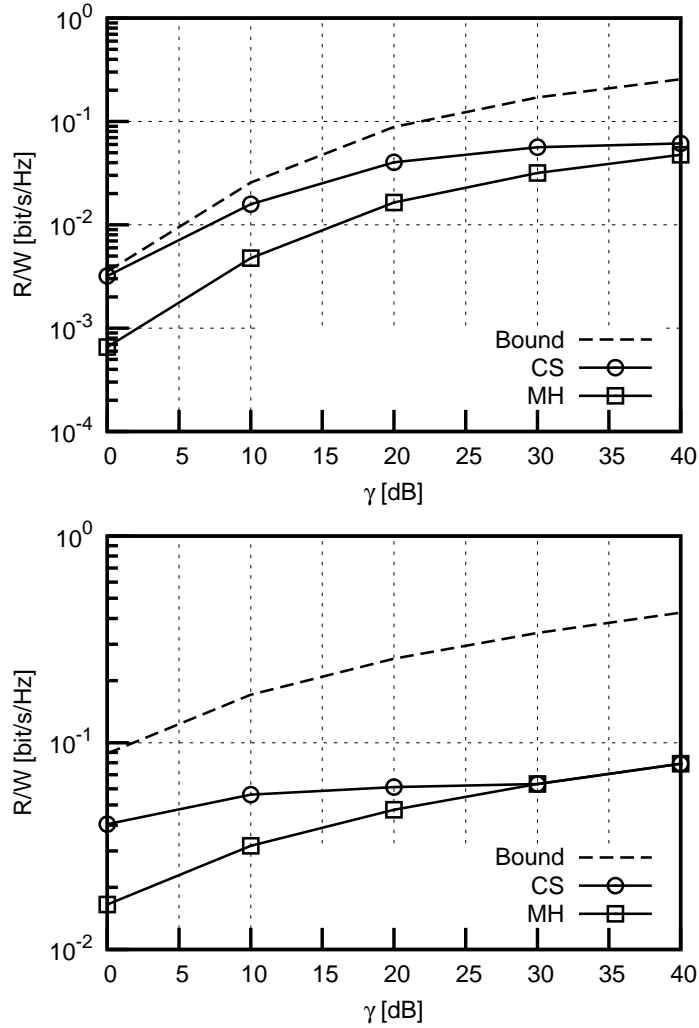


Figure 4.4: Average achievable rate versus γ , for $n = 20$ and $\alpha = 0.1$ (top), and $\alpha = 10$ (bottom). The performance of the cut-set upper bound, the Cooperative Sub-chains strategy and the Multi-hop scheme are compared.

to nodes transmitting simultaneously while in the Multi-hop such interference is not present (nodes are not transmitting simultaneously). Due to the absence of interference, under both these strategies the link capacities are given by \mathcal{C} and, since the average power consumptions π_i are the same, also the ratios $\pi_i/(R/W)$ are the same ($i = 1, \dots, n$).

We then observe that, although the Cooperative Sub-chains outperforms the Multi-hop in terms of average achievable rate, the Multi-hop scheme is more convenient in terms of energy consumption. Indeed, in the latter, nodes are most of the time in the sleep state (i.e., they perform fewer transmissions/receptions than

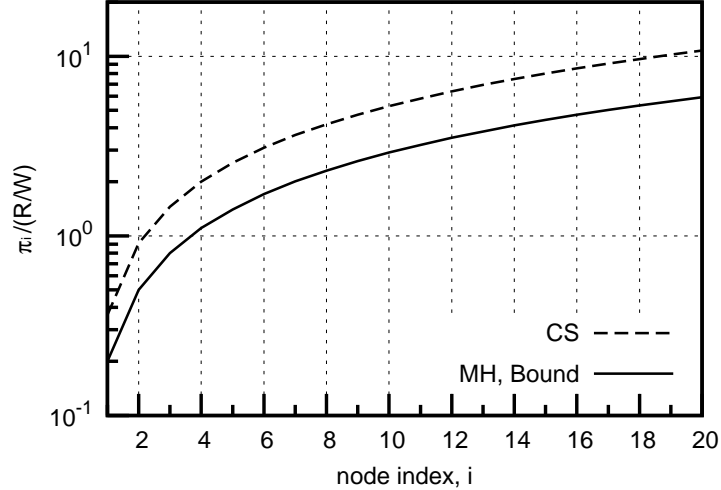


Figure 4.5: Per-node power consumption ($\pi_i, i = 1, \dots, n$) normalized to the average achievable rate, for $n = 20, \gamma = 30$ dB and $\alpha = 1$.

in the Cooperative Sub-chains). Furthermore, as expected, the closer a node to the gateway, the higher its power consumption. This is the well-known energy hole phenomenon, which is due to the higher traffic load experienced by the nodes closer to the gateway. In the next section, we will focus on this issue and analyze the case where each node should experience a target value π of average power consumption.

4.5 Fairness in data rate and energy consumption

We now aim at maximizing the data rate that the network nodes can achieve, constraining the average power consumption at every node to a target value. We stress that, while doing this, we still impose that all nodes achieve the same average data rate.

As done in Section 4.4, we start by deriving the cut-set upper bound to the achievable rate, taking into account the additional constraint on the average power consumption of the nodes. We then envision a strategy that leverages the Multi-hop principles but implements an optimal link scheduling so as to maximize the node data rate while meeting the system constraints. We refer to this strategy as Optimized Multi-hop. Note that we choose to focus on a Multi-hop-based mechanism,

as deriving the optimal link scheduling for the Cooperative Sub-chains would add a great deal of complexity to the analysis and lead to a cumbersome, numerical solution of the problem. Finally, we compare the performance of the Optimized Multi-hop strategy to the bound and derive some guidelines for the system design.

4.5.1 Link capacities providing fairness in average power consumption

While constraining the average power consumption at the nodes to be the same, we assume that the nodes are not restricted any longer to transmit at the same power level, i.e., we have different values $\alpha_i = P_i^{\text{tx}}/P_e$, for $i = 1, \dots, n$. The capacity of the i -th link is thus $\mathcal{C}_i = \log_2(1 + \alpha_i\gamma)$. However, for the average power consumption, we need to have $\pi_i = \pi$, for any $1 \leq i \leq n$. Specifically, by imposing π_i equal to π_{i+1} and using (4.3), we obtain

$$t_i^{\text{r}} + (1 + \alpha_i)t_i^{\text{t}} = t_{i+1}^{\text{r}} + (1 + \alpha_{i+1})t_{i+1}^{\text{t}}.$$

Since node i only receives from node $i - 1$, then $t_i^{\text{r}} = t_{i-1}^{\text{t}}$ and the above expression can be rewritten as a function of the nodes transmit time fractions, as

$$t_{i-1}^{\text{t}} + (1 + \alpha_i)t_i^{\text{t}} = t_i^{\text{t}} + (1 + \alpha_{i+1})t_{i+1}^{\text{t}}. \quad (4.13)$$

Furthermore, since node i has to transmit through the i -th link i times the information transmitted by node 1 on link 1, the transmit time of node i is given by $t_i^{\text{t}} = it_1^{\text{t}}\mathcal{C}_1/\mathcal{C}_i$. Substituting this result in (4.13) and solving for α_{i+1} , we have

$$\frac{1 + \alpha_{i+1}}{\mathcal{C}_{i+1}} = \frac{i}{i+1} \frac{\alpha_i}{\mathcal{C}_i} + \frac{i-1}{i+1} \frac{1}{\mathcal{C}_{i-1}} \quad (4.14)$$

which recursively relates the link capacity \mathcal{C}_{i+1} with \mathcal{C}_i and \mathcal{C}_{i-1} , for $i > 1$. We now prove the theorem below, which allows us to make some important remarks on

(4.14) and on the sequence of link capacities \mathcal{C}_i .

Theorem 4.5.1 *The sequence \mathcal{C}_i , $i = 1, \dots, n$, satisfying (4.14), if it exists, is decreasing with i .*

Proof Let us fix the normalized transmit power of node 1 to α_1 . The capacity of link 1 is then $\mathcal{C}_1 = \log_2(1 + \alpha_1\gamma)$. We prove the theorem by induction and proceed in two steps.

1. We first prove that $\alpha_2 < \alpha_1$. For $i = 1$ we solve (4.14), i.e., we solve $(1 + \alpha_2)/\mathcal{C}_2 = \alpha_1/2\mathcal{C}_1$. For simplicity, we define $f(\alpha) = (1 + \alpha)/\log_2(1 + \alpha\gamma)$. This function is positive for $\alpha \geq 0, \gamma \geq 0$ and shows a minimum $f_{\min} > 0$ at $\alpha_{\min} > 0$. Moreover, it is decreasing with α in the range $\alpha \in [0, \alpha_{\min})$ and increasing with α for $\alpha \in (\alpha_{\min}, +\infty)$. It follows that the equation $y = f(\alpha)$ has solution for α only if $y \geq f_{\min}$, and, in general, two solutions exist. In order to maximize the link capacities, hence the capacity of the network, we take the largest between the two solutions. As for the solution of $f(\alpha_2) = \alpha_1/2\mathcal{C}_1$, we note that $\alpha_1/2\mathcal{C}_1 < (1 + \alpha_1)/\mathcal{C}_1 = f(\alpha_1)$; it follows that $\alpha_2 < \alpha_1$ and $\mathcal{C}_2 < \mathcal{C}_1$.
2. Assuming that the relation $\alpha_i < \alpha_{i-1}$ (hence $\mathcal{C}_i < \mathcal{C}_{i-1}$) is proved, we now show that $\alpha_{i+1} \leq \alpha_i$. Since $\mathcal{C}_i < \mathcal{C}_{i-1}$, from (4.14) we have

$$\begin{aligned}
f(\alpha_{i+1}) &< \frac{i}{i+1} \frac{\alpha_i}{\mathcal{C}_i} + \frac{i-1}{i+1} \frac{1}{\mathcal{C}_i} \\
&= \frac{i}{i+1} \frac{1 + \alpha_i}{\mathcal{C}_i} - \frac{1}{(i+1)\mathcal{C}_i} \\
&< \frac{i}{i+1} \frac{1 + \alpha_i}{\mathcal{C}_i} \\
&< \frac{1 + \alpha_i}{\mathcal{C}_i} \\
&= f(\alpha_i).
\end{aligned} \tag{4.15}$$

This implies $\alpha_{i+1} \leq \alpha_i$, thus $\mathcal{C}_{i+1} < \mathcal{C}_i$.

Remark If for some $i \leq n$ the sum on the right hand side of (4.14) is lower than f_{\min} , a solution to (4.14) for \mathcal{C}_{i+1} does not exist. This implies that a sequence, \mathcal{C}_i , $i = 1, \dots, n$, of link capacities satisfying the average power constraints does not exist and the system has no solution.

Remark The recursive equation in (4.14) allows to find \mathcal{C}_i , $i = 2, \dots, n$, given the output transmit power of node 1, i.e., α_1 . Denoting by $\alpha^{\max} = P^{\text{txmax}}/P_e$ the maximum transmit power of a node (assumed to be the same for all nodes), then the link capacities are maximized when $\alpha_1 = \alpha^{\max}$.

4.5.2 An upper bound to the achievable rate

In order to derive the bound, we exploit some of the results obtained in Section 4.4.1. As before, we simplify the computation of the bound by assuming the network to be a cascade of n discrete memoryless channels. We therefore apply the max-flow min-cut theorem and reduce to n the possible network cuts. For every cut $(\mathcal{S}_i, \bar{\mathcal{S}}_i)$, the rate for reliable communication is again given by (4.5) and, by averaging over all possible network states, we obtain $I(x_i; y_{i+1}) = t_i^t \mathcal{C}_i$. By considering all cuts, the expression of the bound is given by

$$R_b \leq W \max_{\sum_{\sigma} t^{\sigma} = 1} \min_i \frac{\mathcal{C}_i t_i^t}{i}. \quad (4.16)$$

Given the relationship between the amount of data that node 1 and node i have to transmit, for any i we can write

$$t_i^t = i t_1^t \mathcal{C}_1 / \mathcal{C}_i, \quad (4.17)$$

$$t_i^r = (i - 1) t_1^t \mathcal{C}_1 / \mathcal{C}_{i-1}. \quad (4.18)$$

In the above expressions, the ratios $\mathcal{C}_1/\mathcal{C}_i$ and $\mathcal{C}_1/\mathcal{C}_{i-1}$ account for the fact that links 1, $i - 1$, and i have different capacities. From (4.17), we observe that $\mathcal{C}_i t_i^t / i =$

$t_1^t \mathcal{C}_1$, i.e., the argument of (4.16) does not depend on i , therefore the \min_i operator in (4.16) can be removed by arbitrarily setting $i = n$. Next, by substituting the results (4.17) and (4.18) in (4.1) and setting $i = n$, we can solve for $\mathcal{C}_1 t_1^t$ and obtain

$$\mathcal{C}_1 t_1^t = (1 - t_n^s) \frac{\mathcal{C}_n \mathcal{C}_{n-1}}{n \mathcal{C}_{n-1} + (n-1) \mathcal{C}_n}. \quad (4.19)$$

Then, we can rewrite (4.16) as

$$\begin{aligned} R_b &\leq W \max_{\sum_{\sigma} t^{\sigma} = 1} (1 - t_n^s) \frac{\mathcal{C}_{n-1} \mathcal{C}_n}{n \mathcal{C}_{n-1} + (n-1) \mathcal{C}_n} \\ &= W \frac{\mathcal{C}_{n-1} \mathcal{C}_n}{n \mathcal{C}_{n-1} + (n-1) \mathcal{C}_n} \end{aligned} \quad (4.20)$$

where in the last line of (4.20) the maximum is obtained for $t_n^s = 0$.

The bound in (4.20) suggests a communication strategy with n network states $\sigma_1, \dots, \sigma_n$, similar to that shown in Table 4.1. In this case, however, the time fractions that the nodes spend in each state are given by

$$\begin{aligned} t_i^t &= \frac{i}{\mathcal{C}_i} \frac{\mathcal{C}_{n-1} \mathcal{C}_n}{n \mathcal{C}_{n-1} + (n-1) \mathcal{C}_n}, \\ t_i^x &= \frac{i-1}{\mathcal{C}_{i-1}} \frac{\mathcal{C}_{n-1} \mathcal{C}_n}{n \mathcal{C}_{n-1} + (n-1) \mathcal{C}_n}, \\ t_i^s &= 1 - \frac{i \mathcal{C}_{i-1} + (i-1) \mathcal{C}_i}{\mathcal{C}_i \mathcal{C}_{i-1}} \frac{\mathcal{C}_{n-1} \mathcal{C}_n}{n \mathcal{C}_{n-1} + (n-1) \mathcal{C}_n}. \end{aligned} \quad (4.21)$$

The above results are obtained using (4.19) with $t_n^s = 0$ in (4.17) and (4.18). Moreover, the time fractions associated with each network state are given by

$$t^{\sigma_i} = \left(\frac{i}{\mathcal{C}_i} - \frac{i-2}{\mathcal{C}_{i-2}} \right) \frac{\mathcal{C}_{n-1} \mathcal{C}_n}{n \mathcal{C}_{n-1} + (n-1) \mathcal{C}_n}$$

for $i > 1$ and

$$t^{\sigma_1} = \frac{1}{\mathcal{C}_1} \frac{\mathcal{C}_{n-1} \mathcal{C}_n}{n \mathcal{C}_{n-1} + (n-1) \mathcal{C}_n}.$$

This is due to the fact that $t^{\sigma_i} = t_i^t - t_{i-2}^t$, as shown in Table 4.1. Finally, the

normalized average power consumption of the nodes is given by

$$\pi_b = t_1^t(1 + \alpha_1) = \frac{1 + \alpha_1}{C_1} \frac{C_{n-1}C_n}{nC_{n-1} + (n-1)C_n}.$$

4.5.3 Multi-hop strategy with optimal link scheduling (Optimized Multi-hop)

Recall that the communication strategy suggested by the cut-set bound relies on the optimistic assumption that simultaneous transmissions do not interfere with each other. In practice, instead, the signal to noise ratio at the receiver is degraded by the interference power. A communication strategy that avoids such a problem is the Multi-hop, where the network has n states, $\sigma_1, \dots, \sigma_n$, and the time fraction associated to the generic state σ_i corresponds to the time fraction associated to the transmit time of node i , i.e, $t^{\sigma_i} = t_i^t$.

Under the constraint of a fair rate allocation, the rate that can be achieved by any node is equal to the rate obtained by node 1: $R_{\text{mh}} = Wt_1^t C_1$. The transmit time fraction of node i is again given by (4.17). By replacing in (4.17) the expression of R_{mh} and solving for t_i^t , we have

$$t_i^t = \frac{i}{C_i} \frac{R_{\text{mh}}}{W}. \quad (4.22)$$

Since $t_i^t = t^{\sigma_i}$ and $\sum_i t^{\sigma_i} = 1$, we readily obtain

$$R_{\text{mh}} = W \left(\sum_{i=1}^n \frac{i}{C_i} \right)^{-1} \quad (4.23)$$

where, in order to meet the constraints on the average power consumption, the capacities C_i are obtained by (4.14). Since the average power consumption is the same for any node, we can compute it in terms of the transmit time fraction of node 1, i.e., $\pi_{\text{mh}} = t_1^t(1 + \alpha_1)$. However, from (4.22) we have $t_1^t = \frac{R_{\text{mh}}}{WC_1}$. By using the

expression of R_{mh}/W in (4.23), we finally get

$$\pi_{\text{mh}} = \frac{1 + \alpha_1}{\mathcal{C}_1} \left(\sum_{i=1}^n \frac{i}{\mathcal{C}_i} \right)^{-1}.$$

4.5.4 Results

We now compare the performance of the Optimized Multi-hop scheme against the bound. Figure 4.6 depicts the average achievable rate normalized to the available bandwidth, as the target average power consumption at the nodes varies. The results have been obtained for $n = 4$, $\alpha^{\text{max}} = 100$, and $\gamma = 10, 50$ dB.

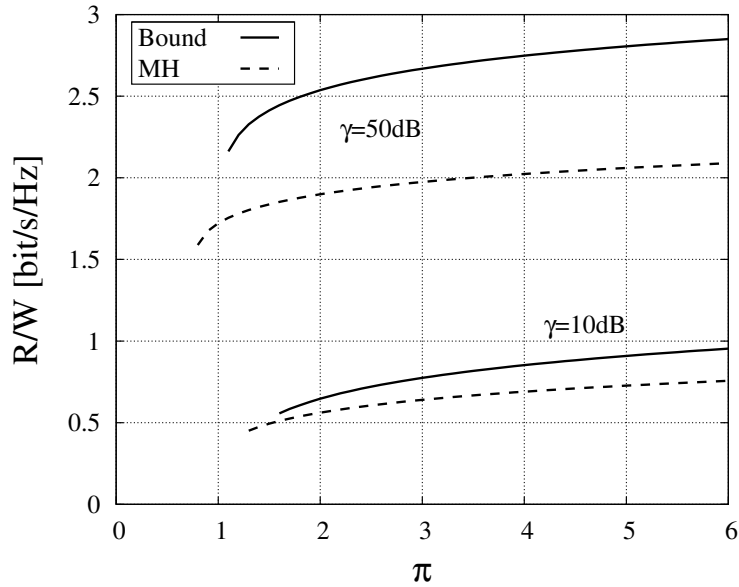


Figure 4.6: Average achievable rate of the multi-hop scheme with optimal link scheduling (Optimized Multi-hop), for $n = 4$, $\alpha^{\text{max}} = 100$ and $\gamma = 10, 50$ dB. The performance is compared to the cut-set bound, as the target average power consumption at the nodes (π) varies.

By looking at the plot, we observe that there is a non-negligible gap between the performance of our scheme and the bound, which increases as the SNR grows. This suggests that, given the target value π , a significant improvement in the achievable rate could be obtained by adopting a different communication strategy. Specifically, such a strategy should let more than one node transmit at the same time, similarly to the Cooperative Sub-chains previously described.

Another interesting fact underscored by the plot is that an optimal link scheduling for the classic multi-hop data transfer that meets the constraints and maximizes the achievable rate may not exist, for low values of π and γ . Figure 4.7 sheds more light on this issue, showing the achievable rate for the Optimized Multi-hop scheme as a function of γ and a varying number of nodes in the network. The results have been obtained again for $\alpha^{\max} = 100$; also, we point out that the different values of the achievable rate appearing on the y-axis correspond to different values of π .

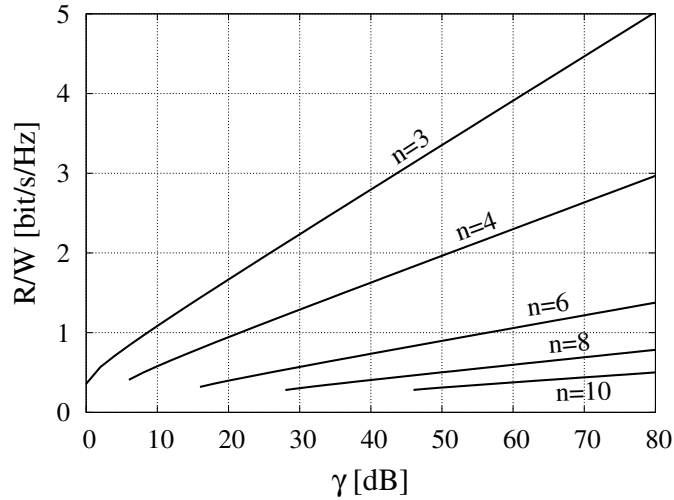


Figure 4.7: Achievable rate for the Optimized Multi-hop strategy, when $\alpha^{\max} = 100$ and both γ and n vary.

Again, we note that, for low values of SNRs and as the number of nodes in the network increases, there is no solution to the optimal scheduling problem. Indeed, under the above conditions, the unfairness in energy consumption between the nodes that are far away from the gateway and those close to the gateway becomes overwhelming. As a consequence, an optimal link scheduling can be found only for sufficiently large values of α^{\max} , i.e., large values of maximum transmit power.

4.6 Concluding Remarks

In this chapter, we studied the achievable rate of communication nodes in a network with linear topology, under the assumption that the nodes are half duplex and all

of them need to deliver data to a gateway node located at one end of the topology. We first examined a fair communication strategy, named Cooperative Sub-chains as introduced earlier in Chapter 2, that allows all nodes to achieve the same data rate. We compared its performance to that of classic multi-hop data transfer as well as to the cut-set upper bound, which we extended to our network scenario. Then, in order to address both the energy hole problem and the energy depletion in energy-harvesting systems, we considered the additional constraint of letting any node experience the same average power consumption. We then derived the cut-set bound in this case and the optimal link schedule in classic multi-hop data transfer that meets the system requirements.

The results show that the Cooperative Sub-chains strategy achieves very good performance, which, for low-medium values of SNR, is close to the bound. As the SNR, hence the interference among simultaneous transmissions, increases, our strategy tends to perform similarly to the classic multi-hop scheme, thus exhibiting the ability to maximize the achievable rate under different conditions. Under energy constraints, we showed that, for low SNR and a large number of nodes in the network, the system requirements can be met only if sufficiently high values of transmit power can be used. The gap we observed between the bound and the rate achieved by the classic multi-hop scheme with optimal link scheduling also suggests that significant improvements could be obtained by applying a strategy similar to the Cooperative Sub-chains. However, deriving the optimal link scheduling for such a scheme would add a great deal of complexity to the analysis and lead to a cumbersome, numerical solution of the problem. This aspect, as well as the study of cases where nodes have different constraints on the achievable rate and power consumption, represent interesting directions for future research.

Chapter 5

Upper Bounds to the Performance of Cooperative Traffic Relaying in Linear Wireless Networks

Wireless networks with linear topology, where nodes generate their own traffic and relay other nodes' traffic, have attracted increasing attention. Indeed, they well represent sensor networks monitoring paths or streets, as well as multi-hop networks for video surveillance of roads or vehicular traffic.

In this chapter we study the performance limits of such network systems when

- (i) the nodes' transmissions can reach receivers farther than one-hop distance from the sender,
- (ii) the transmitters cooperate in the data delivery,
- (iii) interference due to concurrent transmissions is taken into account.

By adopting an information-theoretic approach, we derive analytical bounds to the achievable data rate in both the cases where the nodes have full-duplex and half-duplex radios. The expressions we provide are mathematically tractable and allow the analysis of multi-hop networks with a large number of nodes.

Our analysis highlights that increasing the number of cooperating transmitters beyond two leads to a very limited gain in the achievable data rate.

Also, for half-duplex radios, it indicates the existence of dominant network states, which have a major influence on the bound. It follows that efficient, yet simple, communication strategies can be designed by considering at most two cooperating transmitters and by letting half-duplex nodes operate according to the aforementioned dominant states.

5.1 Introduction

Multi-hop communication systems are primarily implemented to extend the overall coverage of wireless networks, leading to a more efficient use of the available communication resources and to an increased network throughput.

As indicated by the information theory, the capacity of a wireless network increases when the nodes participate cooperatively in relaying the traffic toward their destinations. Thus, various cooperative schemes have been proposed in the literature for networks that include only full-duplex nodes (i.e., nodes that can simultaneously transmit and receive) [31, 40], only half-duplex nodes (i.e., nodes that at any time instant can either transmit or receive) [53], or a mix of full-duplex and half-duplex nodes [51].

In this chapter, we consider a wireless network where n nodes have to deliver their traffic to a common destination node (e.g., a gateway node) through multi-hop data transfers. We focus on a network whose topology can be considered as linear, as, e.g., in the case of sensor networks for path and street monitoring, or multi-hop networks for videosurveillance of roads and vehicular traffic [36]. The nodes share the same radio resources and each of them may generate its own data at a different average rate. We assume that, if needed, the nodes cooperate to relay the traffic based on the decode-and-forward paradigm [20]. The nodes' transmission rates and powers correspond to optimal coding over a discrete-time additive white Gaussian noise (AWGN) channel, although more general channels and coding schemes could be considered as well. Furthermore, unlike previous work, we account for the fact

that receivers may exploit signal transmissions from nodes farther than one-hop distance from the sender, and that nodes in radio visibility can cooperate to transmit toward one or more receiver nodes.

Under these conditions, we adopt an information-theoretic approach and we develop a method to obtain a fairly tight upper bound to the nodes' achievable rate, which also accounts for the interference due to simultaneous transmissions. Specifically, we study the cut-set upper bound [29, 30] of the network system, and obtain the timing and traffic links schedule of such a network under which the upper bound is satisfied. We carry out the analysis in presence of both full-duplex (FD) and half-duplex (HD) nodes; for the former, we study the general case where nodes may choose to operate either in FD or HD mode, as the second operational mode (i.e., HD) can be considered as a subcase of the first one (i.e., FD).

We stress that, since the nodes' operational states in FD mode are a superset of those under the HD mode, an upper bound for an FD network is an upper bound for the HD case too. However, such a bound would be loose for an HD network, where the data transfer towards the destination is expected to be significantly slower than in the FD case (recall that HD nodes cannot transmit and receive at the same time). We therefore carry out a different analysis for FD and HD networks, so as to obtain tight upper bounds under both operational modes.

We start our analysis by adopting the cut-set methodology as introduced in [29, 30]; this, however, would require us to consider all possible network cuts and operational states, which is unfeasible in our case due to the exceedingly high complexity. We therefore limit the number of cuts to be considered and identify the dominant states in which the network can operate, and derive the upper bound to the nodes data rate accounting for such cuts and network states only. Also, in the case of an HD network, whose analysis becomes more complex due to the additional operational constraints, we are able to analyze a large-size network by resorting to an equivalent one, composed of five nodes only. To show the validity of our approach,

we compute a lower bound to the traditional cut-set bound. By comparing our results to the aforementioned lower bound, we demonstrate that the upper bound we derive is tight. Finally, we use the bounds obtained for the FD and the HD case to investigate the system behavior as several parameters, like the signal-to-noise ratio (SNR), the dependence of the signal attenuation with the distance and the number of nodes, vary.

We remark that several works have appeared in the literature addressing a problem similar to the one we study, but for networks with only one node generating traffic and the others acting as relays [35, 39], or with multiple source nodes but operating in FD mode only [31, 40], or for networks with very few HD nodes [41]. The benefits of an integrated FD and HD relaying scheme have been studied in [51], for a network with a source-destination pair and an intermediate relay-only node. However, the solution in [51] holds only if the loop-back interference observed at the relay operating in FD mode is resolved. This imposes further hardware requirements, which limit the application of the strategy proposed there. A network scenario closer to ours has been analyzed in [34, 47], but with a different objective. There, the authors consider the problem of computing transmission powers, rates, and link scheduling for an energy-constrained wireless network and solve it by maximizing the network lifetime through a cross-layer design approach. Beside having different scope, our work differs from [34, 47] in that they consider the data rates of the source nodes as inputs to the problem of transmission scheduling, while we aim at deriving an upper bound to the nodes' achievable rate. Finally, in [42] Lutz et al. analyze relay cascades with HD constraints, in which adjacent node pairs are connected via error-free links. The information transfer is carried out by applying a coding scheme that allocates the transmission and reception time slots at the relays depending on the amount of information to be transferred. Through numerical results, the authors show that their strategy achieves the cut-set bound under certain conditions on the nodes' rates. Together with its rather complex cod-

ing scheme, the strategy in [42] requires the nodes to be synchronized at the symbol level. Unlike [42], in our approach we derive an upper bound to the rates achievable by the nodes, using an AWGN channel model and accounting for interference due to simultaneous transmissions. In summary, to our knowledge, our work is the first one that provides an upper bound to the achievable data rates in a network where (i) the nodes may operate all in FD or HD mode, or some in FD and others in HD mode, (ii) a node's transmission can be exploited at a receiver located at more than one-hop distance from the sender, and (iii) interference is taken into account.

The rest of the paper is organized as follows. First, we describe the system model in Section 5.2 and provide some basic concepts on the cut-set bound in Section 5.3. The upper bound to the nodes' achievable rate is investigated in Sections 5.4 and 5.5 for, respectively, FD and HD networks. There, we also present some numerical results showing the impact of the system parameters on the performance. Finally, in Section 5.6 we draw our conclusions and highlight directions for future research.

5.2 System model

We consider a wireless network with linear topology composed of n nodes and a destination node, as depicted in Fig. 5.1. Without loss of generality, we let node 1 be the node at the left end of the topology, while the destination is located at the right end and is denoted by $n + 1$. For simplicity, we assume that the nodes are equally spaced along the path and denote by d the inter-node distance, which we refer to as the one-hop distance. It follows that the network has length $L = nd$ meters, or, equivalently, it includes n -hops.

Node i ($i = 1, \dots, n$) generates messages at rate R_i , and it can decode and forward other nodes' messages. We consider an additive white Gaussian noise (AWGN) channel, and assume that all nodes transmit with power P while the noise power spectral density at each receiver is N_0 . We then write the SNR measured at

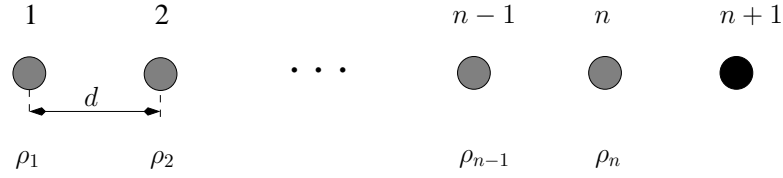


Figure 5.1: Network topology.

distance d from a transmitting node as

$$\gamma = \frac{PG_t G_r}{WN_0} \left(\frac{\lambda}{4\pi d} \right)^a \quad (5.1)$$

where G_t, G_r are, respectively, the transmit and receive antenna gains, λ is the carrier wavelength, and a is the path loss exponent.

We assume that each node $i, i = 1, \dots, n + 1$, is equipped with directional antennas, so that it can receive signals only from upstream transmitting nodes and it can use its whole power to transmit towards downstream nodes. This is a reasonable assumption considering that our objective is to find an upper bound to the achievable data rates and that we deal with a linear network in which all nodes aim at delivering their data to the same destination located at one end of the topology.

Furthermore, since we are interested in finding bounds to practical cooperative communication strategies, for any receiver node, we define k_C as the maximum distance (with respect to the receiver itself) at which collaborating transmitters can be located; we refer to k_C as cooperation range. We define k_I ($k_I \geq k_C$) as the interference range of a node, i.e., the maximum distance at which a transmitted signal can cause interference at a receiver. Both the cooperation and the interference ranges are expressed in hops. From the above definitions, it follows that a node can receive *useful* signals from transmitters within distance k_C hops, while it receives interfering signals from nodes located at distance farther than k_C hops but within k_I hops. All signals arriving at the receiver from farther than k_I hops are assumed to have negligible power. Signals received from collaborating nodes are correlated, while interfering signals received from nodes farther than k_C hops are uncorrelated

and independent of the useful signals. This is a fair assumption as, by definition of cooperation range, the signals from nodes farther than k_C hops are not exploited by a receiver, hence useful and interfering signals can be assumed to be uncorrelated. Also, under the system scenario outlined above, neglecting the correlation among interfering signals represents a best case (i.e., it never overestimates the effect of the interfering signals), thus it does not invalidate the derivation of the upper bound to the nodes' data rate.

Denoting by \mathbf{y} the vector of signals received at the network nodes, we can write:

$$\mathbf{y} = \sqrt{\gamma}\mathbf{H}^T\mathbf{x} + \sqrt{\gamma}\mathbf{W}^T\mathbf{i} + \mathbf{z}. \quad (5.2)$$

In (5.2), $\mathbf{x} = [x_1, \dots, x_n]^T$ is the vector of signals transmitted by nodes $1, \dots, n$; $\mathbf{i} \sim \mathcal{N}(\mathbf{0}, \mathbf{I})$ is the vector of signals transmitted by interfering nodes (assumed to be uncorrelated and independent of \mathbf{x}); \mathbf{H} is the matrix including the coefficients of the channels between the receiver nodes and the transmitters in their cooperation range; \mathbf{W} is the matrix including the coefficients of the channels between the receivers and their corresponding interferers. Finally, $\mathbf{z} \sim \mathcal{N}(\mathbf{0}, \mathbf{I})$ is the noise vector, independent of \mathbf{x} and \mathbf{i} .

We assume that nodes employ Gaussian codebooks and that $\mathbf{x} \sim \mathcal{N}(\mathbf{0}, \Sigma)$, with $(\Sigma)_{ii} = 1, i = 1, \dots, n$. The entries h_{ij} of the $n \times (n + 1)$ channel matrix \mathbf{H} are defined as

$$h_{ij} = \begin{cases} (i - j)^{-a/2} & \text{if } i - k_C \leq j < i \\ 0 & \text{else,} \end{cases} \quad (5.3)$$

while the elements w_{ij} of the $n \times (n + 1)$ interference matrix \mathbf{W} are given by

$$w_{ij} = \begin{cases} (i - j)^{-a/2} & \text{if } i - k_I \leq j < i - k_C \\ 0 & \text{else.} \end{cases} \quad (5.4)$$

Note that the elements h_{ij} and w_{ij} are assumed to be static in order to make the

following analysis more readable; however, our derivations can be easily extended to the case of a time-varying channel model.

At last, we stress that, while most of previous work aims at maximizing the sum rates of source nodes, we consider that every node i may have a different amount of data to deliver to the destination in the unit time. Thus, our goal is to study the *maximum fair rate allocation* to all nodes, i.e., the average data rates that can be achieved by the nodes and that satisfy the desired proportion among the nodes' data generation rates. To do so, we should consider an n -dimensional problem, with the n variables representing the nodes' data rates. However, we can obtain a problem formulation that is mathematically tractable, by expressing the average¹ rate at which node i transfers its own data towards the destination node $n + 1$ as

$$R_i = \rho_i R \quad i = 1, \dots, n. \quad (5.5)$$

In the above equation, the coefficients ρ_i 's are (positive) input parameters representing the relationship among the nodes' data generation rates, hence the desired relationship among the nodes' traffic delivery rates. Such an expression allows us to consider only one system variable, R , which should be maximized.

Given the aforementioned scenario, we are interested in deriving a bound to the maximum achievable rate R , in both the FD and the HD case. FD nodes have the ability to transmit and receive simultaneously over the same frequency band; we denote the corresponding operational state by tt . HD nodes, instead, cannot do both tasks simultaneously, i.e., at a given time instant, they can either transmit (t) or receive (τ). Under certain circumstances, an FD node may also operate in HD mode for a fraction of time, hence it may be in any of the states t , τ and tt . However, for FD nodes, state t can be included in state tt since reception does not increase the interference level at other nodes and it does not decrease the system capacity

¹Note that the average is computed over time, as the generic node i may take different operational states at different time instants (namely, transmit, reception and idle/sleep).

either. Note also that a sleep state could be considered, in which the nodes neither transmit nor receive but they just save energy. However, for the purposes of our analysis, a sleep state is equivalent to the receive state. In conclusion, we can limit our attention to states \mathfrak{r} and \mathfrak{tr} for FD nodes, and to \mathfrak{r} and \mathfrak{t} for HD nodes.

Since any network node can operate in two states, while the destination node $n + 1$ always receives, the number of possible states the network can take is $J = 2^n$. We denote the j -th network state ($j = 1, \dots, J$) by $\boldsymbol{\sigma}_j = [\sigma_{1j}, \dots, \sigma_{nj}]$ where σ_{ij} is the state of node i when the network is in state $\boldsymbol{\sigma}_j$, that is, $\sigma_{ij} \in \{\mathfrak{r}, \mathfrak{tr}\}$ if k is an FD node, and $\sigma_{ij} \in \{\mathfrak{r}, \mathfrak{t}\}$ if k is an HD node. Also, we define the set of network states as $\mathcal{J} = \{\boldsymbol{\sigma}_j, j = 1, \dots, J\}$, while the time fractions the network spends in the possible states are represented by the vector $\mathbf{t} = [t_1, \dots, t_J]^\top$, with $0 \leq t_j \leq 1$ and such that $\sum_{j=1}^J t_j = 1$.

5.3 Background on the cut-set bound

The cut-set bound is an upper-bound to the achievable data rate of a wireless network of generic topology where nodes exchange messages among each other. As mentioned, in our case the network is composed of n wireless nodes and a destination node (see Fig. 5.1). We define the set of network nodes as $\mathcal{T} = \{1, \dots, n + 1\}$ and, as introduced in Section 5.2, we assume that node i , $i = 1, \dots, n$, generates a message W_i , of rate R_i , to be transferred to the destination. The messages W_i 's are assumed to be mutually independent.

Following the notation introduced in [30, Chapter 10.2], we denote by x_i and y_i the random variables representing the signals, respectively, transmitted (channel inputs) and received (channel outputs), by node i , $i = 1, \dots, n + 1$. Moreover, since we assume that the destination node (i.e., node $n + 1$) is always in receive state \mathfrak{r} , we set $x_{n+1} = 0$. The transmitted signals x_i 's are assumed to have zero mean, unit variance and joint distribution p_{x_1, \dots, x_n} . The destination node, on the base of the received signal y_{n+1} , derives estimates \widehat{W}_i of the messages W_i , $i = 1, \dots, n$.

In order to compute the cut-set bound, one should consider all possible partitions, hereinafter called *cuts*, of the network nodes \mathcal{T} into two non overlapping sets, \mathcal{S} and $\mathcal{S}_c = \mathcal{T} \setminus \mathcal{S}$. The former includes some of the nodes generating messages, while the latter contains the destinations of those messages (for which they compute an estimate). Note that, beside the sources and destinations of a set of tagged messages, \mathcal{S} and \mathcal{S}_c can include other nodes as well. In our network scenario, message estimates are derived only at the destination node, thus a valid cut is such that \mathcal{S}_c contains at least node $n + 1$. Let us now consider a generic cut \mathcal{S} . We denote by

- $\mathcal{M}(\mathcal{S})$ the set of messages transmitted by nodes in the cut \mathcal{S} ,
- $R_{\mathcal{M}(\mathcal{S})}$ the sum of the rates of the messages in $\mathcal{M}(\mathcal{S})$,
- $\mathbf{x}_{\mathcal{S}} = \{x_k | k \in \mathcal{S}\}$ the set of channel inputs contained in \mathcal{S} ,
- $\mathbf{x}_{\mathcal{S}_c} = \{x_k | k \in \mathcal{S}_c\}$ the set of channel inputs contained in \mathcal{S}_c , and by
- $\mathbf{y}_{\mathcal{S}_c} = \{y_k | k \in \mathcal{S}_c\}$ the set of channel outputs contained in \mathcal{S}_c .

By [30, Chapter 10.2], the rate $R_{\mathcal{M}(\mathcal{S})}$ can be written as $R_{\mathcal{M}(\mathcal{S})} = \sum_{i \in \mathcal{S}} R_i$, where R_i is the rate of message W_i . Then, the cut-set bound to the network capacity region is given by:

$$\mathcal{C} \subseteq \bigcup_{p_{x_1, \dots, x_n}} \bigcap_{\mathcal{S} \in \Omega} \left\{ R_1, \dots, R_n \mid \sum_{i \in \mathcal{S}} R_i \leq I(\mathbf{x}_{\mathcal{S}}; \mathbf{y}_{\mathcal{S}_c} | \mathbf{x}_{\mathcal{S}_c}) \right\} \quad (5.6)$$

where $\Omega = \{\mathcal{S} | \mathcal{S} \subseteq \mathcal{T}, \mathcal{S} \neq \emptyset\}$ is the set of network cuts, whose cardinality is $|\Omega| = 2^n - 1$. The term $I(\mathbf{x}_{\mathcal{S}}; \mathbf{y}_{\mathcal{S}_c} | \mathbf{x}_{\mathcal{S}_c})$ denotes the mutual information² between the random variables $\mathbf{x}_{\mathcal{S}}$ and $\mathbf{y}_{\mathcal{S}_c}$, given $\mathbf{x}_{\mathcal{S}_c}$ and a joint distribution p_{x_1, \dots, x_n} .

²The mutual information of two random variables measures the mutual dependence of the two variables [20].

5.4 Cut-set bounds: Full-duplex radios

We now derive an upper bound to the achievable data rate by applying the cut-set bound approach. We start by considering the expression in (5.6) and make some observations, as detailed next.

In our scenario, the network can operate in J possible states, i.e., $\boldsymbol{\sigma}_j$, $j = 1, \dots, J$, characterized by the time fractions $\mathbf{t} = [t_1, \dots, t_J]^\top$. The mutual information $I(\mathbf{x}_S; \mathbf{y}_{S_c} | \mathbf{x}_{S_c})$ in (5.6) can therefore be expressed as $I(\mathbf{x}_S; \mathbf{y}_{S_c} | \mathbf{x}_{S_c}) = \sum_{j=1}^J t_j I(\mathbf{x}_S; \mathbf{y}_{S_c} | \mathbf{x}_{S_c}, \boldsymbol{\sigma}_j)$. The rate of the messages generated by the network nodes are such that $R_i = \rho_i R$, therefore we can write $\sum_{i \in S} R_i = R \varrho_S$ where $\varrho_S = \sum_{i \in S} \rho_i$. This allows us to reduce the n -dimensional problem in (5.6) to a formulation with one variable only, i.e., R , where the union and the intersection operators can be replaced with a max and a min operators, respectively. Additionally, the maximization must be performed also over all possible time fractions \mathbf{t} . Hence, using (5.6), we can write the cut-set upper bound to the data rate R as

$$B = \max_{p_{x_1, \dots, x_n}, \mathbf{t}} \min_{S \in \Omega} \frac{1}{\varrho_S} \sum_{j=1}^J t_j I(\mathbf{x}_S; \mathbf{y}_{S_c} | \mathbf{x}_{S_c}, \boldsymbol{\sigma}_j). \quad (5.7)$$

Then, under the assumption of a AWGN channel, FD nodes, a Gaussian codebook and the signal model in (5.2), we obtain the following expression:

$$B_{\text{FD}} = \max_{\boldsymbol{\Sigma}, \mathbf{t}} \min_{S \in \Omega} \left\{ \frac{1}{\varrho_S} \sum_{j=1}^J t_j I_{S,j} \right\} \quad (5.8)$$

where $I_{S,j} = I(\mathbf{x}_S; \mathbf{y}_{S_c} | \mathbf{x}_{S_c}, \boldsymbol{\sigma}_j)$ and the joint density p_{x_1, \dots, x_n} is represented by the covariance matrix $\boldsymbol{\Sigma}$.

However, the computation of a tight cut-set bound, such as that in (5.8) would require us to consider any possible cut of the network, $S \in \Omega$, separating some messages from their corresponding estimates, and its complement, $S_c = \mathcal{T} \setminus S$. Unfortunately, this is impractical for networks with a large number of nodes, since

the number of cuts increases exponentially with n , i.e., as $2^n - 1$. Thus, in the following we derive an upper bound for B_{FD} , i.e., a looser upper bound to the achievable data rate. To demonstrate that our bound is still tight, we derive a lower bound for B_{FD} and show that our upper and lower bounds for B_{FD} are very close.

5.4.1 Upper bound to B_{FD}

A weaker, but mathematically tractable, upper bound to the rate R can be obtained by reducing the cuts to be considered in (5.8) to one cut only, which coincides with \mathcal{T} . Then, we have $B_{\text{FD}} \leq \frac{1}{\varrho_{\mathcal{T}}} \max_{\Sigma, \mathbf{t}} \sum_{j=1}^J t_j I_{\mathcal{T}, j}$ where $I_{\mathcal{T}, j} = I(x_1, \dots, x_n; y_{n+1} | \sigma_j) = I(x_{n-k_C+1}, \dots, x_n; y_{n+1} | \sigma_j)$. It follows that

$$\begin{aligned} B_{\text{FD}} &\leq \frac{1}{\varrho_{\mathcal{T}}} \max_{\Sigma} \sum_{j=1}^J t_j I(x_{n-k_C+1}, \dots, x_n; y_{n+1} | \sigma_j) \\ &= \frac{1}{\varrho_{\mathcal{T}}} \max_{\Sigma} I(x_{n-k_C+1}, \dots, x_n; y_{n+1} | \sigma^*) \\ &= \frac{1}{2\varrho_{\mathcal{T}}} \max_{\Sigma} \log_2 (1 + \gamma \mathbf{h}_{n+1}^{\text{T}} \Sigma \mathbf{h}_{n+1}) . \end{aligned} \quad (5.9)$$

Since we aim at deriving an upper bound, in (5.9) we limited the possible network states to those in which nodes $n - k_C + 1, \dots, n$ are in state tr , nodes $n - k_I + 1, \dots, n - k_C$ are in state τ (so that they do not interfere with the nodes within distance k_C from the destination $n + 1$), and the remaining ones can be either in tr or τ (σ^* represents any of these network states). Note that the vector \mathbf{h}_{n+1} is the $(n + 1)$ -th column of \mathbf{H} and

$$\mathbf{h}_{n+1}^{\text{T}} \Sigma \mathbf{h}_{n+1} \leq \left| \sum_{i=1}^n \sum_{j=1}^n (\mathbf{h}_{n+1})_i (\mathbf{h}_{n+1})_j (\Sigma)_{ij} \right| \leq \left(\sum_{l=1}^{k_C} h_l \right)^2 \quad (5.10)$$

where the second inequality is due to the fact that all elements of \mathbf{h}_{n+1} are positive, $|(\Sigma)_{ij}| \leq 1$, and only the nodes within distance k_C from the destination are

transmitting. By substituting (5.10) in (5.9), we can write

$$B_{\text{FD}} \leq \frac{1}{2 \sum_{i=1}^n \rho_i} \log_2 \left(1 + \gamma \left(\sum_{l=1}^{k_C} h_l \right)^2 \right) = B_{\text{U-FD}}. \quad (5.11)$$

5.4.2 Lower bound to B_{FD}

In order to assess how tight the bound $B_{\text{U-FD}}$ is with respect to B_{FB} , we derive a lower bound for the latter, which we denote by $B_{\text{L-FB}}$. The lower bound $B_{\text{L-FB}}$ is obtained by assuming $\Sigma = \mathbf{I}$ in (5.8), i.e., that the transmitted signals are uncorrelated. Under this condition, a node can decode some data by using one signal only out of the received ones, and it has to consider the latter as interference. Thus, by recalling (5.8) we have

$$B_{\text{FD}} \geq \max_{\mathbf{t}} \min_{S \in \Omega} \left\{ \frac{1}{\rho_S} \sum_{j=1}^J t_j I_{S,j} |_{\Sigma=\mathbf{I}} \right\}, \quad (5.12)$$

where $I_{S,j} |_{\Sigma=\mathbf{I}}$ is the mutual information $I_{S,j}$ conditioned to $\Sigma = \mathbf{I}$, i.e.,

$$I_{S,j} |_{\Sigma=\mathbf{I}} = I(\mathbf{x}_S; \mathbf{y}_{S_c} | \mathbf{x}_{S_c}, \Sigma = \mathbf{I}, \sigma_j).$$

Let us define the $1 \times n$ vector $\boldsymbol{\delta}_S$, whose i -th element is $(\boldsymbol{\delta}_S)_i = 1$ if $i \in S$ and 0 otherwise, and the diagonal matrices $\mathbf{\Delta}_S = \text{diag}(\boldsymbol{\delta}_S)$ and $\bar{\mathbf{\Delta}}_S = \text{diag}([\mathbf{1} - \boldsymbol{\delta}_S, \mathbf{1}])$. Then, the mutual information $I_{S,j} |_{\Sigma=\mathbf{I}}$ can be rewritten as

$$I_{S,j} |_{\Sigma=\mathbf{I}} = I(\mathbf{\Delta}_S \mathbf{x}; \sqrt{\gamma} \bar{\mathbf{\Delta}}_S \mathbf{H}^T \mathbf{x} + \sqrt{\gamma} \bar{\mathbf{\Delta}}_S \mathbf{W}^T \mathbf{i} + \mathbf{z} | (\mathbf{I} - \mathbf{\Delta}_S) \mathbf{x}, \Sigma = \mathbf{I}, \sigma_j)$$

where the matrices $\mathbf{\Delta}_S$ and $\bar{\mathbf{\Delta}}_S$ select the nodes in the cut S and S_c , respectively.

Since $\mathbf{x} = \Delta_S \mathbf{x} + (\mathbf{I} - \Delta_S) \mathbf{x}$ and we assume $\Sigma = \mathbf{I}$, we have

$$\begin{aligned}
I_{S,j} |_{\Sigma=\mathbf{I}} &= I(\Delta_S \mathbf{x}; \sqrt{\gamma} \bar{\Delta}_S \mathbf{H}^T \Delta_S \mathbf{x} + \sqrt{\gamma} \bar{\Delta}_S \mathbf{W}^T \mathbf{i} + \mathbf{z} | \Sigma = \mathbf{I}, \sigma_j) \\
&= h(\sqrt{\gamma} \bar{\Delta}_S \mathbf{H}^T \Delta_S \mathbf{x} + \sqrt{\gamma} \bar{\Delta}_S \mathbf{W}^T \mathbf{i} + \mathbf{z} | \Sigma = \mathbf{I}, \sigma_j) \\
&\quad - h(\sqrt{\gamma} \bar{\Delta}_S \mathbf{W}^T \mathbf{i} + \mathbf{z} | \sigma_j)
\end{aligned} \tag{5.13}$$

where $h(\cdot)$ denotes the differential entropy.

Now, let us define the vector $\mathbf{d}_j = [d_{1j}, \dots, d_{nj}]^T$ whose entries, for $i = 1, \dots, n$, are such that $d_{ij} = 1$ if $\sigma_{ij} = \mathbf{t}$, and $d_{ij} = 0$ if $\sigma_{ij} = \mathbf{r}$. From the above definitions, it follows that the vectors of signals \mathbf{x} conditioned to the network state σ_j can be written as $\mathbf{x} | \sigma_j = \mathbf{D}_j \mathbf{x}$, where $\mathbf{D}_j = \text{diag}(\mathbf{d}_j)$. Similarly, the interference vector conditioned to the network state σ_j is given by $\mathbf{i} | \sigma_j = \mathbf{D}_j \mathbf{i}$. Then, from (5.13) we obtain

$$\begin{aligned}
I_{S,j} |_{\Sigma=\mathbf{I}} &= h(\sqrt{\gamma} \bar{\Delta}_S \mathbf{H}^T \Delta_S \mathbf{x} + \sqrt{\gamma} \bar{\Delta}_S \mathbf{W}^T \mathbf{i} + \mathbf{z} | \Sigma = \mathbf{I}, \sigma_j) \\
&\quad - h(\sqrt{\gamma} \bar{\Delta}_S \mathbf{W}^T \mathbf{i} + \mathbf{z} | \sigma_j) \\
&= h(\sqrt{\gamma} \bar{\Delta}_S \mathbf{H}^T \Delta_S \mathbf{D}_j \mathbf{x} + \sqrt{\gamma} \bar{\Delta}_S \mathbf{W}^T \mathbf{D}_j \mathbf{i} + \mathbf{z} | \Sigma = \mathbf{I}) \\
&\quad - h(\sqrt{\gamma} \bar{\Delta}_S \mathbf{W}^T \mathbf{D}_j \mathbf{i} + \mathbf{z}) \\
&= \frac{1}{2} \log_2 \frac{|\mathbf{I} + \gamma \bar{\Delta}_S (\mathbf{W}^T \mathbf{D}_j \mathbf{W} + \mathbf{H}^T \Delta_S \mathbf{D}_j \mathbf{H}) \bar{\Delta}_S|}{|\mathbf{I} + \gamma \bar{\Delta}_S \mathbf{W}^T \mathbf{D}_j \mathbf{W} \bar{\Delta}_S|} = a_{S,j}
\end{aligned} \tag{5.14}$$

where we used the fact that \mathbf{x} , \mathbf{i} and \mathbf{z} are mutually independent, $\mathbf{D}_j^2 = \mathbf{D}_j$, and $\Delta_S \mathbf{D}_j^2 \Delta_S = \Delta_S \mathbf{D}_j$. Let $\mathbf{a} = [a_{S,1}, \dots, a_{S,J}]^T$ (with $a_{S,j}$ as in (5.14)) and $\mathbf{t} = [t_1, \dots, t_J]^T$. It follows that (5.12) can be rewritten as

$$B_{\text{FD}} \geq \max_{\mathbf{t}} \min_{S \in \Omega} \left\{ \frac{\mathbf{a}^T \mathbf{t}}{\rho_S} \right\}. \tag{5.15}$$

The max-min problem in (5.15) can be turned into the following linear programming

(LP) problem, which can be easily solved:

$$\begin{aligned}
B_{L\text{-FD}} &= \max R \quad \text{s.t.} \\
\frac{\mathbf{a}_S^T \mathbf{t}}{\rho_S} &\geq R, \text{ for any } S \in \Omega \\
\mathbf{1}^T \mathbf{t} &= 1 \\
0 \leq t_j &\leq 1, \text{ for any } j \in \mathcal{J}.
\end{aligned}$$

As a last remark, note that, for the special case where $k_C = k_I = 1$, the expressions we derived for $B_{L\text{-FD}}$, B_{FD} and $B_{U\text{-FD}}$ coincide and take the value, $\frac{1}{2\theta_T} \log_2(1+\gamma)$.

5.4.3 Results

Let us consider a network composed of $n = 10$ nodes plus the destination. By using the above expressions and setting $\rho_i = 1$, $i = 1, \dots, n$, we compute the bounds to the achievable rate R in (5.5) as the value of SNR, γ , and the node cooperation and interference range vary. Recall that, by varying the latter two parameters, the values taken by the bounds in (5.11) and (5.15) vary as well.

Fig. 5.2 presents the results obtained for a path loss exponent, a , equal to 2 (top) and 4 (bottom), respectively. The cooperation range k_C varies between 1 and 4, while the interference range is set to $k_I = 5$. As it can be seen by looking at the plots, in the medium-low SNR region the bounds, $B_{U\text{-FD}}$ and $B_{L\text{-FD}}$, are tight for any value of k_C , while in the high SNR region the gap is very limited for any $k_C \geq 2$. The figures also show that the distance between the two bounds decreases as the path loss exponent increases, especially in the high SNR region. The reason of this behavior is that the larger the k_C 's and a 's, the smaller the impact of the interference, as large k_C 's imply that interferers are very far away from the receiver while large a 's cause severe signal attenuation. Since the bounds $B_{U\text{-FD}}$ and $B_{L\text{-FD}}$ are always close (except for $a = 2$ and $k_C = 1$), we conclude that $B_{U\text{-FD}}$ is a tight upper-bound of the cut-set bound B_{FD} .

Furthermore, we observe that, by increasing k_C , the bounds also increase, as it

can be exploited the cooperation among a larger number of transmitters. However, such a gain is evident only when k_C grows from 1 to 2, while a further increase of k_C to 4 provides only a limited increase in the data rate. Such a gain further reduces as the path loss exponent grows.

In conclusion, our results suggest that increasing the number of cooperating nodes beyond two provides a benefit which is little for medium-low SNR and negligible in the high SNR region. Also, such a gain in the achievable rate significantly decreases for $a > 2$.

It follows that the complexity of designing and implementing a communication strategy that exploits cooperative transmissions from nodes, located farther than two hops away from a receiver, does not pay off in terms of performance.

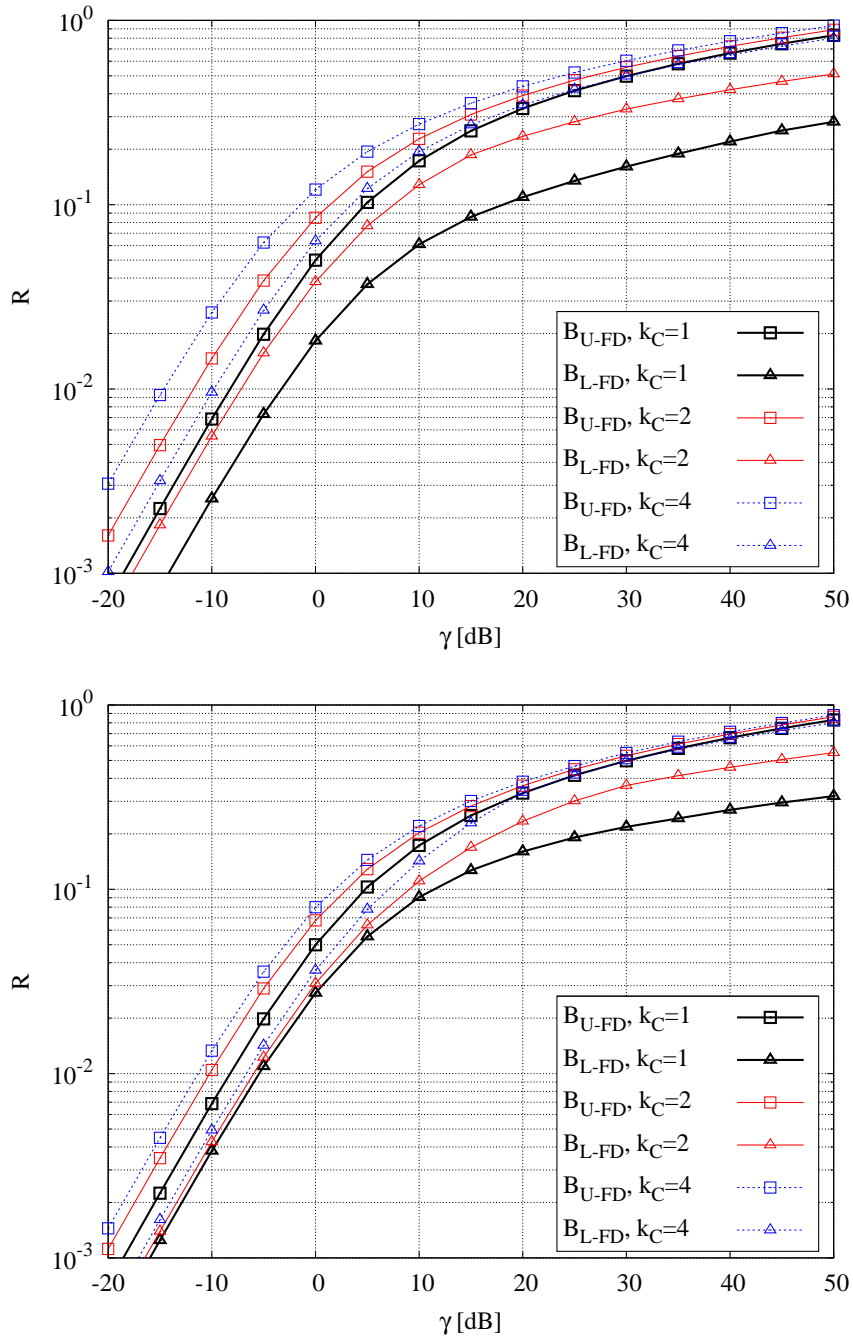


Figure 5.2: Full-duplex radii: bounds for $n = 10$, $a = 2$ (top), and $a = 4$ (bottom), $\rho_i = 1\forall i$, $k_C = 1, 2, 3$ hops and $k_I = 5$.

5.5 Cut-set bounds: Half-duplex radios

We now consider that the n network nodes operate in HD mode, i.e., that at any time instant each node can be either in the transmit (t) or in the receive (r) state. As done in the case of FD radios, we denote by $I_{\mathcal{S},j} = I(\mathbf{x}_{\mathcal{S}}; \mathbf{y}_{\mathcal{S}_c} | \mathbf{x}_{\mathcal{S}_c}, \boldsymbol{\sigma}_j)$ the mutual information associated to cut \mathcal{S} and conditioned to the network being in state $\boldsymbol{\sigma}_j = [\sigma_{1j}, \dots, \sigma_{nj}]$, where $\sigma_{ij} \in \{\text{t}, \text{r}\}$ is the state of node i when the network is in state $\boldsymbol{\sigma}_j$. It follows that the mutual information associated to the cut \mathcal{S} can be written as $I_{\mathcal{S}} = I(\mathbf{x}_{\mathcal{S}}; \mathbf{y}_{\mathcal{S}_c} | \mathbf{x}_{\mathcal{S}_c}) = \sum_{j=1}^J t_j I_{\mathcal{S},j}$.

Following [29], the cut set bound to the rate that can be achieved in the HD scenario is:

$$B_{\text{HD}} = \max_{\mathbf{t}, \boldsymbol{\Sigma}} \min_{\mathcal{S} \in \Omega} \left\{ \frac{I_{\mathcal{S}}}{\rho_{\mathcal{S}}} \right\}. \quad (5.16)$$

where we recall that $\rho_{\mathcal{S}} = \sum_{i \in \mathcal{S}} \rho_i$. The computation of the bound in (5.16) is again mathematically intractable for large networks, since it requires the maximization over the vector \mathbf{t} and the matrix $\boldsymbol{\Sigma}$, and the minimization over $2^n - 1$ cuts. Thus, similarly to what done for the FD case, below we derive an upper and a lower-bound to B_{HD} .

5.5.1 Upper bound to B_{HD}

We first observe that the bound in (5.9) can be obtained again for the HD case by following the same approach as in Sec. 5.4.1, i.e., we can bound (5.16) by reducing the set of possible cuts, Ω . However, it is clear that a different derivation is needed in order to obtain a good bound for the HD case.

We now split the set of nodes \mathcal{T} in two disjoint subsets: \mathcal{T}_1 containing the nodes $\{1, \dots, n - k - 1\}$ and \mathcal{T}_2 including the nodes $\{n - k, \dots, n\}$, where $k \geq k_C$. We then upper-bound B_{HD} by considering only the set of network cuts, $\tilde{\Omega}$, such that, for every $\mathcal{S} \in \tilde{\Omega}$, the nodes in \mathcal{T}_1 are out of the cooperation range of all nodes in \mathcal{S} .

Then, a first upper-bound to B_{HD} can be written as

$$B_{\text{HD}} \leq \max_{\mathbf{t}, \Sigma} \min_{S \in \tilde{\Omega}} \left\{ \frac{I_S}{\rho_S} \right\}. \quad (5.17)$$

Next, motivated by the results obtained for the FD radios (see Fig. 5.2 and related comments), let us limit our attention to the case where the cooperation range is equal to 2 hops, i.e., $k = k_C = 2$. The generalization to the case where $k_C > 2$, although more complicated, can be easily obtained. Under such an assumption, the right hand side of (5.17) can be rewritten as

$$\min_{S \in \tilde{\Omega}} \left\{ \frac{I_S}{\rho_S} \right\} = \min_{1 \leq h \leq 5} \min_{S \in \tilde{\Omega}_h} \left\{ \frac{I_S}{\rho_S} \right\}$$

where the disjoint subsets of cuts, $\tilde{\Omega}_h$'s, satisfy the condition $\tilde{\Omega} = \bigcup_{h=1}^5 \tilde{\Omega}_h$ and are defined below.

1. $\tilde{\Omega}_1 = \{S = \{n - q, \dots, n - 1\}, 2 \leq q \leq n - 1\}$. In this case, we have $S_c = \{1, \dots, n - q - 1, n\}$ for $2 \leq q < n - 1$, and $S_c = \{n, n + 1\}$ for $q = n - 1$. The corresponding mutual information can be written as

$$I_S = I(\mathbf{x}_S; \mathbf{y}_{S_c} | \mathbf{x}_{S_c}) = I(\mathbf{x}_S; y_n, y_{n+1} | \mathbf{x}_{S_c}) \quad (5.18)$$

where the last equality holds since the signals \mathbf{y}_{S_c} , except for y_n , do not depend on \mathbf{x}_S . We recall that the conditioned mutual information $I(X; Y | Z)$ can be written in terms of differential entropy as $I(X; Y | Z) = h(Y | Z) - h(Y | X, Z)$. In our case and for $2 \leq q \leq n - 1$, we have

$$\begin{aligned} I(\mathbf{x}_S; y_n, y_{n+1} | \mathbf{x}_{S_c}) &= h(y_n, y_{n+1} | \mathbf{x}_{S_c}) - h(y_n, y_{n+1} | x_1, \dots, x_n) \\ &\leq h(y_n, y_{n+1} | x_n) - h(y_n, y_{n+1} | x_{n-2}, x_{n-1}, x_n) \\ &= I(x_{n-2}, x_{n-1}; y_n, y_{n+1} | x_n) \end{aligned} \quad (5.19)$$

since conditioning reduces the entropy and, under our assumptions

$$h(y_n, y_{n+1}|x_1, \dots, x_n) = h(y_n, y_{n+1}|x_{n-2}, x_{n-1}, x_n).$$

Recall that in (5.17) we need to minimize the ratio I_S/ρ_S over all possible cuts. Therefore, by using the results in (5.18) and (5.19), we can write:

$$\begin{aligned} \min_{S \in \tilde{\Omega}_1} \frac{I_S}{\rho_S} &\leq \min_{S \in \tilde{\Omega}_1} I(x_{n-2}, x_{n-1}; y_n, y_{n+1}|x_n) \left(\sum_{i \in S} \rho_i \right)^{-1} \\ &= I(x_{n-2}, x_{n-1}; y_n, y_{n+1}|x_n) \min_{2 \leq q \leq n-1} \left(\sum_{i \in \{n-q, \dots, n-1\}} \rho_i \right)^{-1} \\ &= I(x_{n-2}, x_{n-1}; y_n, y_{n+1}|x_n) \left(\sum_{i=1}^{n-1} \rho_i \right)^{-1} = I_1. \end{aligned} \quad (5.20)$$

2. $\tilde{\Omega}_2 = \{\{n-1\}\}$. Following the same procedure as above, we obtain

$$\min_{S \in \tilde{\Omega}_2} \frac{I_S}{\rho_S} \leq \frac{1}{\rho_{n-1}} I(x_{n-1}; y_n, y_{n+1}|x_{n-2}, x_n) = I_2.$$

3. $\tilde{\Omega}_3 = \{S = \{n-q, \dots, n\}, 2 \leq q \leq n-1\}$. Then, we have $S_c = \{1, \dots, n-q-1\}$ for $2 \leq q \leq n-1$, and $S_c = \emptyset$ for $q = n-1$. Again, we obtain

$$\min_{S \in \tilde{\Omega}_3} \frac{I_S}{\rho_S} \leq \frac{1}{\sum_{i=1}^n \rho_i} I(x_{n-1}, x_n; y_{n+1}) = I_3.$$

4. $\tilde{\Omega}_4 = \{\{n-1, n\}\}$, then $\min_{S \in \tilde{\Omega}_4} \frac{I_S}{\rho_S} \leq \frac{1}{\rho_n + \rho_{n-1}} I(x_{n-1}, x_n; y_{n+1}|x_{n-2}) = I_4$.

5. $\tilde{\Omega}_5 = \{\{n\}\}$, then $\min_{S \in \tilde{\Omega}_5} \frac{I_S}{\rho_S} \leq \frac{1}{\rho_n} I(x_n; y_{n+1}|x_{n-2}, x_{n-1}) = I_5$.

Given that the interference range is larger than the cooperation range, i.e., $k_I > k_C$, it is clear that the terms I_h 's also account for the interference. Since interfering signals are assumed to be uncorrelated, for simplicity in the bound computation, the terms of mutual information I_h 's can be upper-bounded by considering $k_I = k_C + 1$. That is, we can account only for a single interfering node.

In conclusion, let \tilde{I}_h be the mutual information I_h conditioned to $k_I = k_C + 1$, $h = 1, \dots, 5$. We can eventually write the upper-bound to B_{HD} as

$$B_{\text{U-HD}} = \max_{\mathbf{t}, \Sigma} \min_{\substack{1 \leq h \leq 5 \\ \sum_{j=1}^J t_j = 1}} \tilde{I}_h. \quad (5.21)$$

Note that the bound in (5.21) refers to an equivalent network composed of 5 nodes (see Fig. 5.3), namely: (a) an interfering node $n-3$; (b) the node $n-2$ whose transmitted signal is considered as useful for nodes $n-1$ and n and as interference for node $n+1$; (c) the nodes $n-1$ and n whose transmitted signals are considered as useful to node $n+1$; and (d) the destination node $n+1$. Also, the terms $\tilde{I}_1, \dots, \tilde{I}_5$ represent the mutual information associated to the cuts, respectively, $\{n-2, n-1\}$, $\{n-1\}$, $\{n-2, n-1, n\}$, $\{n-1, n\}$, $\{n\}$ of the equivalent network, where the equivalent traffic loads are described by the coefficients

$$\hat{\rho}_{n-2} = \sum_{i=1}^{n-2} \rho_i; \quad \hat{\rho}_{n-1} = \rho_{n-1}; \quad \hat{\rho}_n = \rho_n.$$

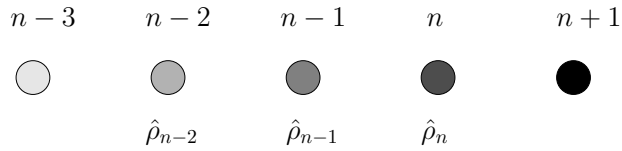


Figure 5.3: Equivalent network for the computation of the bound in (5.21).

Since each node can operate in two states and node $n+1$ is always receiving, the above equivalent network has 2^4 states to be considered in the computation of (5.21).

As the last remark, we observe that the mutual information \tilde{I}_h , $h = 1, \dots, 5$, can be rewritten as $\tilde{I}_h = \sum_j t_j \tilde{I}_{h,j}$, where the terms $\tilde{I}_{h,j}$ are the mutual information conditioned to network state σ_j . Then, the bound in (5.21) can be written as

$$B_{\text{U-HD}} = \max_{\mathbf{t}, \Sigma} \min_{\substack{1 \leq h \leq 5 \\ \sum_j t_j = 1}} \sum_j t_j \tilde{I}_{h,j}.$$

The above max-min problem can be efficiently solved as follows: for each covariance matrix Σ , solve the LP problem

$$\begin{aligned}
B_{\text{U-HD}} &= \max R \quad \text{s.t.} \\
\sum_j t_j \tilde{I}_{h,j} &\geq R, \quad h = 1, \dots, 5 \\
\sum_j t_j &= 1 \\
\sum_{j:\sigma_{j,n-3}=\text{t}} t_j &\geq \frac{\rho_{n-3}R}{\frac{1}{2}\log_2(1+\gamma)}
\end{aligned}$$

and choose the maximum over Σ . Note that $\sum_{j:\sigma_{j,n-3}=\text{t}} t_j$ represents the time fraction during which the interfering node $n - 3$ is transmitting (i.e., it is in state t). The constraint $\sum_{j:\sigma_{j,n-3}=\text{t}} t_j \geq \frac{\rho_{n-3}R}{\frac{1}{2}\log_2(1+\gamma)}$ bounds such a time fraction with the time required by node $n - 3$ to transmit *at least* its own generated data ($\rho_{n-3}R$) through a single-hop channel with capacity $\log_2(1 + \gamma)/2$.

5.5.2 Lower bound to B_{HD}

As done for the FD case, in order to verify that the upper bound $B_{\text{U-HD}}$ is tight enough, we derive a lower bound to B_{HD} and compare it to the $B_{\text{U-HD}}$. Again, we lower bound B_{HD} by assuming $\Sigma = \mathbf{I}$. By doing so, we obtain:

$$B_{\text{HD}} \geq \max_{\text{t}} \min_S \left\{ \frac{\sum_{j=1}^J t_j I_{S,j} |_{\Sigma=\mathbf{I}}}{\rho_S} \right\}. \quad (5.22)$$

The conditioned mutual information $I_{S,j} |_{\Sigma=\mathbf{I}}$ can be expressed similarly to (5.14), as:

$$\frac{1}{2} \log_2 \frac{|\mathbf{I} + \gamma \bar{\Delta}_S \bar{\mathbf{D}}_j (\mathbf{W}^\top \mathbf{D}_j \mathbf{W} + \mathbf{H}^\top \Delta_S \mathbf{D}_j \mathbf{H}) \bar{\mathbf{D}}_j \bar{\Delta}_S|}{|\mathbf{I} + \gamma \bar{\Delta}_S \bar{\mathbf{D}}_j \mathbf{W}^\top \mathbf{D}_j \mathbf{W} \bar{\mathbf{D}}_j \bar{\Delta}_S|} = b_{S,j} \quad (5.23)$$

where the matrix $\bar{\mathbf{D}}_j = \text{diag}([1 - \mathbf{d}, 1])$ accounts for the fact that HD nodes cannot simultaneously transmit and receive, i.e., $\bar{\mathbf{D}}_j$ is used to force to 0 the signal received at the nodes that are transmitting. The right hand side of (5.22) can then be further

bounded as:

$$\max_{\substack{\mathbf{t} \\ \mathbf{1}^\top \mathbf{t} = 1}} \min_{\mathcal{S}} \left\{ \frac{\mathbf{b}_{\mathcal{S}}^\top \mathbf{t}}{\varrho_{\mathcal{S}}} \right\} \geq \max_{\substack{\hat{\mathbf{t}} \\ \mathbf{1}^\top \hat{\mathbf{t}} = 1}} \min_{\mathcal{S}} \left\{ \frac{\hat{\mathbf{b}}_{\mathcal{S}}^\top \hat{\mathbf{t}}}{\varrho_{\mathcal{S}}} \right\} = B_{\text{L-HD}} \quad (5.24)$$

where the column vectors $\hat{\mathbf{b}}_{\mathcal{S}}$ and $\hat{\mathbf{t}}$ are defined as $\hat{\mathbf{b}}_{\mathcal{S}} = \{b_{\mathcal{S},j}\}$, $\hat{\mathbf{t}} = \{t_j\}$, with $j \in \hat{\mathcal{J}}$, and where we only considered a subset $\hat{\mathcal{J}}$ of the possible network states \mathcal{J} . The reduction of the number of considered states to $\hat{\mathcal{J}}$ allows a dramatic reduction of the computational complexity of (5.24) and is justified by the fact that, through numerical analysis, we have observed that most of the network states have little or no influence on the value of the bound. More specifically, the number of dominant states, i.e., those that provide significant contribution, increases just linearly with n . Also, for $k_I = k_C + 1$, the dominant network states are circular shifts of the vector $\sigma = [\dots \text{ttrttrttr} \dots]$ where the pattern ttr is repeated. This result was expected since, for the above value of k_I , the pattern ttr both avoids interference and allows neighboring nodes to cooperate. This finding suggests that efficient communication strategies can be obtained by exploiting such network states. The max-min problem in (5.24) can then be turned into the following LP problem:

$$\begin{aligned} B_{\text{L-HD}} &= \max R \quad \text{s.t.} \\ \frac{\hat{\mathbf{b}}_{\mathcal{S}}^\top \hat{\mathbf{t}}}{\varrho_{\mathcal{S}}} &\geq R, \text{ for any } \mathcal{S} \in \Omega \\ \mathbf{1}^\top \hat{\mathbf{t}} &= 1 \\ 0 \leq t_j &\leq 1, \text{ for any } j \in \hat{\mathcal{J}}. \end{aligned}$$

5.5.3 Results

We now assume HD radios and compare the bounds in (5.21) and (5.24) to the achievable data rate as the SNR varies. We focus on the case where $\rho_i = 1$, $i = 1, \dots, n$, path loss exponent $a = 2, 4$, cooperation range $k_C = 2$ and interference range $k_I = k_C + 1$. The results are shown in Fig. 5.4, for $n = 10$. The bounds we derived show to be very close for any value of γ and a , again proving that the upper-

bound B_{U-HD} in (5.21) is a tight upper bound to the cut-set bound B_{HD} . Similar results have been obtained also varying the values of the system parameters over a larger range.

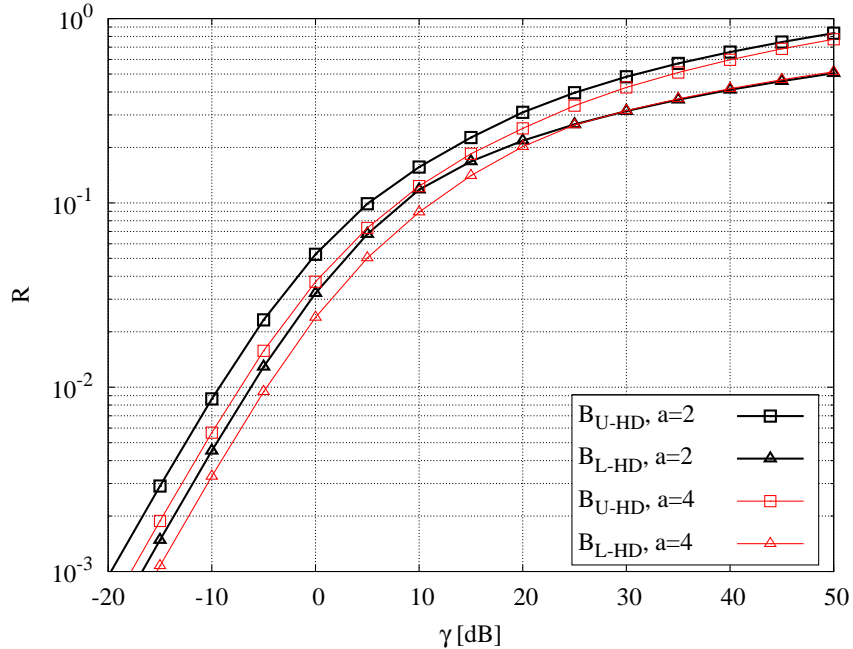


Figure 5.4: Half-duplex radii: bounds for $n = 10$, $a = 2, 4$, $\rho_i = 1 \forall i$, $k_C = 2$ hops and $k_I = 3$.

After assessing the tightness of the bounds in (5.11) and (5.21), we now investigate their behavior for different values of n . In particular, Fig. 5.5 compares the bounds B_{U-FD} and B_{L-FD} for $a = 2, 4$, $k_C = 2$, and for $n = 5$ and $n = 10$, respectively. The bounds for the FD case are clearly higher than those obtained for HD radios, as the latter case constrains the nodes to operate in either transmit or receive mode while in the FD case the best operational mode for each node is selected.

We then analyze the case where the nodes have different traffic loads, i.e., they generate data traffic at different rates ρ_i . In particular, Figs. 5.6 and 5.7 show the case where $\rho_i = i$, $i = 1, \dots, n$, i.e., the closer a node to the destination, the higher its load. The first plot presents the curves obtained for $n = 5$ and path loss exponent a equal to 2 and 4. In this case, we can observe a behavior very similar to the one exhibited by the bounds in Fig. 5.5 (top), i.e., under a constant traffic

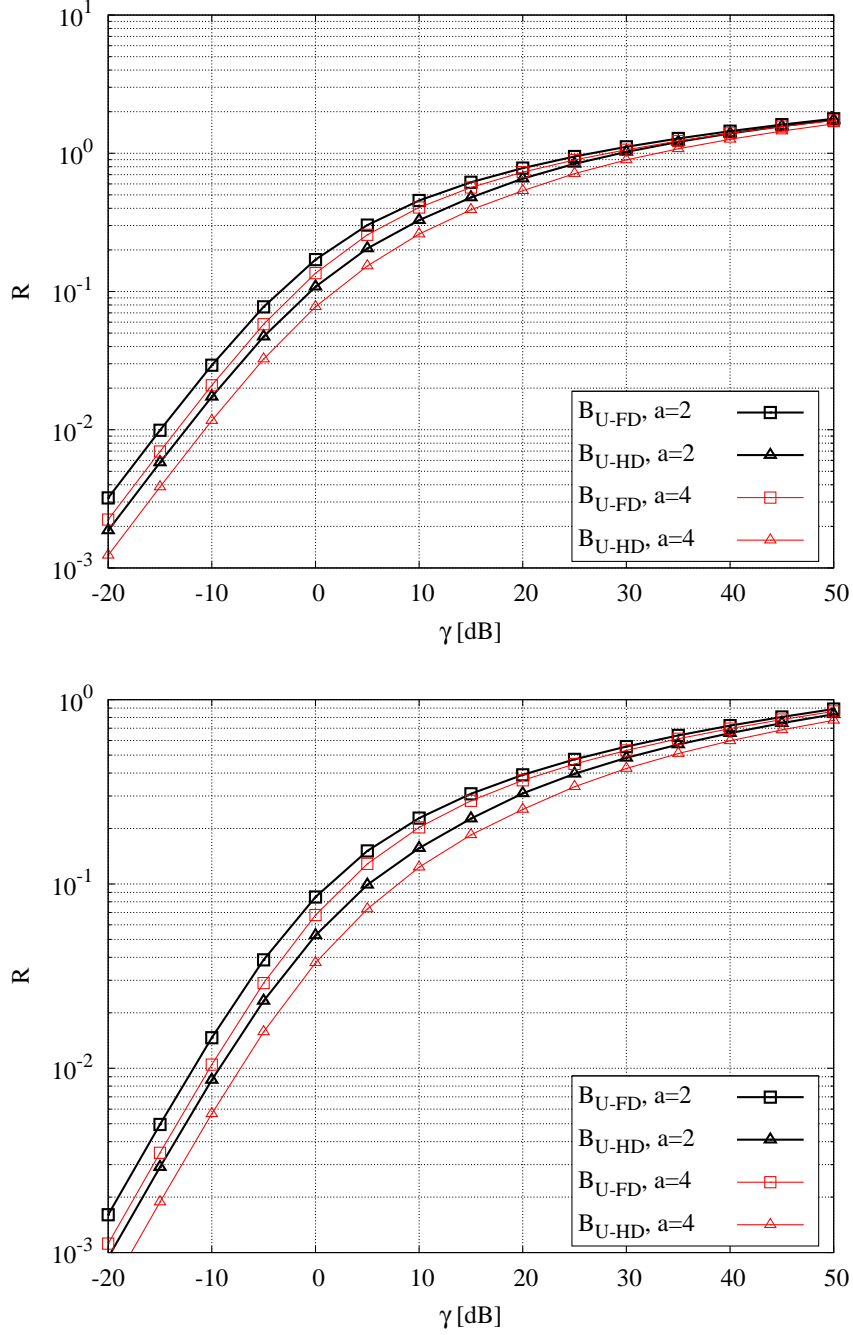


Figure 5.5: Comparison between the cases of half-duplex and full-duplex radios. Bounds for $n = 5$ (top), and $n = 10$ (bottom), with $a = 2, 4$, $\rho_i = 1 \forall i$, $k_C = 2$ hops and $k_I = 3$ hops.

load for all nodes. The plot in Fig. 5.7, instead, refers to the case where $a = 2$ and $n = 5, 10$. Comparing these results with those in Fig. 5.5 (bottom), it is evident that the achievable value of R is greatly affected by the number of nodes n when $\rho_i = i$, $i = 1, \dots, n$. However, recall that, in this case, the average data rate of the generic

node i is $R_i = iR, i = 1, \dots, n$. Thus, although R decreases as n grows, the overall amount of traffic delivered to the destination in a time unit is still high.

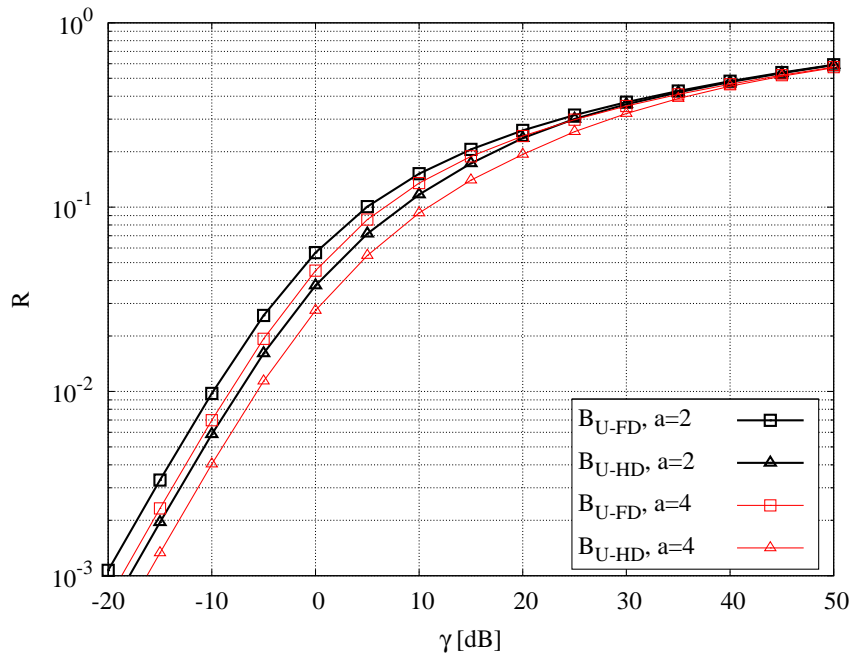


Figure 5.6: Comparison between the cases of half-duplex and full-duplex radios. Bounds for $n = 5, a = 2, 4, k_C = 2$ hops, $k_I = 3$ hops, and different data generation rates at the nodes, namely, $\rho_i = i, i = 1, \dots, n$.

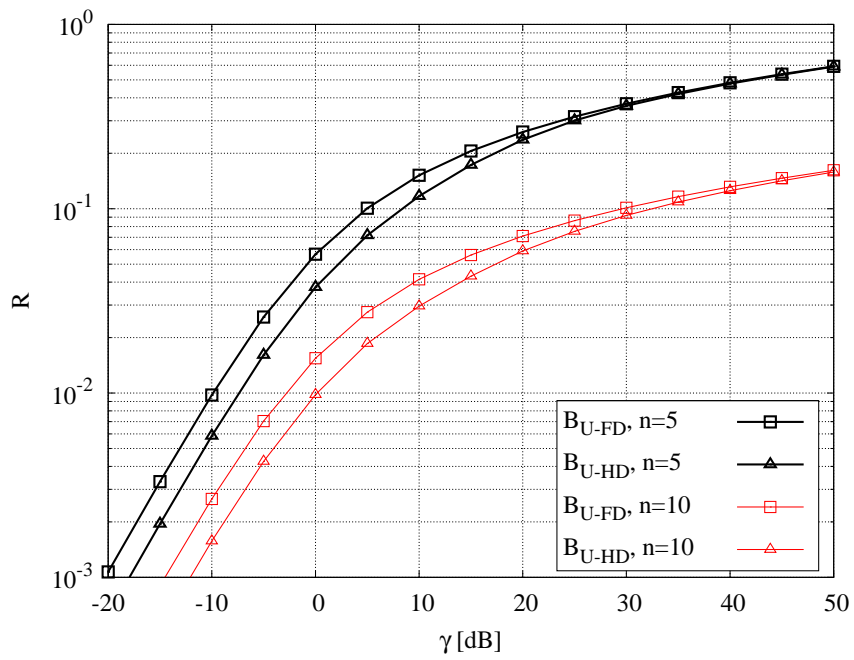


Figure 5.7: Comparison between the cases of half-duplex and full-duplex radios. Bounds for $n = 5, 10$, $a = 2$, $k_C = 2$ hops, $k_I = 3$ hops, and different data generation rates at the nodes, namely, $\rho_i = i, i = 1, \dots, n$.

5.6 Conclusions

We studied the upper bound to the data rate that wireless nodes in a linear network can achieve. We carried out the analysis accounting for the interference due to simultaneous transmissions, and in presence of full as well as half-duplex nodes. Also, unlike previous work, we considered that nodes located at more than one-hop distance can cooperate to deliver the data traffic to the destination, and that nodes may have different requirements in terms of achievable data rate. The expressions we derived are mathematically tractable and allow the analysis of large-scale, multi-hop networks. Numerical results showed the impact on the performance of several system parameters, such as the SNR, the path loss exponent and the number of cooperating transmitters.

Our analysis suggests two important facts. First, in order to design efficient communication strategies, it is sufficient to use pairs of transmitters that cooperate to forward the data to the destination. Second, in half-duplex networks, there exist some dominant network states whose contribution determines the achievable data rate. Effective communication strategies can therefore be obtained by considering pairs of cooperating nodes and by letting the network operate in such states. Future work will focus on the definition of cooperative traffic relaying schemes that provide an achievable rate as close as possible to the upper bound provided in this study.

Chapter 6

Two-hop Cooperative

Communication Strategies for

Wireless Sensor Networks

We study multi-hop wireless sensor networks composed of a cascade of nodes that may both generate their own traffic and relay other nodes' data. Nodes operate in half-duplex mode and aim at delivering their data to a common destination node. We analyze the above network scenario considering that the nodes can relay traffic over up to two hops, and devise suitable communication strategies. We show that the proposed schemes exhibit good performances in terms of average achievable rate when compared to non-cooperative techniques as well as to the cut-set upper bound.

6.1 Introduction

In this chapter, we present two multi-hop traffic relaying strategies for linear wireless networks whose nodes all operate in half-duplex mode. More precisely, we consider a wireless network where the nodes have to deliver their traffic to a destination node, possibly through multi-hop data transfers. The nodes share the same

radio resources and generate their own traffic at an equal average rate. We assume that the nodes cooperate to relay the traffic based on the decode-and-forward paradigm [20]. The node transmission rates and powers correspond to optimal coding over a discrete-time additive white Gaussian noise (AWGN) channel, although more general channels and coding schemes could be considered as well. Furthermore, unlike previous work, we account for the fact that the *transmission range of the source/relay nodes may span over more than one hop*. Under these conditions, we derive the average rate that can be achieved by the node under each proposed strategy, and we compare it to the cut-set upper bound on the network data rate.

The rest of the chapter is organized as follows. We first discuss related work in Section 6.2, then we introduce the system model we consider in Section 6.3. The proposed transmission strategies are described in Section 6.4, while their performances are evaluated in Section 6.5. Finally, in Section 6.6 we draw our conclusions and highlight directions for future research.

6.2 Related Work

Traffic relaying in wireless networks has been widely investigated, under different network topologies and assumptions on the nodes capabilities. As an example the works in [39, 50] address the case where one node is a traffic source while the others act as relays only. Specifically, the study in [50], analyzes, among others, a cascaded, cooperative, two-hop relaying scheme. Such a strategy, although being different from ours and considering only one source, relies on the same assumption we make on the node transmission range.

Multiple source nodes have been considered in [31] under the assumption that all network nodes are full-duplex [31, 40], or in [41] where just a small number of nodes operate in half-duplex mode. A transmission strategy that integrates both full- and half-duplex schemes has been presented in [51], for a network with a source-destination pair and only one relay node. Such a strategy outperforms those that

can be designed in the case of a full- or half-duplex relay only, but it cannot be extended to more general network scenarios. A network of half-duplex source/relay cascades, similar to the one we study, has been analysed in [42]. The work there presents a coding scheme, through which the cut-set bound to the data rate can be achieved when the rates of relay sources fall below certain thresholds. However, the work considers one-hop communications only, and the obtained result holds under the assumption of error-free communication links and of nodes being synchronized at the symbol level.

Finally, energy-efficient, cooperative, traffic relaying schemes have been proposed in [32, 33]. However, the scope and methodology of these works differ from ours, as they focus either on the design of algorithms and protocols for sensor networks, or target different scenarios, e.g., MIMO communications. In [34, 47], the problem of computing transmission powers, rates, and link schedule for an energy-constrained wireless network has been addressed by maximizing the network lifetime through a cross-layer design approach. Besides having different scope, our study differs from [34, 47] in that these works consider the data rates of the source nodes as the inputs to the problem of transmission scheduling.

6.3 System Model

Network topology: We consider a wireless network with linear topology composed of n nodes and a destination in which node 1 is the node at the left end of the topology, while the destination is located at the right end and is denoted by $n + 1$. For simplicity, we assume that the distance between every two nodes (including the destination) is the same, and is denoted by d . The network topology is depicted in Fig. 6.1. The nodes in the network serve as both data sources and data relays. Every node i , $i = 1, \dots, n$ generates messages, denoted by W_i , with W_i being independent of W_j , for $i \neq j$. We assume that the data traffic generated by the nodes should be delivered to the destination at the same average rate, denoted by R .



Figure 6.1: Network with linear topology, the destination is shown in black.

Node and network states: Each node in the network is equipped with a half-duplex transceiver, implying that it cannot transmit and receive at the same time. This prompts the node i to operate in three different states, namely *transmit*, *receive*, and *sleep*, denoted by \mathfrak{t} , \mathfrak{r} , \mathfrak{s} respectively. The state of the node i is denoted by σ_i in which $\sigma_i \in \{\mathfrak{t}, \mathfrak{r}, \mathfrak{s}\}$. Moreover, the network state σ is defined as the vector $[\sigma_1, \sigma_2, \dots, \sigma_n]$ containing the states of all nodes. In general a network may operate in M states, each denoted by σ_h , $h = 1, \dots, M$. Since there are three possible states for each node, a network may have up to 3^n states, i.e., $M \leq 3^n$. We denote by t_i^σ the fraction of time the node i spends in state σ , and we maintain that $t_i^\mathfrak{t} + t_i^\mathfrak{r} + t_i^\mathfrak{s} = 1$. The network remains in state σ_h for the time t_h where accordingly $\sum_h t_h = 1$.

Communication channel: We adopt the decode-and-forward paradigm [20] as the relaying technique in the network. The nodes transmit information at the same average rate R through the same frequency channel of bandwidth B shared among them. Due to the adopted linear topology of the network, the traffic flow is unidirectional, i.e., from the lower indexed nodes toward those with higher indexes. To avoid an exceedingly high level of complexity of the communication strategies, we assume that node i , while being in state \mathfrak{r} , is able to decode only the signals transmitted from the nodes that are located no farther than two-hop distance, $2d$. In other words, it treats the signals from the nodes located farther than $2d$ -distance as interference. Moreover, the nodes in the network are assumed to have two antennas; one dedicated to transmission and directed toward the destination (downstream), and the other dedicated to reception and directed to the opposite side of the destination (upstream). This limits the interfering signals to the upstream ones only. All nodes transmit with power P , and the channel noise is considered to be AWGN

with the power spectral density N_0 . The signal-to-noise ratio (SNR) with respect to the one-hop distance d and in the absence of interference is denoted by γ defined as

$$\gamma = \frac{PG_tG_r}{N_0B} \left(\frac{\lambda}{4\pi d} \right)^a \quad (6.1)$$

where G_t, G_r are, respectively, the transmit and receive antenna gains, λ is the carrier wavelength, and a is the path loss exponent. Finally, by denoting the transmission bandwidth by B , we define the one-hop channel capacity as $\mathcal{C}(\gamma) = B \log_2(1 + \gamma)$.

6.4 Communication strategies

In this section, we describe our two proposed communication strategies, namely TTR (Transmit-Transmit-Receive) and TTRR (Transmit-Transmit-Receive-Receive). For each strategy, we adopt an information-theoretic approach and derive the average data rate that can be achieved.

6.4.1 The TTR strategy

The TTR strategy transfers the nodes traffic to the destination in n steps, each denoted by $h, h = 1, \dots, n$. According to such a strategy, at each step h , the network nodes plus the destination are grouped into $L(h)$ non-overlapping triplets of adjacent nodes, each triplet denoted by $\mathcal{T}_\ell^{(h)}, \ell = 1, \dots, L(h)$. Also, let us label the three nodes in the generic triplet by $\{\nu_1, \nu_2, \nu_3\}$.

The procedure through which the TTR strategy is accomplished is detailed below. An example of the network operation, representing the node and network states is given in Fig. 6.2, for a network with $n = 6$ nodes plus the destination.

Initial step, $h = 1$:

All nodes $\{1, \dots, n\}$, plus the destination, take part in the data transfer, hence

$L(1) = \lceil n/3 \rceil$. Each triplet $\mathcal{T}_\ell^{(1)}$ ($\ell = 1, \dots, L(1)$) includes the nodes $\{3(\ell - 1) + 1, 3(\ell - 1) + 2, 3(\ell - 1) + 3\}$; e.g., $\mathcal{T}_1^{(1)} = \{1, 2, 3\}$. Within the ℓ -th triplet, node ν_1 sends message $W_{3\ell-2}$ to node ν_2 at rate $\mathcal{R}^{(1)}$, using a transmit power level equal to P . Node ν_3 , instead, is in sleep mode (see Fig. 6.2); thus, at step $h = 1$, each triplet is in the state $[\sigma_{\nu_1}, \sigma_{\nu_2}, \sigma_{\nu_3}] = [\mathfrak{t}, \mathfrak{r}, \mathfrak{s}]$. Upon successful decoding, $W_{3\ell-2}$ will be available at node ν_2 .

Steps $h = 2, \dots, n$:

The number of nodes involved in the data transfer is $n - h + 2$, plus the destination, while the remaining $h - 2$ nodes are in sleep state. Hence, we have $L(h) = \lfloor (n - h + 3)/3 \rfloor$ and each triplet $\mathcal{T}_\ell^{(h)}$ ($\ell = 1, \dots, L(h)$) includes the nodes $\{3(\ell - 1) + h, 3(\ell - 1) + h + 1, 3(\ell - 1) + h + 2\}$. Within the ℓ -th triplet, the two leftmost nodes, ν_1, ν_2 , transmit the messages in the set $\{W_{3\ell-2}, W_{3\ell-1}, W_{3\ell}\}$, while the rightmost node, ν_3 , receives (see Fig. 6.2). Thus, at step h each triplet is in state $[\sigma_{\nu_1}, \sigma_{\nu_2}, \sigma_{\nu_3}] = [\mathfrak{t}, \mathfrak{t}, \mathfrak{r}]$, after which the strategy has been named. Specifically, nodes ν_1 and ν_2 dedicate a portion of their transmit power, $\alpha_j^{(h)}P$ and $\beta_j^{(h)}P$, respectively, to send the j -th element in the message set $\{W_{3\ell-2}, W_{3\ell-1}, W_{3\ell}\}$ toward node ν_3 , at rate $\mathcal{R}^{(h)}$, where $j = 1, 2, 3$ and $\sum_j \alpha_j^{(h)} = \sum_j \beta_j^{(h)} = 1$. Note, however, that for $h = 2, 3$, some of the messages in the set may not be available at ν_1 (ν_2) yet; in these cases, the corresponding power coefficient $\alpha_j^{(h)}$ ($\beta_j^{(h)}$) will be set to zero.

Table 6.1 reports the expression of the power coefficients $\alpha_j^{(h)}$ and $\beta_j^{(h)}$, for $j = 1, 2, 3$ and the generic h . Upon the completion of step h , the leftmost transmitter in the network has no more data to send, hence it will not take part in the following operational steps and the triplets are shifted toward the destination by one node.

Next, let $x_j^{(\ell)}$, $j = 1, 2, 3$, be the signal transmitted in the triplet $\mathcal{T}_\ell^{(h)}$ that carries the j -th element of the set $\{W_{3\ell-2}, W_{3\ell-1}, W_{3\ell}\}$. For example, for $h = 2$, $x_1^{(2)}$ denotes the signal transmitted by node ν_1 and ν_2 in the second triplet $\mathcal{T}_2^{(2)}$ that carries W_4 . All $x_j^{(\ell)}$ are assumed to be unit-variance signals. Moreover, let $y_i^{(\ell)}$

h	$\alpha_1^{(h)}$	$\alpha_2^{(h)}$	$\alpha_3^{(h)}$	$\beta_1^{(h)}$	$\beta_2^{(h)}$	$\beta_3^{(h)}$
2	1	0	0	$\beta_1^{(2)}$	$1 - \beta_1^{(2)}$	0
3	$\alpha_1^{(3)}$	$1 - \alpha_1^{(3)}$	0	$\beta_1^{(3)}$	$\beta_2^{(3)}$	$\beta_3^{(3)}$
$4, \dots, n$	$\alpha_1^{(h)}$	$\alpha_2^{(h)}$	$\alpha_3^{(h)}$	$\beta_1^{(h)}$	$\beta_2^{(h)}$	$\beta_3^{(h)}$

Table 6.1: Power coefficients $\alpha_j^{(h)}$ and $\beta_j^{(h)}$ ($j = 1, 2, 3$) for $2 \leq h \leq n$, ($\alpha_3^{(h)} = 1 - \alpha_1^{(h)} - \alpha_2^{(h)}$ and $\beta_3^{(h)} = 1 - \beta_1^{(h)} - \beta_2^{(h)}$).

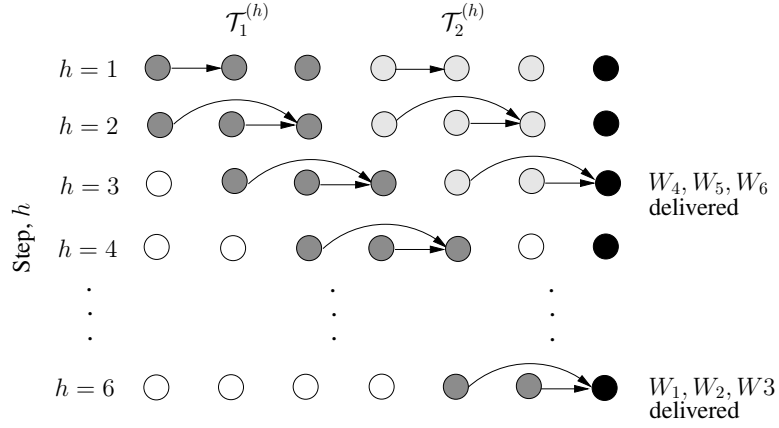


Figure 6.2: TTR strategy in a network with $n = 6$ nodes.

denote the received signal at node ν_i , whenever being in receive mode, in the triplet $\mathcal{T}_\ell^{(h)}$.

As mentioned, for $h = 1$, the first and the second nodes within each triplet act, respectively, as transmitter and receiver, while the third node is in sleep state and does not participate in the network operations. Thus, for $h = 1$ the received signal at node ν_2 is given by:

$$y_2^{(\ell)} = \sqrt{\gamma} x_1^{(\ell)} + \sqrt{\gamma} \sum_{k=1}^{\ell-1} \frac{x_1^{(k)}}{(3(\ell - k) + 1)^{\alpha/2}} + z_2^{(\ell)} \quad (6.2)$$

where the second term refers to the interference coming from those upstream nodes that belong to the previous $\ell - 1$ triplets, and $z_2^{(\ell)}$ is the noise.

Similarly, for $h = 2, \dots, n$, each triplet has its first two nodes acting as transmitters and the third node as a receiver. Hence, the received signal $y_3^{(\ell)}$ is

$$\begin{aligned}
y_3^{(\ell)} &= \sqrt{\gamma} \sum_{j=1}^3 \left(2^{-a/2} \sqrt{\alpha_j^{(h)}} + \sqrt{\beta_j^{(h)}} \right) x_j^{(\ell)} \\
&+ \sqrt{\gamma} \sum_{k=1}^{\ell-1} \sum_{j=1}^3 \left(\frac{\sqrt{\alpha_j^{(h)}}}{(3(\ell-k)+2)^{\frac{a}{2}}} + \frac{\sqrt{\beta_j^{(h)}}}{(3(\ell-k)+1)^{\frac{a}{2}}} \right) x_j^{(k)} \\
&+ z_3^{(\ell)}
\end{aligned} \tag{6.3}$$

with the last term accounting for the interference coming from the upstream nodes.

By investigating the denominator of the terms corresponding to the interference in (6.2) and (6.3), some simplifications are possible. In fact, the power of interfering signals is proportional to $(3(\ell-k)+1)^{-a}$ or $(3(\ell-k)+2)^{-a}$, hence it experiences drastic drops as the difference $\ell-k$ exceeds one. It follows that we can approximate the interference as that due to the nearest upstream triplet, and rewrite (6.2) and (6.3) as

$$y_2^{(\ell)} = \sqrt{\gamma} x_1^{(\ell)} + 2^{-a} \sqrt{\gamma} x_1^{(\ell-1)} + z_2^{(\ell)} \tag{6.4}$$

$$\begin{aligned}
y_3^{(\ell)} &= \sqrt{\gamma} \sum_{j=1}^3 \left(2^{-a/2} \sqrt{\alpha_j^{(h)}} + \sqrt{\beta_j^{(h)}} \right) x_j^{(\ell)} + z_3^{(\ell)} \\
&+ \sqrt{\gamma} \sum_{j=1}^3 \left(5^{-a/2} \sqrt{\alpha_j^{(h)}} + 2^{-a} \sqrt{\beta_j^{(h)}} \right) x_j^{(\ell-1)}
\end{aligned} \tag{6.5}$$

Moreover, since the last three steps, $h = n-2, n-1, n$, involve only one active triplet, i.e., $L(h) = 1$, (see Fig. 6.2), there will be no interference at all, and the received signals will be given by (6.5) with the interference terms removed, i.e., $y_3^{(\ell)} = \sqrt{\gamma} \sum_{j=1}^3 \left(2^{-a/2} \sqrt{\alpha_j^{(h)}} + \sqrt{\beta_j^{(h)}} \right) x_j^{(\ell)} + z_3^{(\ell)}$.

6.4.1.1 Deriving the rate constraints in TTR strategy

Let us now denote by $\mathcal{R}^{(h)}$ the rate of the traffic transfer during step h ($h = 1, \dots, n$). Regarding the initial step, $h = 1$, and according to (6.4), the first term

denotes the desired signal, while the second and third terms denote the interfering signal and the noise, respectively. Thus, according to [20], the constraint on the traffic transfer rate $\mathcal{R}^{(1)}$ is given by:

$$\mathcal{R}^{(1)} \leq \mathcal{C}\left(\frac{\gamma}{1 + 4^{-a}\gamma}\right) = \mathcal{C}\left(\frac{1}{\gamma^{-1} + 4^{-a}}\right) \quad (6.6)$$

As for $h \geq 2$, (6.5) refers to the multiple access transmission of independent messages carried by the signals $x_j^{(\ell)}$, $j = 1, 2, 3$, in the presence of independent interfering signals $x_j^{(\ell-1)}$ and AWGN noise [20]. As a consequence, the corresponding rate constraints are

$$R_j \leq \mathcal{C}\left(\frac{\gamma\left(2^{-a/2}\sqrt{\alpha_j^{(h)}} + \sqrt{\beta_j^{(h)}}\right)^2}{1 + \gamma \sum_{j=1}^3 \left(5^{-a/2}\sqrt{\alpha_j^{(h)}} + 4^{-a/2}\sqrt{\beta_j^{(h)}}\right)^2}\right) \quad (6.7a)$$

$$\sum_{j=1,2} R_j \leq \mathcal{C}\left(\frac{\gamma \sum_{j=1,2} \left(2^{-a/2}\sqrt{\alpha_j^{(h)}} + \sqrt{\beta_j^{(h)}}\right)^2}{1 + \gamma \sum_{j=1}^3 \left(5^{-a/2}\sqrt{\alpha_j^{(h)}} + 4^{-a/2}\sqrt{\beta_j^{(h)}}\right)^2}\right) \quad (6.7b)$$

$$\sum_{j=1,3} R_j \leq \mathcal{C}\left(\frac{\gamma \sum_{j=1,3} \left(2^{-a/2}\sqrt{\alpha_j^{(h)}} + \sqrt{\beta_j^{(h)}}\right)^2}{1 + \gamma \sum_{j=1}^3 \left(5^{-a/2}\sqrt{\alpha_j^{(h)}} + 4^{-a/2}\sqrt{\beta_j^{(h)}}\right)^2}\right) \quad (6.7c)$$

$$\sum_{j=2,3} R_j \leq \mathcal{C}\left(\frac{\gamma \sum_{j=2,3} \left(2^{-a/2}\sqrt{\alpha_j^{(h)}} + \sqrt{\beta_j^{(h)}}\right)^2}{1 + \gamma \sum_{j=1}^3 \left(5^{-a/2}\sqrt{\alpha_j^{(h)}} + 4^{-a/2}\sqrt{\beta_j^{(h)}}\right)^2}\right) \quad (6.7d)$$

$$\sum_{j=1}^3 R_j \leq \mathcal{C}\left(\frac{\gamma \sum_{j=1}^3 \left(2^{-a/2}\sqrt{\alpha_j^{(h)}} + \sqrt{\beta_j^{(h)}}\right)^2}{1 + \gamma \sum_{j=1}^3 \left(5^{-a/2}\sqrt{\alpha_j^{(h)}} + 4^{-a/2}\sqrt{\beta_j^{(h)}}\right)^2}\right) \quad (6.7e)$$

Since we have assumed that at each step all messages are transferred at the same rate $\mathcal{R}^{(h)}$, we set $R_j = \mathcal{R}^{(h)}$, $j = 1, 2, 3$.

Thus, by expanding the terms in (6.7), we finally obtain

$$\mathcal{R}^{(h)} \leq \mathcal{C}\left(\left(2^{-a}\alpha_1^{(h)} + \beta_1^{(h)} + 2^{(1-a/2)}\sqrt{\alpha_1^{(h)}\beta_1^{(h)}}\right)\delta\right) \quad (6.8a)$$

$$\mathcal{R}^{(h)} \leq \mathcal{C}\left(\left(2^{-a}\alpha_2^{(h)} + \beta_2^{(h)} + 2^{(1-a/2)}\sqrt{\alpha_2^{(h)}\beta_2^{(h)}}\right)\delta\right) \quad (6.8b)$$

$$\mathcal{R}^{(h)} \leq \mathcal{C} \left(\left(2^{-a} \alpha_3^{(h)} + \beta_3^{(h)} + 2^{(1-a/2)} \sqrt{\alpha_3^{(h)} \beta_3^{(h)}} \right) \delta \right) \quad (6.8c)$$

$$\mathcal{R}^{(h)} \leq (1/2) \mathcal{C} \left(\left(2^{-a} (1 - \alpha_3^{(h)}) + 1 - \beta_3^{(h)} + 2^{(1-a/2)} \sum_{j=1,2} \sqrt{\alpha_j^{(h)} \beta_j^{(h)}} \right) \delta \right) \quad (6.8d)$$

$$\mathcal{R}^{(h)} \leq (1/2) \mathcal{C} \left(\left(2^{-a} (1 - \alpha_2^{(h)}) + 1 - \beta_2^{(h)} + 2^{(1-a/2)} \sum_{j=1,3} \sqrt{\alpha_j^{(h)} \beta_j^{(h)}} \right) \delta \right) \quad (6.8e)$$

$$\mathcal{R}^{(h)} \leq (1/2) \mathcal{C} \left(\left(2^{-a} (1 - \alpha_1^{(h)}) + 1 - \beta_1^{(h)} + 2^{(1-a/2)} \sum_{j=2,3} \sqrt{\alpha_j^{(h)} \beta_j^{(h)}} \right) \delta \right) \quad (6.8f)$$

$$\mathcal{R}^{(h)} \leq (1/3) \mathcal{C} \left(\left(1 + 2^{-a} + 2^{(1-a/2)} \sum_{j=1,2,3} \sqrt{\alpha_j^{(h)} \beta_j^{(h)}} \right) \delta \right) \quad (6.8g)$$

with $\delta = \left(\gamma^{-1} + 4^{-a} + 5^{-a} + 2 \cdot 4^{-a/2} \cdot 5^{-a/2} \sum_{j=1}^3 \sqrt{\alpha_j^{(h)} \beta_j^{(h)}} \right)^{-1}$.

Hence, the maximum achievable rate becomes

$$\mathcal{R}^{(h)} = \max_{0 \leq \alpha_j^{(h)}, \beta_j^{(h)} \leq 1} \min \left\{ (6.8a), (6.8b), (6.8c), (6.8d), (6.8e), (6.8f), (6.8g) \right\} \quad (6.9)$$

6.4.1.2 Computing the average Achievable rate, R

Finally, we compute the average achievable data rate. Recall that, according to the TTR strategy, at each step $h \geq 2$, the triplets $\mathcal{T}_\ell^{(h)}$, $\ell = 1, \dots, L(h)$, operate in parallel, and each of them transfers the messages $W_{3\ell-2}, W_{3\ell-1}, W_{3\ell}$. After each step is completed, the triplets are shifted toward the destination by one node. Thus, the time it takes to transfer all data to the destination corresponds to the time necessary to deliver the messages generated by the first three nodes in the network, W_1, W_2, W_3 . Also, as mentioned, each step h corresponds to a different network operational state, denoted by σ_h . Recall that t_h is the fraction of time the network stays in state σ_h , and that we have assumed that the average transmission rate is equal to R . Then, we have $R = t_h \mathcal{R}^{(h)}$, and $\sum_{h=1}^n R / \mathcal{R}^{(h)} = \sum_{h=1}^n t_h = 1$. It follows that, under the TTR strategy, the *average* achievable rate of traffic transfer,

R , is given by:

$$R = \left(\sum_{h=1}^n \frac{1}{\mathcal{R}^{(h)}} \right)^{-1}.$$

6.4.2 The TTRR strategy

The TTRR strategy allows to efficiently deliver messages from nodes to the destination, by using quadruplets of adjacent active nodes in an iterative fashion. For clarity of presentation, we describe the proposed communication strategy in three network scenarios of increasing complexity.

Scenario 1. Consider the case where, in our network of n nodes, only nodes 1 and 2 have messages of rate \mathcal{R} , denoted by W_1 and W_2 , respectively, to be delivered to the destination. In this scenario, the TTRR strategy works in n steps denoted by $h = 1, \dots, n$. During step h , the strategy assumes that only the quadruplet of nodes $\mathcal{Q}^{(h)} = \{h, h + 1, h + 2, h + 3\}$ is active while all other nodes are in sleep state. Specifically nodes h and $h + 1$ transmit while nodes $h + 2$ and $h + 3$ receive; the quadruplet is in state $[\sigma_h, \sigma_{h+1}, \sigma_{h+2}, \sigma_{h+3}] = [\mathfrak{t}, \mathfrak{t}, \mathfrak{r}, \mathfrak{r}]$, after which the strategy has been named.

Let us now fix $h = 1$, then only the quadruplet $\mathcal{Q}^{(1)} = \{1, 2, 3, 4\}$ is active, with nodes 1 and 2 transmitting, and 3 and 4 receiving. In particular, consider that node 1 transmits its whole message W_1 , with rate \mathcal{R} , which will be received by node 3 only. Node 2, instead, splits its message, W_2 , in two parts with rates $\rho_2 \mathcal{R}$ and $(1 - \rho_2) \mathcal{R}$, respectively ($0 \leq \rho_2 \leq 1$). The message of rate $\rho_2 \mathcal{R}$ is sent immediately, and is received by both nodes 3 and 4, while the message of rate $(1 - \rho_2) \mathcal{R}$ is left to be transmitted in the following time step. As a consequence, at time step $h = 2$, node 1 is not active any longer as it has completed its data transfer already, and a new quadruplet is formed, namely, $\mathcal{Q}^{(2)} = \{2, 3, 4, 5\}$. The same communication scheme described for step $h = 1$ is repeated, except that now the transmitters are nodes 2 and 3, with the former sending the remaining portion of its message, $(1 - \rho_2) W_2$, and the latter splitting the received message W_1 in two parts

(see Fig. 6.3).

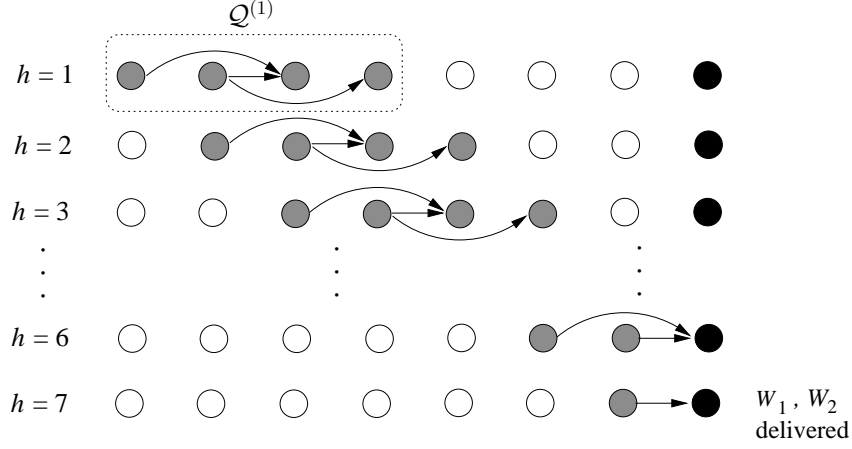


Figure 6.3: TTRR strategy, Scenario 1; the network has $n = 7$ nodes.

In general, at step h ($h = 2, \dots, n - 2$), the first two nodes of quadruplet $Q^{(h)}$, namely, h and $h+1$, have stored in memory two independent messages, respectively, $W_1^{(h)}$ and $W_2^{(h)}$, with $W_1^{(h)}$ having rate $\rho_1^{(h)}\mathcal{R} = (1 - \rho_2^{(h-1)})\mathcal{R}$ and $W_2^{(h)}$ having rate \mathcal{R} . Node h transmits the whole message $W_1^{(h)}$ in step h , while node $h+1$ splits $W_2^{(h)}$ in two parts with rates $\rho_2^{(h)}\mathcal{R}$ and $(1 - \rho_2^{(h)})\mathcal{R}$, respectively ($0 \leq \rho_2^{(h)} \leq 1$). The first part is immediately transmitted, while the second one is sent in the following time step, i.e., $h + 1$. The signals received at nodes $h + 2$ and $h + 3$ are therefore given by:

$$y_{h+2} = \sqrt{\gamma} (2^{-a/2} x_h + x_{h+1}) + z_{h+2} \quad (6.10)$$

$$y_{h+3} = 2^{-a/2} \sqrt{\gamma} x_{h+1} + z_{h+3} \quad (6.11)$$

where x_h and x_{h+1} denote, respectively, the signals transmitted by nodes h and $h+1$ in $Q^{(h)}$, that carry independent messages, while z_{h+2} and z_{h+3} account for the noise.

Regarding (6.10), it describes the multiple access transmission of the two independent messages carried by x_h and x_{h+1} at rates $\rho_1^{(h)}\mathcal{R}^{(h)}$ and $\rho_2^{(h)}\mathcal{R}^{(h)}$.

Thus, according to [20], the rate constraints are

$$\rho_1^{(h)} \mathcal{R}^{(h)} \leq \mathcal{C}(2^{-a}\gamma) \quad (6.12a)$$

$$\rho_2^{(h)} \mathcal{R}^{(h)} \leq \mathcal{C}(\gamma) \quad (6.12b)$$

$$(\rho_1^{(h)} + \rho_2^{(h)}) \mathcal{R}^{(h)} \leq \mathcal{C}((1 + 2^{-a})\gamma) \quad (6.12c)$$

As for node $h + 3$, (6.11) implies that

$$\rho_2^{(h)} \mathcal{R}^{(h)} \leq \mathcal{C}(2^{-a}\gamma) \quad (6.13)$$

Since the rate constraint given by (6.13) dominates that given by (6.12b), the maximum achievable rate $\mathcal{R}^{(h)}$, for a given $\rho_1^{(h)}$, becomes

$$\mathcal{R}^{(h)} = \max_{0 \leq \rho_2^{(h)} \leq 1} \min \left\{ \frac{\mathcal{C}(\gamma/2^{-a})}{\rho_1^{(h)}}, \frac{\mathcal{C}(\gamma/2^{-a})}{\rho_2^{(h)}}, \frac{\mathcal{C}(\gamma + \gamma/2^{-a})}{\rho_1^{(h)} + \rho_2^{(h)}} \right\} \quad (6.14)$$

Remark (*Quadruplets having less than four nodes*): In TTRR strategy, when approaching the destination and in the last two steps, i.e., $h = n - 1, n$, the set of active nodes does not constitute a quadruplet any longer, since there are less than four nodes within the set. Fig. 6.4 depicts such cases where the last set of nodes has respectively three and two nodes only (including the gateway).

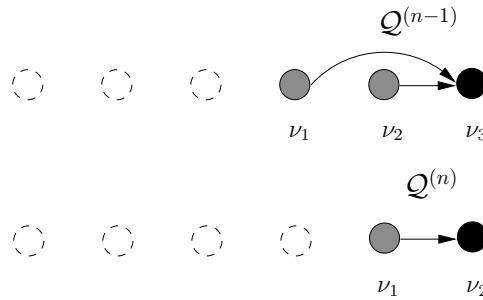


Figure 6.4: Approaching the destination in Scenario 1; the number of active nodes in the last set is less than four, it is actually three (top), and two (bottom).

In step $h = n - 1$ where there are only three active nodes in the last set, only

(6.12) accounts for the rate constraints corresponding to $\mathcal{Q}^{(n-1)}$ since in this case the expression for the received signal is given by (6.10), which yields

$$y_{n+1} = \sqrt{\gamma} (2^{-a/2} x_{n-1} + x_n) + z_{n+1}$$

Hence the maximum achievable rate of traffic transfer in this case is

$$\mathcal{R}^{(n-1)} = \max_{0 \leq \rho_2^{(h)} \leq 1} \min \left\{ \frac{\mathcal{C}(\gamma/2^{-a})}{\rho_1^{(h)}}, \frac{\mathcal{C}(\gamma)}{\rho_2^{(h)}}, \frac{\mathcal{C}(\gamma + \gamma/2^{-a})}{\rho_1^{(h)} + \rho_1^{(h)}} \right\} \quad (6.15)$$

Furthermore, in the last step, i.e. $h = n$, there is only a set of two active nodes, $\mathcal{Q}^{(n)}$ remained (see Fig. 6.4, bottom). Indeed, the received signal at the gateway is given by $y_{n+1} = \sqrt{\gamma} x_n + z_{n+1}$. Accordingly, the rate constraint becomes

$$\mathcal{R}^{(n)} \leq \frac{1}{\rho_1^{(h)}} \mathcal{C}(\gamma) \quad (6.16)$$

Once the optimal value of $\rho_2^{(h)}$ and the maximum achievable rate $\mathcal{R}^{(h)}$ have been determined for any step h , similarly to what done for the TTR scheme, the average achievable rate R can be computed as

$$R = \left(\sum_{h=1}^n \frac{\rho_1^{(h)}}{\mathcal{R}^{(h)}} \right)^{-1}.$$

Scenario 2. Next, we consider a more general case where, given the n network nodes, only two every four nodes generate messages to be delivered to the destination. More formally, only the nodes $4\ell_1 + 1$ and $4\ell_2 + 2$, with $\ell_1 = 0, \dots, \lfloor (n-1)/4 \rfloor$ and $\ell_2 = 0, \dots, \lfloor (n-2)/4 \rfloor$, have independent messages of rate \mathcal{R} to be delivered to the destination. In this case, data can be efficiently transferred by employing the above described n -step communication strategy, in a parallel fashion.

More specifically, at every step $h = 1, \dots, n$, the network nodes plus the destination are divided into $L(h) = \lceil (n-h+2)/4 \rceil$ non-overlapping sets of adjacent nodes, denoted by $\mathcal{Q}_\ell^{(h)} = \{h + 4\ell, h + 4\ell + 1, h + 4\ell + 2, h + 4\ell + 3\}$,

$\ell = 0, \dots, L(h) - 2$, and $\mathcal{Q}_{L(h)-1}^{(h)} = \{h + 4(L(h) - 1), \dots, n + 1\}$. In general, each of these sets is a quadruplet, except for the rightmost which, depending on n and h , may be composed of only 3 or 2 nodes. As shown in Fig. 6.5, the quadruplet $\mathcal{Q}_\ell^{(h)}$, in time steps $h = 1, \dots, n - 4\ell$ forwards the messages $W_{4\ell+1}$ and $W_{4\ell+2}$ to the destination employing the procedure described in Scenario 1.

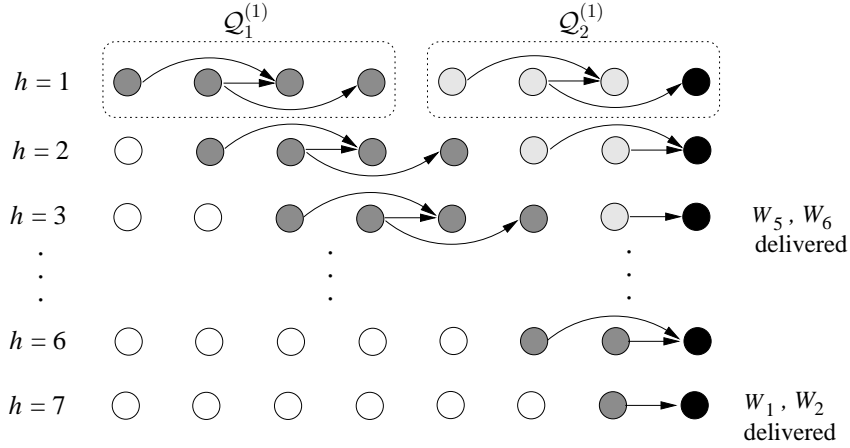


Figure 6.5: TTRR strategy, Scenario 2; delivery of W_1, W_2, W_5, W_6 to the destination in a network with $n = 7$ nodes.

Note also that, in the presence of quadruplets working in parallel, interference between the quadruplets that are active at the same time step, must be taken into account. The signals received within the ℓ -th quadruplet in step h can be therefore written as

$$y_{h+4\ell+2} = \sqrt{\gamma} (2^{-a/2} x_{h+4\ell} + x_{h+4\ell+1}) \quad (6.17)$$

$$+w_{h+4\ell+2} + z_{h+4\ell+2}$$

$$y_{h+4\ell+3} = 2^{-a/2} \sqrt{\gamma} x_{h+4\ell+1} + w_{h+4\ell+3} + z_{h+4\ell+3} \quad (6.18)$$

In (6.17), $x_{h+4\ell}$ and $x_{h+4\ell+1}$ denote, respectively, the signals transmitted by nodes $h + 4\ell$ and $h + 4\ell + 1$ in $\mathcal{Q}_\ell^{(h)}$ (see Fig. 6.6), that carry independent messages, and

$$w_{h+4\ell+2} = \sqrt{\gamma} (6^{-a/2} x_{h+4(\ell-1)} + 5^{-a/2} x_{h+4(\ell-1)+1})$$

accounts for the interfering signals originated from nodes $h + 4(\ell - 1)$ and $h + 4(\ell - 1) + 1$ in $\mathcal{Q}_{\ell-1}^{(h)}$ (refer to Fig. 6.6), and $z_{h+4\ell+2}$ denotes AWGN noise. Similarly, in (6.18), $w_{h+4\ell+3} = \sqrt{\gamma} (7^{-a/2} x_{h+4(\ell-1)} + 6^{-a/2} x_{h+4(\ell-1)+1})$ accounts for the interference from the transmitting nodes in $\mathcal{Q}_{\ell-1}^{(h)}$.

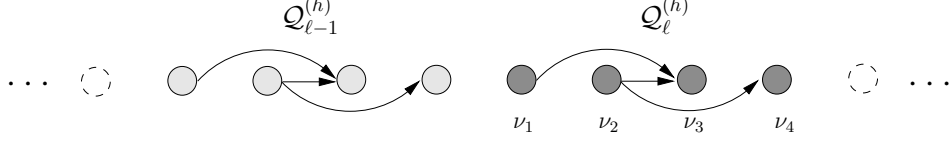


Figure 6.6: Two consecutive quadruplets.

We note that (6.17) describes the multiple access transmission of the two independent messages carried by $x_{h+4\ell}$ and $x_{h+4\ell+1}$ at rates $\rho_1^{(h)} \mathcal{R}^{(h)}$ and $\rho_2^{(h)} \mathcal{R}^{(h)}$, with $w_{h+4\ell+2}$ as interference, and $z_{h+4\ell+2}$ as noise.

Thus, the rate constraints are [20]

$$\rho_1^{(h)} \mathcal{R}^{(h)} \leq \mathcal{C} \left(\frac{(2^{-a/2} \sqrt{\gamma})^2}{1 + (6^{-a/2} \sqrt{\gamma})^2 + (5^{-a/2} \sqrt{\gamma})^2} \right) \quad (6.19a)$$

$$\rho_2^{(h)} \mathcal{R}^{(h)} \leq \mathcal{C} \left(\frac{(\sqrt{\gamma})^2}{1 + (6^{-a/2} \sqrt{\gamma})^2 + (5^{-a/2} \sqrt{\gamma})^2} \right) \quad (6.19b)$$

$$(\rho_1^{(h)} + \rho_2^{(h)}) \mathcal{R}^{(h)} \leq \mathcal{C} \left(\frac{(2^{-a/2} \sqrt{\gamma})^2 + (\sqrt{\gamma})^2}{1 + (6^{-a/2} \sqrt{\gamma})^2 + (5^{-a/2} \sqrt{\gamma})^2} \right) \quad (6.19c)$$

in which by expanding the terms we get

$$\mathcal{R}^{(h)} \leq \frac{1}{\rho_1^{(h)}} \mathcal{C} \left(\frac{2^{-a}}{\gamma^{-1} + 5^{-a} + 6^{-a}} \right) \quad (6.20a)$$

$$\mathcal{R}^{(h)} \leq \frac{1}{\rho_2^{(h)}} \mathcal{C} \left(\frac{1}{\gamma^{-1} + 5^{-a} + 6^{-a}} \right) \quad (6.20b)$$

$$\mathcal{R}^{(h)} \leq \frac{1}{\rho_1^{(h)} + \rho_2^{(h)}} \mathcal{C} \left(\frac{1 + 2^{-a}}{\gamma^{-1} + 5^{-a} + 6^{-a}} \right) \quad (6.20c)$$

As for node $h + 4\ell + 3$, (6.18) gives the expression of the received signal, in which there is only one desired signal involved (i.e., $x_{h+4\ell+1}$). Hence, the rate constraint

is

$$\mathcal{R}^{(h)} \leq \frac{1}{\rho_2^{(h)}} \mathcal{C} \left(\frac{2^{-a}}{\gamma^{-1} + 6^{-a} + 7^{-a}} \right) \quad (6.21)$$

Between the rate constraint given by (6.21) and (6.20b), the first one is dominant, so the maximum achievable rate $\mathcal{R}^{(h)}$, for a given $\rho_1^{(h)}$, becomes

$$\mathcal{R}^{(h)} = \max_{0 \leq \rho_2^{(h)} \leq 1} \min \left\{ (6.20a), (6.20b), (6.20c), (6.21) \right\} \quad (6.22)$$

Remark (*Quadruplets having less than four nodes*) There are some steps for which the last active quadruplet, $\mathcal{Q}_{L^{(h)}-1}^{(h)}$ does not have four nodes any longer (see Fig. 6.7). In the case that there are only three active nodes in $\mathcal{Q}_{L^{(h)}-1}^{(h)}$ (Fig. 6.7, top), (6.20) is still valid as the rate constraints since the expression for the received signal is the same as given by (6.17), i.e. we have

$$y_{n+1} = \sqrt{\gamma} \left(2^{-a/2} x_{n-1} + x_n \right) + w_{n+1} + z_{n+1}$$

Hence (6.22) gives the maximum achievable rate of traffic transfer.

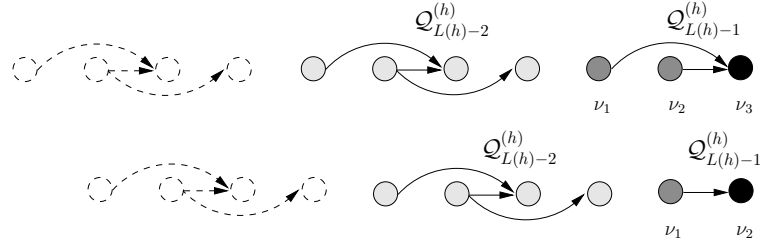


Figure 6.7: Special cases in TTRR strategy, where the number of active nodes in the last set is less than four, it is actually three (top), and two (bottom).

However, an additional equation is introduced as for the received signal referred to the case where $\mathcal{Q}_{L^{(h)}-1}^{(h)}$ has only two active nodes (see Fig. 6.7, bottom). Indeed, the received signal at the gateway is

$$y_{n+1} = \sqrt{\gamma} x_n + \sqrt{\gamma} \left(5^{-a/2} x_{n-4} + 4^{-a/2} x_{n-3} \right) + z_{n+1} \quad (6.23)$$

where the second term denotes the interference from the transmitters in $\mathcal{Q}_{L(h)-2}^{(h+1)}$. Accordingly, the rate constraint becomes

$$\mathcal{R}^{(h)} \leq \frac{1}{\rho_1^{(h)}} \mathcal{C}\left(\frac{1}{\gamma^{-1} + 5^{-a} + 4^{-a}}\right) \quad (6.24)$$

Hence, for this step, the maximum achievable rate is instead

$$\mathcal{R}^{(h)} = \max_{0 \leq \rho_2^{(h)} \leq 1} \min \left\{ (6.20a), (6.20b), (6.20c), (6.21), (6.24) \right\}. \quad (6.25)$$

Let $\mathcal{R}_\ell^{(h)}$ be the rate achieved by the ℓ -th quadruplet in step h . The communication rates $\mathcal{R}_\ell^{(h)}$ can be obtained similarly to what has been done under Scenario 1, in absence of interference. Then, the average communication rate R achieved in this scenario is given by

$$R = \left(\sum_{h=1}^n \max_{\ell} \frac{\rho_{1,\ell}^{(h)}}{\mathcal{R}_\ell^{(h)}} \right)^{-1} \quad (6.26)$$

where $\rho_{1,\ell}^{(h)}$ is the rate coefficient associated to the ℓ -th quadruplet in step h . Since the time required by quadruplet $\mathcal{Q}_\ell^{(h)}$ to complete step h may vary with ℓ , the rate is dominated, at each time step, by the slowest quadruplet, i.e., the one whose transmission time $\rho_{1,\ell}^{(h)}/\mathcal{R}_\ell^{(h)}$ is the longest.

Scenario 3. At last, we consider that all nodes in the network have a message of rate \mathcal{R} to send to the destination. In this case, data can be efficiently delivered by organizing the transmissions in two phases, in each of which we apply the procedure described for Scenario 2. In the first phase, we assume that only the set of nodes considered in Scenario 2 (i.e., $4\ell_1 + 1$ and $4\ell_2 + 2$, $\ell_1 = 0, \dots, \lfloor (n-1)/4 \rfloor$, $\ell_2 = 0, \dots, \lfloor (n-2)/4 \rfloor$) generate messages, which are forwarded to the destination in n steps (see Fig.6.8). In the second phase, only the set of nodes complementary with respect to the previous one (i.e., $4\ell_1 + 3$, and $4\ell_2 + 4$, $\ell_1 = 0, \dots, \lfloor (n-3)/4 \rfloor$, $\ell_2 = 0, \dots, \lfloor (n-3)/4 \rfloor$) have their own messages to be transferred. Such messages are forwarded to the destination in $n-2$ steps, since, after phase 1, the messages of

nodes 1 and 2 have already reached the destination, hence only the last $n - 2$ nodes are involved in the procedure (refer to Fig.6.8).

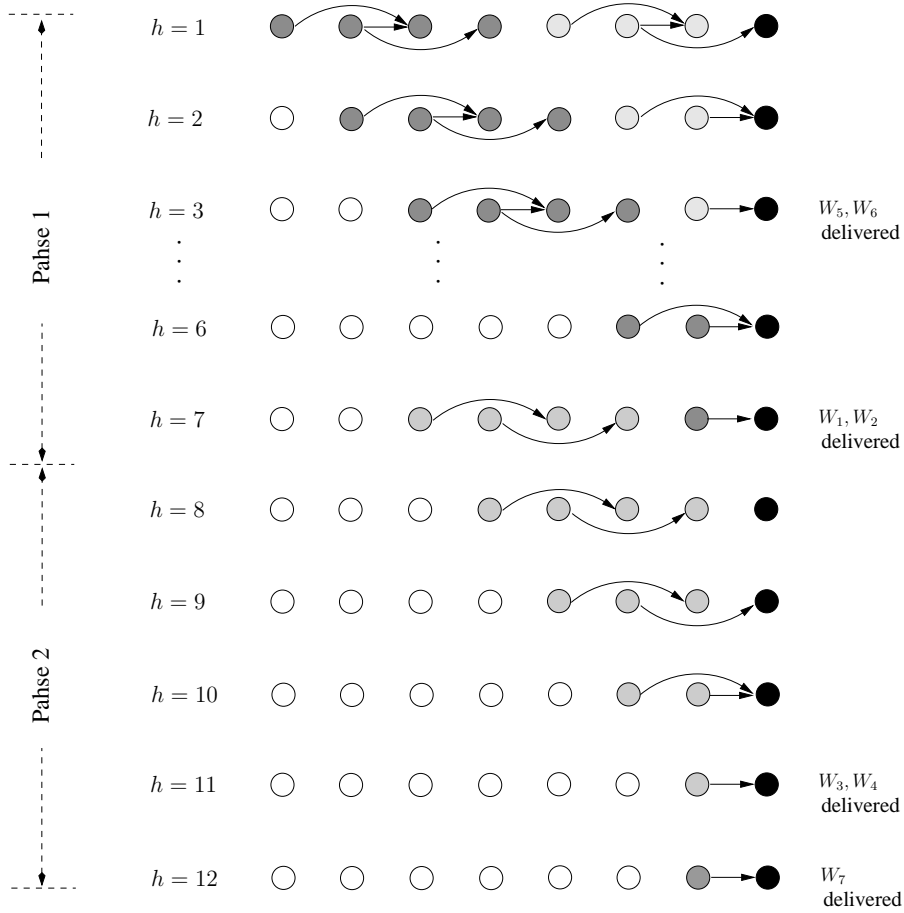


Figure 6.8: TTRR strategy, Scenario 3; a network with $n = 7$ nodes.

The corresponding rate constraints in this scenario is the same as given for Scenario 2.

Let $\mathcal{R}_\ell^{(1,h)}$ and $\mathcal{R}_\ell^{(2,h)}$ be the rates achieved in step h of phases 1 and 2, respectively, and let $\rho_{1,\ell}^{(1,h)}$ and $\rho_{1,\ell}^{(2,h)}$ be the corresponding rate coefficients. Such quantities can be easily derived as done for $\mathcal{R}_\ell^{(h)}$ and $\rho_{1,\ell}^{(h)}, \rho_{2,\ell}^{(h)}$ in Scenario 2. Then, applying (6.26) and accounting for the two phases of the scheme, the average rate achieved by the TTRR strategy is given by:

$$R = \left(\sum_{h=1}^n \max_{\ell} \frac{\rho_{1,\ell}^{(1,h)}}{\mathcal{R}_\ell^{(1,h)}} + \sum_{h=1}^{n-2} \max_{\ell} \frac{\rho_{1,\ell}^{(2,h)}}{\mathcal{R}_\ell^{(2,h)}} \right)^{-1}.$$

6.5 Results

We consider a network with $n = 10$ nodes, plus the destination, and take the signal-to-noise ratio over one-hop distance, γ , and the path loss exponent, a , as the varying parameters of the system; similar results have been obtained for larger values of n . Without loss of generality, we set $B = 1$ MHz, and the transmit and receive gains of the antennas, G_t and G_r , both equal to 1. We compare the rate performance of the TTR and the TTRR (the latter in the most general scenario, namely, Scenario 3) against the cut-set upper bound obtained in Chapter 5 and reported in [52], and the non-cooperative one-hop transmission scheme¹, first by neglecting the interference, and then by taking interference into account. We stress that the analysis in the first case is motivated by the fact that it reflects the condition under which the cut-set bound can be derived.

Fig. 6.9 compares the rate performance of the three strategies, namely, TTR, TTRR, and one-hop, to the cut-set upper bound in the absence of interference and in the cases where $a = 1.5$ (top) and $a = 3$ (bottom). As shown in the figure, for lower γ 's, the TTR strategy outperforms both the TTRR and the one-hop scheme. However, as the system moves into mid-to-high range of γ , the TTRR strategy gives a higher average achievable rate than the other two. For $a = 3$, the average rate achieved by the TTR strategy approaches the upper bound for low values of SNR, while TTRR does the same, but at high SNRs. This suggests that the use of either one of the proposed schemes should be chosen depending on the propagation conditions in the working environment.

Now, we turn our attention to the more realistic case where the interference due to simultaneous transmissions is taken into account. Fig. 6.10 presents the impact of interference on the average achievable rate of the strategies for $a = 1.5, 3$. This figure clearly shows the superiority of the two strategies TTR and TTRR over the one-hop scheme in both low and high values of SNR when the interference is

¹In the non-cooperative one-hop transmission, each message is forwarded downstream toward the node at one-hop distance from the sender, till it is received by the destination.

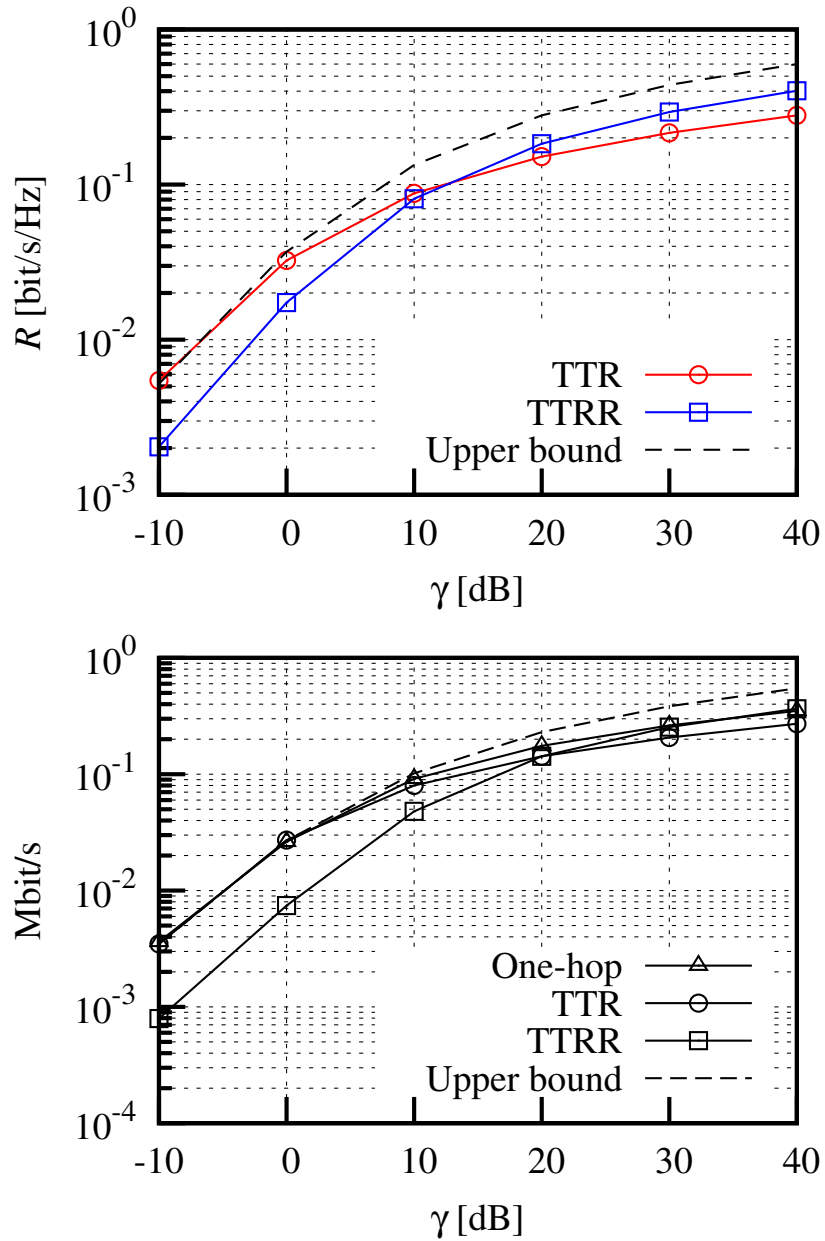


Figure 6.9: Average achievable rates in the absence of signal interference, $a = 1.5$ (top) and $a = 3$ (bottom).

considered. In fact, as the TTR strategy performs well for very low amounts of SNR, at mid-to-high SNRs we see a major difference between the performance of TTRR and the other two schemes.

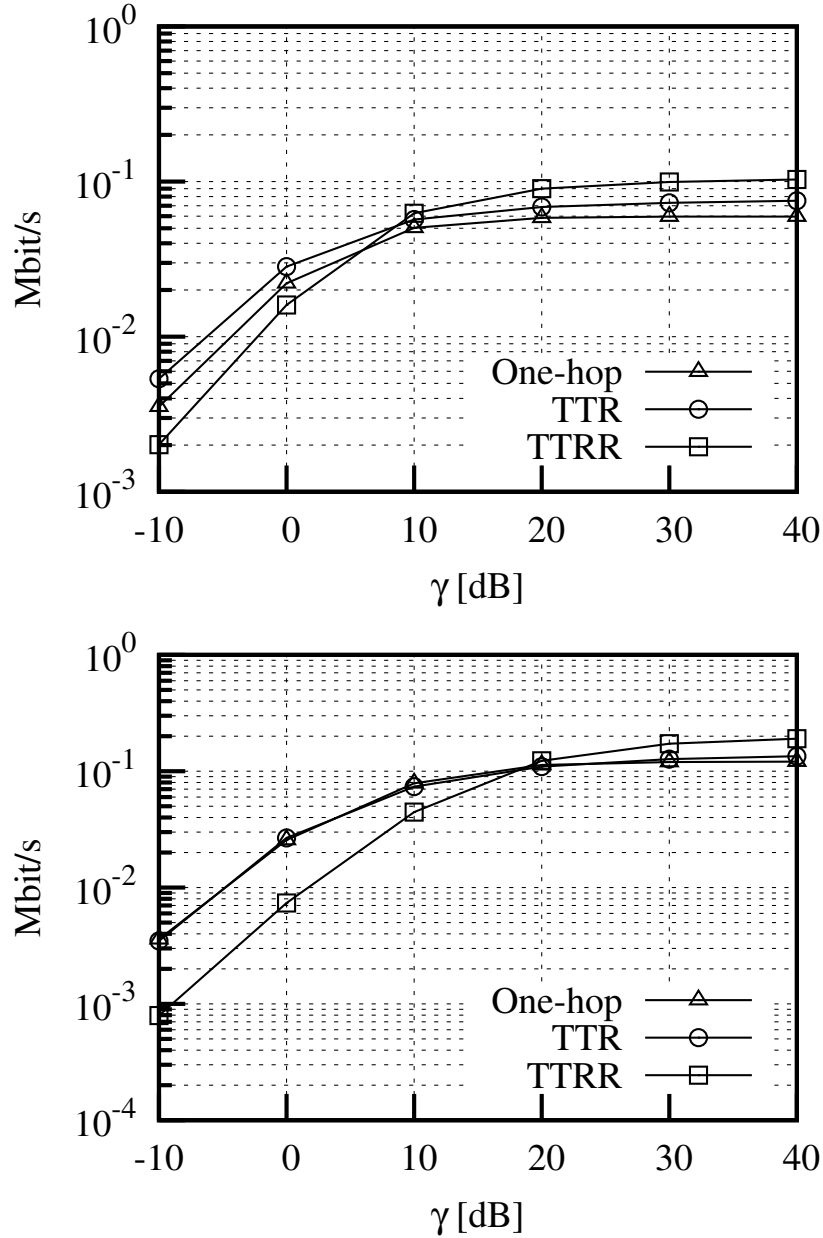


Figure 6.10: Average achievable rates in the presence of signal interference, $a = 1.5$ (top) and $a = 3$ (bottom).

6.6 Concluding Remarks

In this chapter, we considered the case of a multi-hop network with linear topology and half-duplex nodes serving as both traffic sources and relays, and devised two traffic relaying strategies, namely, TTR and TTRR. We studied the rate performance of these schemes in terms of average achievable traffic rate, by taking an information theoretical approach. We showed that the proposed strategies perform well in

realistic scenarios where the signal interference among simultaneous transmissions cannot be neglected. As implied by the results, the superior performance of the strategies along with their simple operation nominate them as efficient data transfer schemes in applications such as wireless sensor networks where these two criteria should be satisfied accordingly. Future work will be the analysis of performance of the proposed strategies with respect to the energy consumption issues, and trying to improve the performance by taking into account both the average achievable rate and energy consumption.

Bibliography

- [1] D. Bhattacharyya, T. Kim, *et al.*, “A Comparative Study of Wireless Sensor Networks and Their Routing Protocols,” *Sensors*, no. 10, 10506–10523, 2010.
- [2] I.F. Akyildiz, W. Su, *et al.*, “Wireless sensor networks, a survey,” *Computer Networks, Elsevier*, 38, 393–422, 2002.
- [3] A. Koubaa, M. Alves, *et al.*, “Lower Protocol Layers for Wireless Sensor Networks, A Survey,” *Technical Report, TR-051101, Version: 1.0*, 2005.
- [4] P. Rentala, R. Musunuri, *et al.*, “Survey on Sensor Networks,” *Survey paper submitted as per the requirements of Mobile Computing (CS 6392) Course*.
- [5] J. Yick, B. Mukherjee, D. Ghosal, “Wireless sensor networks survey,” *Computer Networks, Elsevier*, 52, 2292–2330, 2008.
- [6] E. Bjornemo, “Energy Constrained Wireless Sensor Networks, Communication Principles and Sensing Aspects,” *Ph.D. dissertation, Uppsala University, Sweden*, 2009.
- [7] A. Bari, “Relay Nodes in Wireless Sensor Networks, A Survey,” *University of Windsor*, 2005.
- [8] D. Puccinelli, M. Haenggi, “Wireless Sensor Networks: Applications and Challenges of Ubiquitous Sensing,” *IEEE Circuits and Systems Magazine*, 19–29, Third Quarter 2005.
- [9] J.L. Hill, “System Architecture for Wireless Sensor Networks,” *Ph.D. dissertation, University of California, Berkeley*, 2003.
- [10] V. Rai and R. Mahapatra., “Lifetime Modeling of a Sensor Network,” *IEEE International Conference on Design, Automation and Test in Europe (DATE)*, vol. 1, 202–203, 2005.
- [11] S.K. Singh, M.P. Singh, *et al.*, “Routing Protocols in Wireless Sensor Networks – A Survey,” *International Journal of Computer Sciences & Engineering Survey (IJCSES)*, vol. 49, no. 2, 2010.
- [12] J.M. Kahn, R.H. Katz, *et al.*, “Next century challenges: mobile networking for smart dust,” *Proceedings of the ACM MobiCom*, 271–278, Washington, USA, 1999.

- [13] G.J. Pottie, W.J. Kaiser, “Wireless integrated network sensors”, *Communications of the ACM*, vol. 43, no. 5, 551–558, 2000.
- [14] E. Shih, S. Cho, N. Ickes, *et al.*, “Physical layer driven protocol and algorithm design for energy-efficient wireless sensor networks”, *Proceedings of ACM MobiCom*, 272–286, Rome, Italy, 2001.
- [15] A. Porret, T. Melly, *et al.*, “A low-power low-voltage transceiver architecture suitable for wireless distributed sensors network”, *IEEE International Symposium on Circuits and Systems*, vol. 1, 56–59, Geneva, Switzerland, 2000.
- [16] K.D. Wong, “Physical layer consideration for wireless sensor networks”, *Proceedings of the IEEE International Conference on Networking, Sensing and Control*, Taipei, Taiwan, 2004.
- [17] W. Dargie, C. Poellabauer, “Fundamentals of Wireless Sensor Networks, Theory and Practice”, *Wiley Publications*, 2010.
- [18] Z. Wang, X. Qian, X. Zhao, “The strategies of avoiding energy holes in wireless sensor networks,” *IEEE International Congress on Image and Signal Processing*, 2011.
- [19] H.S. Ramos, Eduardo M.R. Oliveira, *et al.*, “Characterization and Mitigation of the Energy Hole Problem of Many-to-One Communication in Wireless Sensor Networks”, *International Conference on Computing, Networking and Communications*, 2010.
- [20] T.M. Cover, J.A. Thomas, *Elements of Information Theory*, John Wiley & Sons, 1991.
- [21] M.A. Khojastepour, “Distributed Cooperative Communications in Wireless Networks,” *Ph.D. Dissertation*, Rice University, 2003.
- [22] A.S. Avestimehr, S.N. Diggavi, D.N.C. Tse, “Wireless Network Information Flow: A Deterministic Approach,” *IEEE Transactions on Information Theory*, vol. 57, no. 4, April 2011.
- [23] L. Xie, P.R. Kumar, “A Network Information Theory for Wireless Communication: Scaling Laws and Optimal Operation,” *IEEE Transactions on Information Theory*, vol. 50, no. 5, 2004.
- [24] C.E. Shannon, “Two-way communication channels,” *Proceedings of the 4th Berkeley Symp. on Mathematics, Statistics, and Probability*, 1961.
- [25] R. Ahlswede, “Multi-way communication channels,” *Proceedings of 2nd Int. Symp. on Information Theory*, 1971.
- [26] T.M. Cover, “Broadcast channels,” *IEEE Transactions on Information Theory*, vol. 18, pp. 2–14, 1972.
- [27] E.C. Van der Meulen, “Three-terminal communication channels,” *Advances in Applied Probability*, vol. 3, pp. 120–154, 1971.

- [28] T.M. Cover, A. El Gamal, “Capacity theorems for the relay channel,” *IEEE Transactions on Information Theory*, vol. 25, no. 5, pp. 572–584, 1979.
- [29] M.A. Khojastepour, B. Aazhang, A. Sabharwal, “Bounds on Achievable Rates for General Multi-terminal Networks with Practical Constraints,” *ACM IPSN*, Palo Alto, CA, 2003.
- [30] G. Kramer, “Topics in Multi-User Information Theory,” *Foundations and Trends in Communications and Information Theory*, vol. 4, no. 4–5, pp. 265–444, 2007.
- [31] L. Xie, P.R. Kumar, “Multisource, Multidestination, Multirelay Wireless Networks,” *IEEE Transactions on Information Theory*, vol. 53, no. 10, pp. 3586–3595, 2007.
- [32] Z. Zhou, S. Zhou, J. Cui, and S. Cui, “Energy-Efficient Cooperative Communication Based on Power Control and Selective Single-Relay in Wireless Sensor Networks,” *IEEE Transactions on Wireless Communications*, vol. 7, no. 8, pp. 3066–3078, Aug. 2008.
- [33] S. Cui, A. J. Goldsmith, and A. Bahai, “Energy-efficiency of MIMO and cooperative MIMO techniques in sensor networks,” *IEEE J. on Selected Area in Communications*, vol. 22, no. 6, pp. 1089–1098, Aug. 2004.
- [34] R. Madan, S. Cui, S. Lall, and A. J. Goldsmith, “Modeling and optimization of transmission schemes in energy-constrained wireless sensor networks,” *IEEE/ACM Trans. on Networking*, vol. 15, no. 6, pp. 1359–1372, Dec. 2007.
- [35] R. Nabar, H. Bolcskei, F. W. Kneubuehler, “Fading relay channels: performance limits and space-time signal design,” *IEEE J. on selected Areas in Communications*, vol. 22, no. 6, pp. 1099–1109, Aug. 2004.
- [36] Z. Hang, T. Dongbao, “City Traffic Detector Optimization Method Study,” *Journal of Wuhan University of Technology*, vol. 32, no. 6, pp. 1161–1164, 2008.
- [37] J. Li, P. Mohapatra, “Analytical Modeling and Mitigation Techniques for the Energy Hole Problem in Sensor Networks,” *Pervasive and Mobile Computing*, vol. 3, no. 3, June 2007.
- [38] X. Wu, C. Guihai, S.K. Das, “Avoiding Energy Holes in Wireless Sensor Networks with Nonuniform Node Distribution,” *IEEE Transactions on Parallel and Distributed Systems*, vol. 19, no. 5, pp. 710–720, May 2008.
- [39] I. Maric, R.D. Yates, “Bandwidth and Power Allocation for Cooperative Strategies in Gaussian Relay Networks,” *IEEE Transactions on Information Theory*, vol. 56, no. 4, pp. 1880–1889, Apr. 2010.
- [40] C. Edemen, O. Kaya, “Achievable Rates for the Three User Cooperative Multiple Access Channel,” *IEEE WCNC*, Las Vegas, NV, 2008.

- [41] C.W. Sung, Q. Wang, K.W. Shum. “Capacity Region of the Linear Four-node Half-duplex Wireless Relay,” *IEEE Communications Letters*, vol. 13, no. 4, Apr. 2009.
- [42] T. Lutz, C. Hausl, R. Koetter, “Bits Through Deterministic Relay Cascades with Half-Duplex Constraint,” *IEEE Transactions on Information Theory*, vol. 58, no. 1, pp. 369–381, 2012.
- [43] E. Uysal-Biyikoglu, B. Prabhakar, A. El Gamal, “Energy-efficient Packet Transmission over a Wireless Link,” *IEEE/ACM Transactions on Networking*, vol. 10, no. 4, pp. 487–499, 2002.
- [44] E. Uysal-Biyikoglu, A. El Gamal, “On Adaptive Transmission for Energy Efficiency in Wireless Data Networks,” *IEEE Transactions on Information Theory*, vol. 50, no. 12, pp. 3081–3094, 2004.
- [45] S. Pollin, B. Bougard, R. Mangharam, F. Catthoor, I. Moerman, R. Rajkumar, L. Van der Perre, ”Optimizing Transmission and Shutdown for Energy-efficient Real-time Packet Scheduling in Clustered Ad Hoc Networks,” *EURASIP Journal on Wireless Communications and Networking*, vol. 2005, no. 5, Oct. 2005.
- [46] K. Rajgopal, S. Wei, “Scheduling with Rate and Duty-Cycle Constraints for Wireless Networks over an Interference Channel,” *40th Annual Conference on Information Sciences and Systems*, Princeton, NJ, Mar. 2006.
- [47] R. Madan, S. Cui, S. Lall, A.J. Goldsmith, “Cross-Layer Design for Lifetime Maximization in Interference-Limited Wireless Sensor Networks,” *IEEE Transactions on Wireless Communications*, vol. 5, no. 11, pp. 3142–3152, 2006.
- [48] J. Hsu, A. Kansal, J. Friedman, V. Raghunathan, M. Srivastava, “Design Considerations for Solar Energy Harvesting Wireless Embedded Systems,” *SPOTS track at ACM IPSN*, Los Angeles, CA, 2005.
- [49] C.H. Papadimitriou, K. Steiglitz, “The Max-Flow, Min-Cut Theorem,” in *Combinatorial Optimization: Algorithms and Complexity*, Dover, pp. 120-128, 1998.
- [50] P. Herhold, E. Zimmermann, G. Fettweis, “Cooperative Multi-hop Transmission in Wireless Networks,” , vol. 49, pp. 299-324, 2005.
- [51] K. Yamamoto, K. Haneda, H. Murata, *et al.*, “Optimal Transmission Scheduling for a Hybrid of Full- and Half-Duplex Relaying,” *IEEE Communications Letters*, vol. 15, no. 3, 2011.
- [52] A. Nordio, V. Forutan, C.-F. Chiasserini, “Upper Bounds to the Performance of Traffic Relaying in Wireless Linear Networks,” submitted to *IEEE Transactions on Wireless Communications*.

- [53] H. Bagheri, A. Matahari, A. Khandani, “On the Capacity of the Half-Duplex Diamond Channel,” *IEEE ISIT*, pp. 649–653, Jun. 2010.